ISSN number 0971 - 9709

The Journal of Indian Geophysical Union

VOLUME 21, ISSUE 3 I MAY 2017

AN OPEN ACCESS BIMONTHLY JOURNAL OF IGU

EDITORIAL OFFICE

Indian Geophysical Union, NGRI Campus, Uppal Road, Hyderabad- 500 007
Telephone: +91 -40-27012799; 27012734; Telefax:+91-04-27171564
E. mail: jigu1963@gmail.com, website: www.j-igu.in

The Open Access Journal with six issues in a year publishes articles covering
Solid Earth Geosciences; Marine Geosciences; and Atmospheric, Space and Planetary Sciences.

Annual Subscription

Individual ₹ 1000 per issue and Institutional ₹ 5000 for six issues

Payments should be sent by DD drawn in favour of "The Treasurer, Indian Geophysical Union", payable at Hyderabad, Money Transfer/NEFT/RTGS (Inter-Bank Transfer), Treasurer, Indian Geophysical Union, State Bank of Hyderabad, Habsiguda Branch, Habsiguda, Uppal Road, Hyderabad- 500 007
A/C: 52191021424, IFSC Code: SBHY0020087, MICR Code: 500004020, SWIFT Code: SBHYINBB028.

For correspondence, please contact, Hon. Secretary, Indian Geophysical Union, NGRI Campus, Uppal Road, Hyderabad - 500 007, India; Email: igu123@gmail.com; Ph: 040 27012799

ISSN: 0257-7968 (Thomson Reuters)
ISSN: 0971-9709 (NISCAIR)

Approved as ESCI journal by Thomson Reuters
Cited in Indian Citation Index (ICI), New Delhi
Evaluated by NISCAIR, New Delhi

CONTENTS

Searching for alien life on exoplanets :
Researchers study Archean Earth during the First 1-billion-year period

New NASA study suggests that the atmosphere of the Earth appears to have been different during the Archean era. The reason could be little availability of oxygen and high levels of methane, ammonia and other organic chemicals.

Researchers have been searching for life on planets other than Earth since long. A team of researchers studied the Earth, specifically the Archean Earth during 1-1/2-billion-year period early in the planet's history in order to better understand which hazy and distant exoplanet could have habitable conditions to sustain life. For years, astronomers have been trying to look out for alien life by studying distant planets for habitable conditions.

New NASA study suggests that the atmosphere of the Earth appears to have been different during the Archean era. The reason could be little availability of oxygen and high levels of methane, ammonia and other organic chemicals. The haze might have come and disappeared sporadically from the Archean atmosphere, geological evidence suggests. But researchers are not quite sure why. In order to better understand the hazy earth-like exoplanets, the researchers studied the haze formation during the Archean era. The study suggested that Archean Earth is the most alien planet and we have geochemical data of it.

In order to see how haze affected the surface temperature of Archean Earth in turn and in turn how the temperature influenced the chemistry in the atmosphere, the researchers put together sophisticated computer modelling. "The new modelling indicates that as the haze got thicker, less sunlight would have gotten through, inhibiting the types of sunlight-driven chemical reactions needed to form more haze. This would lead to the shutdown of haze-formation chemistry, preventing the planet from undergoing runaway glaciation due to a very thick haze," said the report. This phenomenon is called 'self-limiting haze' as named by the by the research team. Their work is to first make the case that this is what happened on Archean Earth.

That self-limiting haze could have cooled Archean Earth by about 36 degrees Fahrenheit (20 Kelvins) - enough to make a difference but not to freeze the surface completely, the researchers concluded. "Our modelling suggests that a planet like hazy Archean Earth orbiting a star like the young sun would be cold. But we're saying it would be cold like the Yukon in winter, not cold like modern-day Mars". Such a planet could sustain life and can be considered habitable, even if the mean global temperature is below freezing, as long as there is some liquid water on the surface, the report added.

(**Source:** https://www.nasa.gov/vision/universe/starsgalaxies/search_life_I.html)

Editorial

In the last two editorials we have had very good exposure to MAGMA through invigorating interaction. In this issue another fascinating topic is selected for editorial. Length of the editorial has increased as it is an important topic containing various details.

*****Plate Tectonics-revisited**

Any study that involves a percentage of subjectivity needs to be re-evaluated using new data and new models that have taken in to consideration the subjectivity based limitations. However, none can unequivocally state any of these refined models can provide ultimate answers to many questions posed earlier by the learned way back in 19th and 20th century. This enigmatic and intriguing reality allows earth science researchers to be active continuously both in the field, laboratory and before a computer, hoping to find apt solutions. As a part of subjective cutting edge research activity I have selected an interesting topic for this issue`s main editorial-**Plate Tectonics.**

Our readers, young and senior, are informed about Plate Tectonics that gained worldwide significance nearly five decades back. However, a series of studies carried out in the recent past made me to bring out this editorial to excite the inquisitive researcher to go into details of various facets of the plate tectonics. I have collected some relevant information covering the basics and the recent studies and the same are detailed below.

The plate tectonics theory tries to explain the movement of the Earth's lithosphere. The Earth's surface is made up of a series of large plates that can travel up to 2 or 3 cm per year. Convection currents beneath the plates drive the plates in different directions; the source of the heat driving the convection currents is from the radioactive decay taking place within the Earth's core. The idea behind the plate tectonics theory originated from meteorologist Alfred Wegner's ideas of continental drift. He observed that the continents seemed to fit together like a jigsaw forming a super continent called Pangaea. Overall there are seven major plates: North America, South America, Eurasia, Africa, Indo-Australian, Pacific and Antarctica. Mantle convection, Earth rotation and gravity are all drivers of the movement. As these plates interact they form plate boundaries, which cause many different features to emerge.

***The Theory of Plate Tectonics**

The basic theory of plate tectonics is that along seafloor spreading zones, the continents are separating from one another. As they spread apart, magma comes to the surface and becomes new continental crust. As the tectonic plates move away from spreading zones, they collide with one another. In some cases, the edges of two different plates will grind against each other in a horizontal fashion. These areas, called transform boundaries, experience many earthquakes. In other cases, the plates directly collide, forcing one plate upward while the other plate is forced back into the mantle. These collision areas, called convergent boundaries, create mountain ranges. An active convergent boundary is under the Himalayan Mountains, which are being created by the subduction of the Indian crust sliding under the Tibetan crust.

Evidence for Plate Tectonic Theory:

1. Sea Floor Magnetism: Stripes of magnetic material in the seafloor provide strong evidence for tectonic theory. The stripes alternate between those with magnetic material orientated toward magnetic north, and those oriented in the opposite direction. Seafloor spreading is the mechanism behind this phenomenon. As new magma forces its way up to the surface, magnetized minerals in the liquid rock orient along the Earth's magnetic field and then harden as the lava cools. As spreading continues, the material moves away from the spreading zone as if on a conveyor belt. The Earth's magnetic field flips every few hundred thousand years, and the stripes on the ocean floor show a record of those changes. By estimating when the flips occurred and pairing that with the distance the stripes have moved from the spreading zone, scientists can estimate how fast the continents are moving. This supports plate tectonic theory as it shows that there has to be plates for continents to move independently to each other.

2. Fossil Evidence: The continents have moved a great deal in the history of the planet, but they carry records of where they've been. Some of this evidence is the fossils of animals and plants. Palaeomagnetic evidence is a stronger piece of evidence. Magnetic strata within the fossil record show how the land masses were oriented at different times during Earth's history. By constructing detailed records of changes in land mass orientation, scientists can reconstruct paths of tectonic movement much further back in history than they can from the magnetic striping on the sea floor.

3. Direct Measurement: Modern technology gives us a range of ways to directly measure the movement of tectonic plates. These methods are based around the idea of measuring distance between two points on Earth by using some intermediary transmitter in space. Using these measurements, scientists can accurately estimate movement of the tectonic plates today.

Evidence against Plate Tectonic Theory:

The evidence against is due to the mechanism of plate movement. This is because convection cell currents have not been proved conclusively to exist due to technological limitations. We have never been able to get deep enough into earth to prove the theory. The main fault in convection cell currents is the evidence collected, which suggests that these cells are impossible to occur. Their occurrence is only supported by theory. More questions have surfaced about the formation of plates and how energy is gained through convection to move truly slabs of rock. Finally convection cell currents do not have the force to form mountain ranges such as the Andes and Himalayas.

(**Source:** http://education.seattlepi.com/list-describe-evidence-plate-tectonics-theory-5600.html;
http://mrrudgegeography.weebly.com/plate-tectonic-theory.html)

Researchers added to the above by stating that much of the theory based on continuing observations of the sea floor and continental margins. The initial determination was that, as the continents spread apart, new oceanic crust is formed at the mid-oceanic ridges. But what happens to it then? Somewhere it has to be consumed. If not, the earth would have to keep getting bigger to accommodate the additional crust (Originally proposed, but generally discounted). Earth would have had to start out real small if spreading rates historically approached today's rates. Harry Hess in the early 1960's Proposed that old oceanic crust is consumed at island arcs. Amidst plausible supporting evidences major opposition emerged questioning what causes the plates to move? This always been the weak point of the theory and the rallying cry of the non-believers.

Lots of possibilities have been proposed. Lunar drag; Centrifugal pull due to rotational velocity (these first two were Wegener's original proposal-Demonstrated to be too small); Gravitational sliding away from the topographic highs of the spreading centers; Expansion of the earth-Possible mechanism to start it off; Lithosphere cracks; New material rises to fill the void; Density differences between descending lithosphere; mantle drags plate behind; Pulls open at the ridges-Slab-pull, ridge-push; Mantle Convection. Currently popular theory-Most probably a combination of several of the above, as well as others not imagined yet.

(**Source:** http://jersey.uoregon.edu/~mstrick/RogueCom College/RCC_Lectures/ConDrift_PlateTec.html)

As stated in the beginning when there is subjectivity in our proposals/theories scores of knowledgeable researchers make it a point to find apt solutions. Some of the recent studies are listed below to show where we stand with regard to Plate Tectonics.

***Plate tectonics on the early Earth: Limitations imposed by strength and buoyancy of subducted lithosphere**

The tectonic style and viability of modern plate tectonics in the early Earth is still debated. Field observations and theoretical arguments both in favour and against the uniformitarian view of plate tectonics back until the Archaean continue to accumulate. Authors of a study published in "Lithos" presented the first numerical modelling results that address for a hotter Earth the viability of subduction, one of the main requirements for plate tectonics. A hotter mantle has mainly two effects: 1) viscosity is lower, and 2) more melt is produced, which in a plate tectonic setting will lead to a thicker oceanic crust and harzburgite layer (**P.S**: Harzburgite is an ultramafic, igneous rock, a variety of peridotite consisting mostly of the two minerals, olivine and low-calcium (Ca) pyroxene (enstatite). Harzburgite layers play significant role in the morphology of subducting plates and the behavior of oceanic crustal layers).

Although compositional buoyancy resulting from these thick crust and harzburgite might be a serious limitation for subduction initiation, modelling results show that eclogitization significantly relaxes this limitation for a developed, ongoing subduction process. Furthermore, the lower viscosity leads to more frequent slab break-off, and sometimes to crustal separation from the mantle lithosphere. Unlike earlier propositions, not compositional buoyancy considerations, but this lithospheric weakness could be the principle limitation to the viability of plate tectonics in a hotter Earth. These results suggest a new explanation for the absence of ultrahigh-pressure metamorphism (UHPM) and blue-schists in most of the Precambrian: early slabs were not too buoyant, but too weak to provide a mechanism for UHPM and exhumation.

(**Source:** Jeroen van Hunen and Arie P. van den Berg, Lithos,Volume 103, Issues 1–2, June 2008, 217–235)

***Tiny Mineral Grains Could Drive Plate Tectonics**

The idea of plate tectonics—that Earth's plates smash into each other to form mountains, slide underneath one another to form ocean trenches, and pull apart to form new oceans and continents—is well known. The underlying mechanism driving these processes, which scientists think may be vital to the evolution of life, remains unclear. No one knows for sure how plate tectonics even evolved.

At a global scale, individual plates can be easy to see—their borders are defined by where earthquakes occur. Global perspectives have also allowed scientists to precisely map the movement of plates over millennia by tracking magnetic signatures on the bottoms of the oceans. In addition, vast networks of GPS receivers can also track minute movements of plates today.

To fully understand plate tectonics, we need to zoom in from the global scale into the microscale. However, investigating the factors that first triggered plate tectonics requires a different perspective, said David Bercovici, a geophysicist from Yale University.

At many plate boundaries, scientists find a metamorphic rock made of deformed, very fine grained minerals called mylonite. The origin of mylonite is still unknown. The grains within mylonite are much smaller than the rocks in the plates around them, which makes mylonite relatively weak. Because of this relative weakness, mylonite seems to support or permit very, very rapid, focused deformation. Bercovici and colleagues suggest that the small-grained mylonite fuels a feedback mechanism that creates the weak spots on Earth that we know as active plate boundaries. As you deform [mylonite], somehow the grains in rocks become so small that it softens the rock up, and softened rock supports rapid deformation to allow you to have these plate boundaries. Small-grained mylonite fuels a feedback mechanism that creates the weak spots on Earth that we know as active plate boundaries. Scientists remain in the dark about exactly how mylonite forms at a granular level. However, decades of collaborative research gave Bercovici's team an idea.

In most rocks, minerals grow grain by grain, gobbling up the grains next to them—much like how the bubbles in foam get bigger by "eating" neighbouring bubbles. When a growing mineral grain swells up against a different type of mineral, its growth is blocked by the boundary between the two minerals in a process called "pinning." This process forces the grains into smaller and smaller sizes by further damaging the grain-to-grain interface.

As the grains get smaller and smaller, the resulting mylonite gets weaker and weaker. "By damaging the [grain] interface, we can drive the grains to smaller sizes and therefore get the self-softening feedback mechanism," Bercovici said.

Origins of Plate Boundaries

The last piece of the puzzle required a peek back in time—via exhaustive research on samples of 4.4-billion-year-old zircon. Zircon forms when granites crystallize from magma heated by the hot fluids that sweat off subduction zones.

The age of the zircon falls as much as 1 billion years before scientists think plate tectonics became a global phenomenon. This presents a puzzle—how did a mineral known to form from subduction processes crystallize before subduction became mainstream? Bercovici speculates that primitive subduction zones might have formed on Earth's surface early in its history, when cool, heavy mantle rock near the surface began to drip down deeper into the mantle, pulling overlying crust down with it.

Bercovici applied his theoretical model of mylonite formation to simulations that mimicked the formation of subduction zones. He found that where primitive subduction formed, a mylonitic-type weak zone formed. When the drip-like subduction ceased and started again elsewhere, it left behind a weak zone that would persist without healing for many millions of years.

Although the research may be the first to show how initial damage in surface plates can propagate through tectonic cycles, it needs to be tested using more realistic rock mechanics, said Jun Korenaga, professor of geophysics at Yale University. Although Bercovici's work gives clues about how plates on Earth started to move, it does not solve the plate tectonic mystery completely. For example, what happens when two continents collide? In the future, Bercovici hopes to include the effects of continent-to-continent interaction in his models of mylonite-induced tectonics.

(**Source:** Wendel, J. (2015), Tiny mineral grains could drive plate tectonics, *Eos, 96,* doi:10.1029/ 2015EO024967.)

Another interesting article was published recently, keeping the dialogue interesting.

***Heat from earth's core could be underlying force in plate tectonics**

For decades, scientists have theorized that the movement of Earth's tectonic plates is driven largely by negative buoyancy created as they cool. New research, however, shows plate dynamics are driven significantly by the additional force of heat drawn from the Earth's core. The new findings also challenge the theory that underwater mountain ranges known as mid-ocean ridges are passive boundaries between moving plates. The findings show the East Pacific Rise, the Earth's dominant mid-ocean ridge, is dynamic as heat is transferred. David B. Rowley, professor of geophysical sciences at the University of Chicago, and fellow researchers came to the conclusions by combining observations of the East Pacific Rise with insights from modeling of the mantle flow there.

"We see strong support for significant deep mantle contributions of heat-to-plate dynamics in the Pacific hemisphere," said Rowley, lead author of the paper. "Heat from the base of the mantle contributes significantly to the strength of the flow of heat in the mantle and to the resultant plate tectonics." The researchers estimate up to approximately 50 percent of plate dynamics are driven by heat from the Earth's core and as much as 20 terawatts of heat flow between the core and the mantle. Unlike most other mid-ocean ridges, the East Pacific Rise as a whole has not moved east-west for 50 to 80 million years, even as parts of it have been spreading asymmetrically. These dynamics cannot be explained solely by the subduction -- a process whereby one plate moves under another or sinks. Researchers in the new findings attribute the phenomena to buoyancy created by heat arising from deep in the Earth's interior. "The East Pacific Rise is stable because the flow arising from the deep mantle has captured it," Rowley said. "This stability is directly linked to and controlled by mantle upwelling," or the release of heat from Earth's core through the mantle to the surface. The Mid-Atlantic Ridge, particularly in the South Atlantic, also may have direct coupling with deep mantle flow, he added.

Some researchers pointed out that the consequences of this research are very important for all scientists working on the dynamics of the Earth, including plate tectonics, seismic activity and volcanism.

The forces at work

Convection, or the flow of mantle material transporting heat, drives plate tectonics. As envisioned in the current research, heating at the base of the mantle reduces the density of the material, giving it buoyancy and causing it to rise through the mantle and couple with the overlying plates adjacent to the East Pacific Rise. The deep mantle-derived buoyancy, together with plate cooling at the surface, creates negative buoyancy that together explain the observations along the East Pacific Rise and surrounding Pacific subduction zones. A debate about the origin of the driving forces of plate tectonics dates back to the early 1970s. Scientists have asked: Does the buoyancy that drives plates primarily derive from plate cooling at the surface, analogous with cooling and overturning of lakes in the winter? Or, is there also a source of positive buoyancy arising from heat at the base of the mantle associated with heat extracted from the core and, if so, how much does it contribute to plate motions? The latter theory is analogous to cooking oatmeal: Heat at the bottom causes the oatmeal to rise, and heat loss along the top surface cools the oatmeal, causing it to sink. Until now, most assessments have favored the first scenario, with little or no contribution from buoyancy arising from heat at the base. The new findings suggest that the second scenario is required to account for the observations, and that there is an approximately equal contribution from both sources of the buoyancy driving the plates, at least in the Pacific basin.

Based on models of mantle convection, the mantle may be removing as much as half of Earth's total convective heat budget from the core," Rowley said. Much work has been performed over the past four decades to represent mantle convection by computer simulation. Now the models will have to be revised to account for mantle upwelling, according to the researchers.

The research could have broader implications for understanding the formation of the Earth. It has important consequences for the thermal budget of the Earth and the so-called 'secular cooling' of the core. If heat coming from the core is more important than we thought, this implies that the total heat originally stored in the core is much larger than we thought.

Also, the magnetic field of the Earth is generated by flow in the liquid core, so the findings of Rowley and co-authors are likely to have implications for our understanding of the existence, character and amplitude of the Earth's magnetic field and its evolution through geological time. (**Citation**: David B. Rowley, et al. Kinematics and dynamics of the East Pacific Rise linked to a stable, deep-mantle upwelling**.** *Science Advances*, 2016; 2 (12): e1601107 DOI: 10.1126/sciadv.1601107).

Increase in the Mantle Temperature

It is stated in the previous sub-section that the mantle may be removing as much as half of Earth`s total convective heat budget from the core. However, if the mantle temperature is higher than normally believed the picture may change. The mantle - the mostly solid, rocky part of Earths interior - is about 60 degrees Celsius hotter than previously thought, a new study has found. The findings led by Woods Hole Oceanographic Institution (WHOI) in the US could change how scientists think about many issues in Earth science including how ocean basins form. A 60-degree increase may not sound like a lot compared to a molten mantle temperature of more than 1,400 degrees Celsius, researchers said.

However, the result is significant *as a hotter mantle would be more fluid, helping to explain the movement of rigid tectonic plates.*

Since it is not possible to measure the mantles temperature directly, geologists have to estimate it through laboratory experiments that simulate the high pressures and temperatures inside the Earth. Water is a critical component of the equation: the more water (or hydrogen) in rock, the lower the temperature at which it will melt.

The peridotite rock that makes up the upper mantle is known to contain a small amount of water. To figure out how the water content of mantle rock affects its melting point, a researcher (Emily Sarafian), conducted a series of lab experiments.

Following standard experimental methodology, she created a synthetic mantle sample. She used a known, standardised mineral composition and dried it out in an oven to remove as much water as possible. She modified her starting sample by adding spheres of a mineral called olivine, which occurs naturally in the mantle. The spheres were large enough for her to analyse their water content using secondary ion mass spectrometry (SIMS). From there, she was able to calculate the water content of her entire starting sample. To her surprise, she found it contained approximately the same amount of water known to be in the mantle.

Based on her results, she concluded that mantle melting had to be starting at a shallower depth under the seafloor than previously expected. To verify her results, she made use of magnetotellurics - a technique that analyses the electrical conductivity of the crust and mantle under the seafloor. Reconciling the temperatures and pressures she measured in her experiments the melting depth from an earlier study. It led her to a startling conclusion: The oceanic upper mantle must be 60 degrees Celsius hotter than current estimates. (**Source:** INDIA TODAY NEWS, 5th March, 2017).

Adding spice to the debate another study surfaced to motivate Indian researchers.

***India was by no means as isolated as Plate Tectonists thought**

India harbours many unique species of flora and fauna that only occur in this form on the subcontinent. The prerequisite for such a unique development of species is that no exchange takes place with other regions. For a long time, scientists assumed that India was isolated in this way due to continental drift. The supercontinent Gondwana, which included South America, Africa, Antarctica, Australia, Madagascar and India, broke up over the course of geological history. What is now India also began moving towards the north east around 130 million years ago. It was common belief among researchers that, before it collided with the Eurasian plate, India was largely isolated for at least 30 million years during its migration. However, according to current findings by paleontologists at the University of Bonn, the Indian subcontinent may not have been as isolated on its journey as we have thought. "Certain midges that occurred in India at this time display great similarity to examples of a similar age from Europe and Asia," says lead author. These findings are a strong indicator that an exchange did occur between the supposedly isolated India, Europe and Asia.

Mining for amber in the Indian coal seams

A scientist from the University of Bonn mined for amber in seams of coal near the Indian city of Surat. Small midges, among other things, were encased in tree resin 54 million years ago and preserved as fossils. The paleontologist investigated a total of 38 biting midges encased in amber and compared them with examples of a similar age from Europe and China. Scientists from the University of Gdansk (Poland) and Lucknow (India) were also involved in this. It has been possible to assign a total of 34 of these insect fossils to those that are already known. There was significant conformity with biting midges in amber from the Baltic and Fushun in north-east China.

Chains of islands presumably created a link to India

Scientists assume that a chain of islands that existed at that time between India, Europe and Asia could have helped the biting midges to spread. As if from stepping stone to stepping stone, the insects could have gradually moved forward along the islands.

(**Source**: Stebner et al. 2017, Jes Rust. Biting Midges from Cambay Amber Indicate that the Eocene Fauna of the Indian Subcontinent Was Not Isolated. *PLOS ONE*, 12 (1): e0169144 DOI: 10.1371/journal.pone.0169144)

From the basic studies carried out five decades back and many interesting more recent studies (some are given above) it is clear that researchers have to adapt to a changed perception, namely, look at micro level to understand the basic mechanism underlying Plate Tectonics. In other words try to see a grain of rock as the main component and formation of mylonite as the vital source in initiating and sustaining Plate Tectonics. We find it difficult to invoke in real time the role of forces associated with the slabs of rocks and mammoth crustal segments to understand the basic mechanism responsible for the plates to move, slide and subduct. The strongest part of the lithosphere that has to be softened, which is thus, the plate tectonic bottle-neck (as proposed by Bercovici) is the cold ductile region, below where failure and frictional sliding become ineffective. This is at about 50-100km in depth and ranging mostly around temperatures of 1000K. It turns out that rocks in deformation zones exhumed from these depths and temperatures exhibit very localized deformation and at the same time unusual grain-size reduction. In summary Bercovici would say that the main features of **plate tectonicness**, are (1) one-sided subduction of tectonic plates that involves entraining surface material (and from this the other unique feature of continental crust pops out), (2) focussed but passive divergent zones or spreading centers, and (3) significant strike-slip motion. If we want to recognize plate tectonics in all its glory on another planet or identify how, when and why it started on Earth, we need to find these features. But, then it also helps to understand why we have these features at all. This debate goes on and on, until theory is supported by in situ experiments; a reality in an unspecified time scale. As micro and macro structures tell us the striking similarity, a section of a leaf and a sea of cosmic world (full of galaxies, dark matter and innumerable number of unknown features) let us enjoy the beauty of William Blake's quote about a grain of sand: ***"To see a world in a grain of sand and heaven in a wild flower Hold infinity in the palms of your hand and eternity in an hour."--William Blake.***

***In this issue & status of JIGU**

In this issue apart from editorial and news at a glance we have 7 research publications. I place on record our thanks to authors for communicating good articles for publication in JIGU. I am indebted to learned scientists for sparing their valuable time in reviewing the manuscripts, following ethical norms. Couple of editorial board members extended their unequivocal support and help in editing the manuscripts and providing useful inputs for authors (especially students and young researchers) to enhance quality of the manuscripts. I am trying to meet various norms with my limited capabilities. Since I wish to be relatively stress free I seek the help of one and all to share more responsibility in managing the journal, by voluntarily monitoring day to day activities of JIGU, especially when I am not in a position to visit JIGU office.

I am happy to inform our readers and contributors that our journal is included in the "Indian citation Index" apart from Thomson Reuters ESCI. If we can maintain the good standards of publication and ensure timely release of bi-monthly issues we will definitely get better recognition.

P.R.Reddy

J. Ind. Geophys. Union (May 2017)
v.21, no.3, pp: 183-190

Variations of Total Magnetic Field before two small magnitude Earthquakes in Kachchh, Gujarat, India

Shivam Joshi*, C.P. Simha, K.M. Rao and M.S.B.S. Prasad
Institute of Seismological Research, Department of Science &Technology, Gandhinagar, Gujarat, India
*Corresponding Author: iamshivamjoshi@gmail.com

ABSTRACT
In this study, variations of Total Magnetic field recorded in overhauser magnetometer at Multi Parametric Geophysical Observatories (MPGO) of Badargadh and Desalpar are analysed to correspond with small magnitude earthquakes occurred in 2014 in Kachchh, Gujarat employing different techniques such as power spectral density, fractal dimensions and principal component analysis. To reduce the effects of manmade and atmospheric perturbations magnetic data of mid night (i.e., 18-21 UTC) times were considered. Two small magnitude earthquakes occurred on 9th March 2014 (Mw 4.1, R=58 km) and 29th April 2014 (Mw 3.8, R=43 km) within the preparatory zone were studied in this analysis. In order to discriminate the effect of geomagnetic storm activity, the planetary index Kp and Dst were also analyzed in the corresponding period. These parameters are found to be normal during 9th March event and high during 29th April event. Total Magnetic field however, recorded considerable enhancement (10 nT for 9th March event and 30 nT for 29th April event) three days prior to these events. These enhancements persisted during the event and latter decreased exponentially. The difference between the total magnetic field data of the two MPGO Observatories (Badargadh and Desalpar), which is free of the secular trend of the geomagnetic field showed exponential increase prior to these events. We here by conclude that the observed magnetic anomaly prior to 9th March earthquake might be related to seismogenic origin while we cannot attribute the variations before 29th April with local earthquake activity as there was a record of global geomagnetic effects during this period.

Key words: Total magnetic field, Principal Component analysis, Fractal dimension, PSD, earthquake.

INTRODUCTION

The pre seismic anomalies related to electromagnetic effects are promising tools among the short term earthquake precursors. Various studies have shown that these pre-seismic electromagnetic emissions occur in a wide frequency band ranging from few Hz to MHz (Fraser-Smith et al., 1990; Hayakawa and Fujinawa, 1994). Pre earthquake anomalies are often observed in the magnetic observations close to earthquake epicentres (Hattori, 2004). Merzer and Klemperer (1997) suggest that geomagnetic anomalies are caused by induced electric currents flowing in the fault zone during the earthquake preparation period. All most all global pre-earthquake electromagnetic studies hither to conduct are based on large magnitude earthquakes. Efforts were little for similar studies in the case of small magnitude earthquakes. The purpose of the present paper is to apply modern techniques on geomagnetic data to see whether it is possible to identify any anomalies before small-magnitude earthquakes. Few such attempts reported in literature, unfortunately, did not show positive results. However, Seokhoon Oh, (2012), Bella et al., (1998), among others observed positive anomalies prior to local seismic activity. In the present paper we report the outcome of our study on the geomagnetic variations before small magnitude earthquakes (4.0 or smaller) occurred in Kachchh region of Gujarat that may probably be related to pre-seismic signatures. Here, we used the techniques of Fractal analysis, Principal component analysis and Power spectral densities for analysing the geomagnetic data.

Data and Method

The Kachchh basin is a western margin pericratonic rift basin of India and is considered to be an excellent site for studying pre-earthquake geomagnetic anomalies as this region is seismically active. Institute of Seismological Research (ISR) established three multi-parametric geophysical observatories (MPGO) at Desalpar, Badargadh and Vamka in this region. In order to monitor geomagnetic total field, one Overhauser magnetometer with a sample rate of 1sec is installed at each of these MPGO sites, which are located at remote places away from man-made noise and the electric field disturbances. The total geomagnetic data of Desalpar (DES) and Badargadh (BAD) during 25th Jan - 10th May 2014 are taken in this analysis. The locations of Badargadh ($23^0.47$ N, $70^0.62$ E) and Desalpar ($23^0.74$ N, $70^0.69$ E) observatories along with the two earthquake epicentres are shown in Figure 1. Details of the two local earthquakes being considered, which are within 50 km epicentre distance from our observatories are shown in Table 1.

Table 1. Details of local earthquakes being studied.

EVENT (Date)	TIME (GMT)	Mw	LAT. (°N)	LONG. (°E)	Epicentral dist (km) DES	Epicentral dist (km) BAD	Hy.Dist. (km) DES	Hy.Dist. (km) BAD	Depth (km)
09th Mar 2014	19:01	4.1	23.359	70.293	33	16	49	39	36.2
29th Apr 2014	05:55	3.8	23.491	70.281	32	15	34	19	12.5

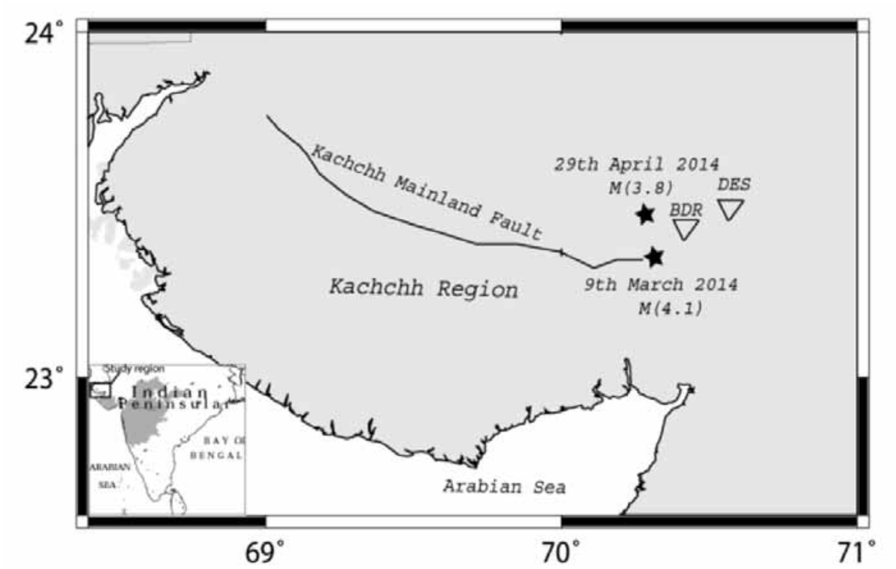

Figure 1. Locations of Magnetic observatories (triangles) along with earthquake locations (star). The study region is shown as rectangle in India map (inset).

The following procedure of data analysis was adopted:

1. We used the data of 3hrs during the local midnight (18-21 UTC) with the sampling interval of 1 sec.
2. We performed the Power Spectral Density (PSD) at five different frequencies. By averaging over the 6 segments, we obtained the daily average spectrum.
3. The Principal Component Analysis and Fractal dimensions were obtained.

Principal Component Analysis

Principal component analysis (PCA) involves a mathematical procedure that transforms a number of (possibly) correlated variables into a (smaller) number of uncorrelated variables called principal components. The mathematical technique used in PCA is called eigen analysis: we solved for the eigen values and eigenvectors of a square symmetric matrix with sums of squares and cross products. In this Principal Component Analysis, we have to subtract the mean from each of the data dimensions; the mean is the average across each dimension. Then, we calculate the covariance matrix. Subsequently, we calculate the Eigen values and Eigen vectors of the covariance matrix.

Fractal Dimensions

We analysed the fractal dimensions which are based on self-organized critical (SOC) concept, using Berry's method (Berry, 1979). The concept of SOC was first introduced by Bak et al., (1987). In the Berry's method, the hourly time series is divided into segments of 1024 data points, with 50% overlapping the previous segment. Each segment is subjected to Fast Fourier Transform. Power spectrum of five segments in 3 h is then averaged to obtain the most coherent and persistent spectral characteristics. Slope (β) of averaged spectrum is then estimated using linear fit to the spectrum plotted on log-log scale in the frequency band 0.03-0.1 Hz. This slope can be linked with fractal dimension using Berry's equation ($D = (5 - \beta)/2$) (Berry, 1979).

RESULTS AND DISCUSSION

The local earthquakes in Kachchh considered in this study fall within the limits of Earthquake preparatory zone (Dobrovolsky et al., 1979) and Es parameter(Hattori et al., 2006). The Es parameter is found to be $0.6*10^8$ for

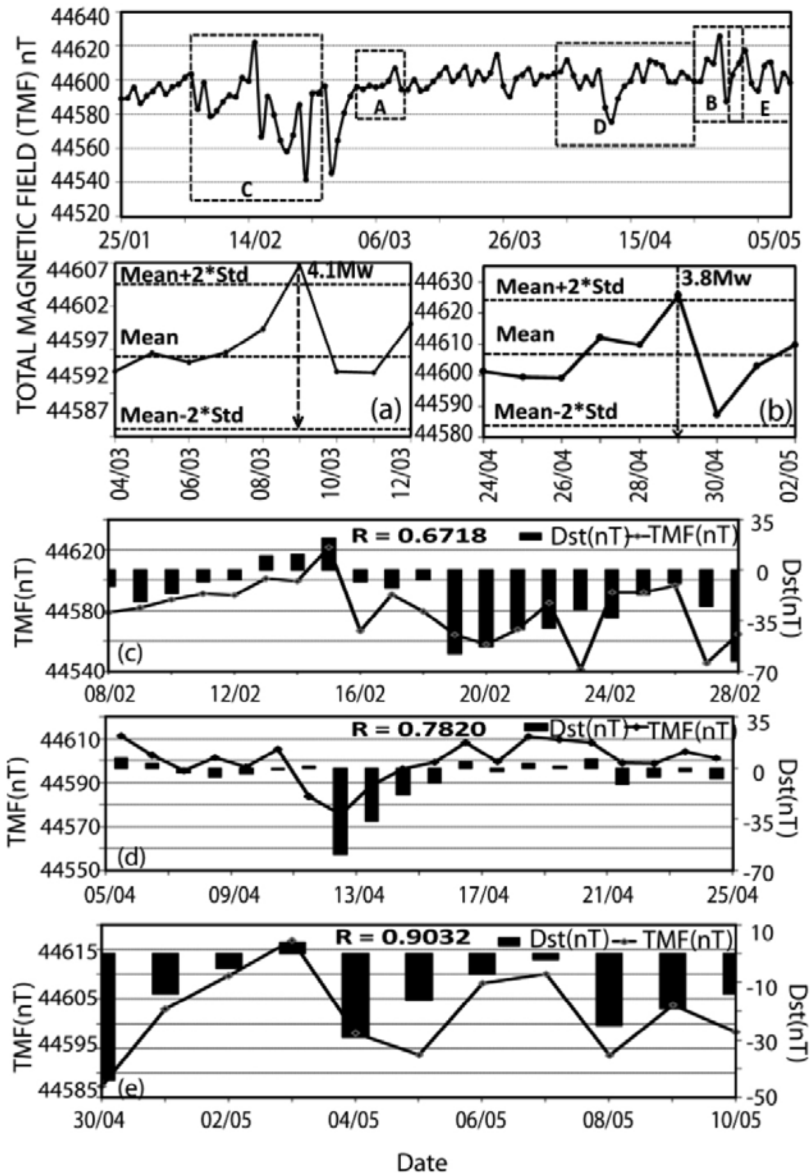

Figure 2. Total Magnetic Field of Badargadh site during 9th March and 29th April events. Panels a, b are 5 days before and 3 days after the local earthquakes respectively; panel c, d, e during the regime of high Dst. R is corr-coefficient between TMF and Dst.

the 9th March event and $0.8*10^8$for the 29th April event at Badargadh station.

Total Magnetic Field Variations

Daily night time 3 hours (18-21 UT) averaged Total Magnetic Field from 25th Jan to 10th May 2014 recorded at the MPGO sites of Badargadh and Desalpar are shown in Figures 2 & 3. These sites are situated within the radial distance of 50 km from each other. Total Magnetic Field values varied from 44540 to 46260nT at Badargadh and Desalpar sites respectively. We can clearly see the enhancement in the data series at few instances which are marked as a -e segments in these figures. The a, b segments are categorised as seismogenic and the c, d, e segments are categorised as global geomagnetic effects. This categorisation has been made based on timings of local earthquakes and global geomagnetic storms. The segments a & b represent 5 days before and 3 days after the earthquakes (Table 1). These segments clearly show considerable enhancement of 10nT for 9th March event and 30 nT for 29th April event. The enhancement started on 6th March from 44495 nT to 44605 nT on 9 th March. Similarly, the segment b is shown as middle panel, the enhancement started on 26th April from 44600 nT to 44630 nT on 29th April.

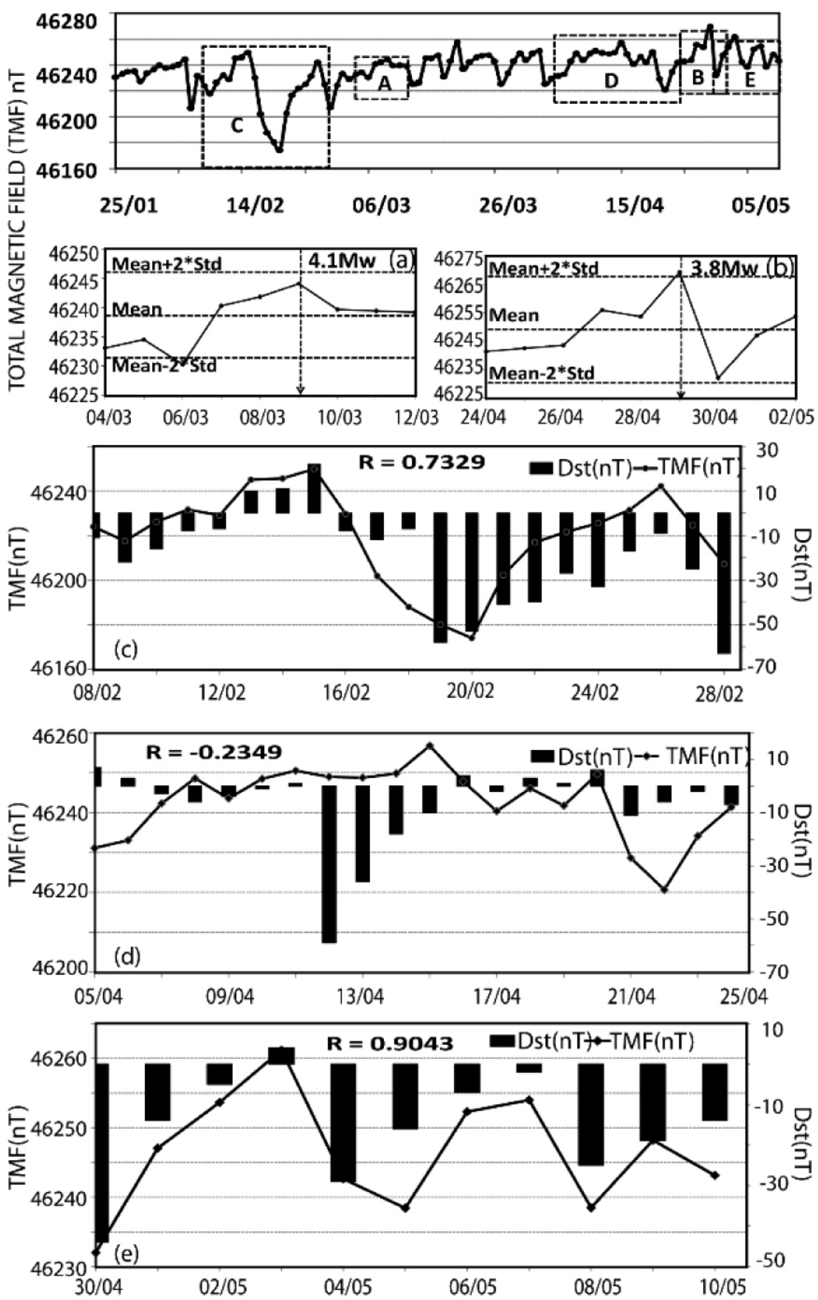

Figure 3. Total Magnetic Field of Desalpar site during 9th March and 29th April events. Panels a, b are 5 days before and 3 days after the local earthquakes respectively; panel c, d, e during the regime of high Dst. R is corr-coefficient between TMF and Dst.

The enhancement persists during the event and exponentially decreases after one day onwards. In order to identify the anomalies in the time series, statistical limits of Mean+2*sigma and Mean-2*sigma is computed for the 9 days regime during these earthquakes. The data series around 9th March event is found to be geomagnetic storm free data as it satisfies the conditions of $\Sigma Kp<10$ and Dst<-20nT during this period (Hayakawa et al., 1996). The other event on 29 April is not satisfying these conditions and fall in geomagnetic storm effect. We found that the signal crossed statistical limits just before these two earthquakes. It is generally believed that signal crossing this limit is anomalous. We can certainly attribute the anomalies before 9th March event as signatures of pre-earthquake geomagnetic variations. However, the data around 29th April event is influenced by storm, and therefore we cannot attribute this signal to local earthquake activity.

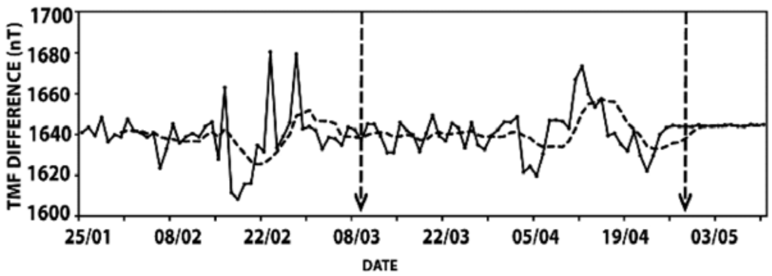

Figure 4. Difference plot of TMF of Badargadh- Desalpar.

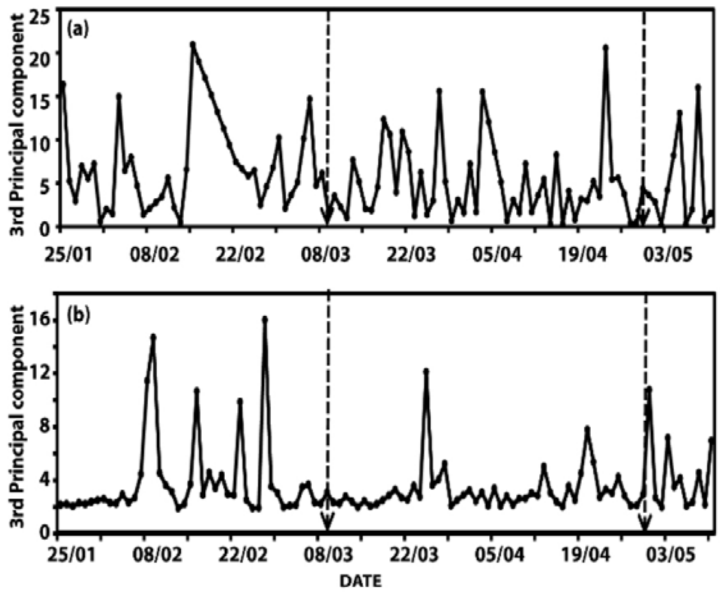

Figure 5. 3rd Principal Component Analysis of (a) Desalpar and (b) Badargadh.

Variation of difference of Total Magnetic Field of two stations

The main sources of Total Magnetic field are the earth's interior, localised stresses, currents in the ionosphere, magnetosphere and geomagnetic storms. It is essential to remove the effect of external sources from local stresses. So that we can retain the noise free signal and easily correlate with earthquakes. We first assume that the effect of external causes are similar to both the stations and therefore the difference between them will be free from the external effects. Figure 4 shows the differenced time series of TMF during 25Jan-10May 2014 of the two stations Badargadh and Desalpar. In order to see the trend, 10 days running mean is shown as dashed line in Figure 4. Many researchers reported that the differenced signal has shown anomalies in the form of offsets before earthquakes (Shapiro and Abdullabekov, 1982; Johnston and Mueller, 1987; Mueller and Johnston, 1990). In our case, the offset started on 25th February before 9th March event and on 5th April before 29th April event. The time series of differenced signal during these periods have shown linearly increasing trend with a rate of 1.04 nT/day for 9th March event and 0.41 nT/day for 29th April event.

Variations of 3rd Principal Component

We performed 3rd Principal component analysis on the time series of Total Magnetic Field data of Badargadh and Desalpar during 25th Jan-10th May 2014. The results of the 3rd PCA are shown as Figure 5.The peaks in 3rd principle component are observed on Feb 3, 15 and March 1 at Desalpar station and similar peaks on Feb 9, 16, 23 and 27are observed at Badargadh station before 9th March event. Eigen value increases from 3.5 on 1st March onwards to 16.67 on 7th March which is showing an enhancement of 88.68% in PCA signal at Desalpar. A sharp peak from 2 nT to 15 nT was observed on 1st March at Badargadh station. Similarly, we observed peaks on April 23 and April 20 before 29th April event with an increase of eigen values to 20.54 which is showing an enhancement of 78.67%.

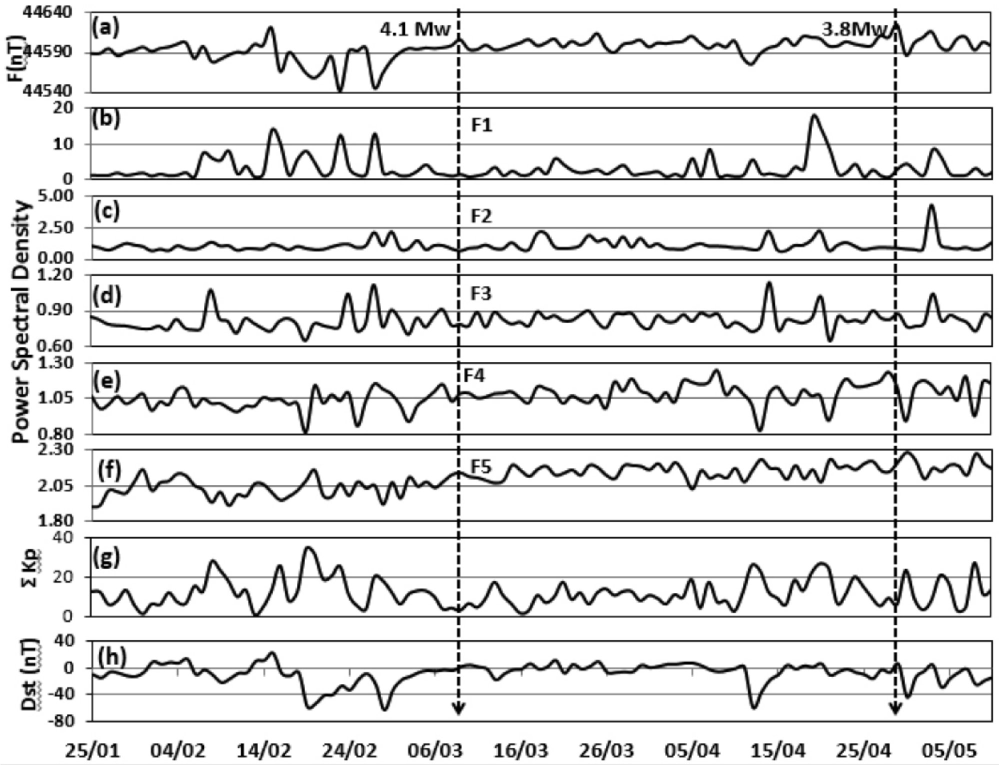

Figure 6. (a) night time (18-21UT) average value variations of total magnetic field (F) at Badargadh;(b-f) are PSD variations in five frequency bands f1-f5; (g) & (h) global kp sum & Dst values.

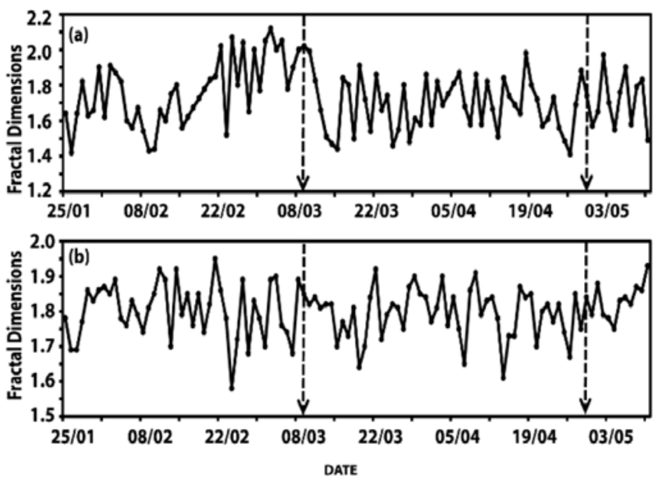

Figure 7. Fractal Dimensions of (a) Desalpar site (b) Badargadh site.

Variations in Power Spectral Density (PSD)

Power Spectral Density (PSD) is the frequency response of a random or periodic signal. The PSD analysis has been carried out in five frequency bands as f1(0.001-0.005Hz), f2(0.005-0.01Hz), f3(0.01-0.05Hz), f4(0.05-0.1Hz) and f5(0.1-0.5Hz) on TMF time series of both Badargadh and Desalpar. In Figure 6, Panel b-d shows the response of the frequencies (0.001-0.05 Hz). These frequencies responded more than other frequency ranges as shown in panel e-f in the frequency range 0.05-0.5 Hz. Hayakawa et al., (1996) have also reported the frequency band 0.005-0.01 is more responsive to seismogenic signal. There are few peaks in 20-25 February and 1-3 March before 9th March event.

There is a rise in Kp values during 20-25 February and we may relate the rise of PSD values during this period to global geomagnetic effects. The Kp values are quite normal during the time of 9th March event and the peaks during 1-3 March may be correlated with local earthquake activity. The Kp values during the 29th April event are high and the peaks observed in PSD around this time cannot be attributed to local earthquake activity. A rise of 40- 50% of the signal has been observed before the seismogenic effects. Similarly, 50-65% rise of the PSD values are observed before global geomagnetic effects. We can clearly see the distinct increase of signal in response to both global geomagnetic effects and local earthquake effects.

Variations of Fractal Dimensions

We calculated the fractal dimensions of TMF time series of both Badargadh and Desalpar observatories during 25th January - 10th May 2014using Berry's method and the same are shown in Figure 7. The fractal dimension D fluctuates from 1.4 - 2.1 at both the observatories. It increases gradually from 22nd February to reach a maximum of 2.1 just before 9th March event. Fractal dimensional values have shown good one –to –one variance with geomagnetic disturbance regime and seismogenic regime especially few days before 9th March earthquake. There is no prominent change in fractal dimensions observed during the time of 29th April event. An increase in the fractal dimension before earthquakes is widely reported in literature (Hayakawa et al., 1999; Rawat, 2014).

CONCLUSIONS

Two small magnitude earthquakes occurred on 9th March 2014 (Mw 4.1, R=58 km) and 29th April 2014 (Mw 3.8, R=43 km) and located near to Multi Parametric Geophysical Observatories (MPGO) of ISR at Badargadh and Desalpar in Kachchh region, Gujarat are studied. These two earthquakes are within the preparatory zone. The planetary index (Kp) and Dst are also analyzed in the corresponding period. These parameters are found to be normal during 9th March event and relatively high during 29th April event. An enhancement of 10 nT for 9th March event and 30 nT for 29th April event have been observed. The enhancement persists during the event and exponentially decreases after the event. Eigen value analysis (Principal Component Analysis) clearly showed enhancement of 88.68% in PCA signal before 9th March event and 78.67% before 29th April event. Fractal dimensions also showed 16-20% rise before 9th March event. Power Spectral Densities (PSD) in 0.001-0.05 Hz has shown good correlation with these events. The differenced signal of the total magnetic field data of Badargadh and Desalpar is enhanced exponentially prior to these events. These results facilitate us to conclude that the observed magnetic anomaly prior to 9th March event might be related to seismogenic origin. We cannot, however attribute the variations before 29th April event as seismogenic as there is high global geomagnetic influence during this period.

ACKNOWLEDGEMENT

The authors are thankful to the Director General, ISR for his encouragement, scientific support and permitting us to publish this work. Authors are thankful to Prof. B.V.S. Murty for constructive review and apt editing of the manuscript. We thank the Chief Editor for his continued support, guidance and encouragement.

Compliance with ethical Standards

The authors declare that they have no conflict of interest and adhere to copyright norms.

REFERENCES

Bak, P., Tang, C., and Wiesenfeld K., 1987. Self-organized criticality: an explanation of 1/f noise. Phys Rev Lett., v.59, pp: 381-384.

Bella, F., Biagi, P.F., Caputo, M., Cozzi, E., Della Monica, G., Ermini, A., Plastino, W., and Sgrigna, V., 1998. Field strength variations of LF radio waves prior to earthquakes in Central Italy, Phys. Earth Planet. Int., v.105, pp: 279–286.

Berry, M.V., 1979. Diffractals. J. Phys A Math Gen, v.12, pp: 781-797.

Dobrovolsky, L.R., Zubko, S.I., and Myachkin, V.I., 1979. Estimation of the size of earthquake preparation zones, Pageoph, v.117, pp: 1025-1044.

Fraser-Smith, A.C., Bernardy, A., McGill, P.R., Ladd, M.E., Helliwell, R.A., and Villard Jr., O.G, 1990. Low frequency magnetic field measurements near the epicenter of the Loma-Prieta earthquake, Geophys. Res. Lett., v.17, pp: 1465–1468.

Hattori, K., 2004. ULF Geomagnetic changes associated with large earthquakes. Terr. Atmo. Ocean Sci., v.15, pp: 329–360.

Hattori, K., Serita, A., Yoshino, C., Hayakawa, M., and Isezaki, N., 2006. Singular spectral analysis and principal component analysis for signal discrimination of ULF geomagnetic data associated with 2000 Izu Island earthquake swarm, Phys. Chem. Earth, v.31, pp: 281–291.

Hayakawa, M., Kawate, R., Molchanov, O. A., and Yumoto, K., 1996. Results of ultra-low-frequency magnetic field measurements during the Guam earthquake of 8 August 1993, Geophys. Res. Lett., doi: 10.1029/95GL02863., v.23, pp: 241–244.

Hayakawa, M., Itoh, T., and Smirnova, N., 1999. Fractal analysis of ULF geomagnetic data associated with the Guam earthquake on 8 August 1993, Geophys. Res. Lett., v.26, pp: 2797–2800.

Hayakawa, M., and Fujinawa, Y., (Eds.), 1994. Electromagnetic Phenomena Related to Earthquake Prediction, Terra Scientific Publishing Co., Tokyo, pp: 677.

Johnston, M.J.S., and Mueller, R.J., 1987. Seismomagnetic observation during the 8 July 1986 magnitude 5.9 North Palm Springs earthquakes, Science, v.237, pp: 1201–1203.

Merzer, M., and Klemperer, S.L., 1997. Modeling low-frequency magnetic-field precursor to the Loma Prieta earthquake with a precursory increase in fault-zone conductivity, Pure Appl. Geophys., v.150, pp: 217–248.

Mueller, R.J., and Johnston, M.J.S., 1990. Seismo magnetic effect generated by the October18, 1989, Ms7.1 Loma Prieta California earthquake, Geophys. Res.Lett., v.17, pp: 1231-1234.

Rawat, G., 2014. Characteristic ULF band magnetic field variations at MPGO, Ghuttu for the 20 June 2011 earthquake in Garhwal Himalaya, CurrSci India., v.106, pp: 88-93.

Seokhoon, Oh., 2012. Geomagnetic variation and its relation to micro earthquakes in the seismically inactive Korean Peninsula, Geosciences Journal, March, DOI 10.1007/s12303-012-0001-z., v.16, no.1, pp: 47–58.

Shapiro, V.A., and Abdullabekov, K.N., 1982. Anomalous variations of the geomagnetic field in East Fergana - magnetic precursor of the Alay earthquake with M=7.0 (November 2, 1978), Geophys. J. R. Astron. Soc., v.68, pp: 1-5.

Received on: 19.9.16; Revised on: 17.1.17; Accepted on: 28.1.17

More Frequent Glacial Quakes on Greenland Signal Ice Retreat

Between 1993 and 2011, the annual number of earthquakes caused by gigantic blocks of ice breaking away from Greenland's glaciers has increased; further evidence of accelerating ice loss.

Since the 1990s, researchers have seen a rise in the number of glacial earthquakes emanating from Greenland’s glaciers—earthquakes that stem from massive blocks of ice calving from glacier fronts. Nearly half of the glacial earthquakes in the past quarter century occurred between 2011 and 2013, a team of researchers has now found after digging through seismic data. These earthquakes could be a signal of a warming climate’s effect on the stability of the ice sheet itself.

“The rise in glacial earthquakes is part of the larger pattern of ice loss that is happening all over the Greenland ice sheet.” “The rise in glacial earthquakes is part of the larger pattern of ice loss that is happening all over the Greenland ice sheet”. Along with recorded ice loss and melt runoff, more frequent glacial earthquakes provide “another piece of evidence that Greenland is rapidly losing ice.” said Kira Olsen, Columbia University, New York, who led the new study. (**Citation:** Wendel, J. (2017), More frequent glacial quakes on Greenland signal ice retreat, Eos,98, doi:10.1029/2017EO065855).

J. Ind. Geophys. Union (May 2017)
v.21, no.3, pp: 191-197

Meandering-braiding aspects of the middle-lower part of the Ganga River, India

Raghunath Pal
Centre for the Study of Regional Development, School of Social Science,
Jawaharlal Nehru University, New Delhi-110067, India
raghunath.geo17@gmail.com

ABSTRACT
The present study is focused on the analysis of some geometric characteristics regarding meandering and braiding of the middle-lower part of the Ganga River at different axes. The middle-lower part of the Ganga River is the study reach and it ranges from Bhagalpur to Jangipur. The methods that applied in this study are: braid-channel ratio, sinuosity index and different parameters of maximum asymmetry. The relationship between the relative bend-entry curvature or channel width ratio and relative bend curvature is very strong and positive. The relationship between bend-entry curvature and meander wavelength is positive along with the positive relationship between relative bend curvature and meander wavelength. In the study reach sinuosity ranges from 1.08 to 1.90 and braid-channel ratio ranges from 1.21 to 4.26. The sinuosity index and range of sinuosity are not very high compared to the braid-channel ratio and its range. Statistically the relation between sinuosity and the braid-channel ratio is negative but the value is not significant in the reach. Hence, the channel lies in between the sinuous-braided structure or the meander-braided structure in the study reach.

Key words: Ganga River, channel geometry, braid-channel ratio, sinuosity index, maximum asymmetry.

INTRODUCTION

While carrying out geomorphologiocal changes along big rivers researchers recreate in a geographic information system (GIS) environment using data obtained from Landsat TM/ETM+/OLI satellite images. This helps to have proper knowledge of the temporal changes in the sinuosity and braiding characteristics of the river during different periods. This further helps the right and left banks morphology of a river, the shorelines of islands and bars within the river channel automatically from the satellite images by integrating the normalized difference water index (NDWI) and modified normalized difference water index (MNDWI) (Derya Ozturk and Faik Ahmet Sesli, 2015). Due to various limitations in the present study the above technique could not be used. While admitting non utilisation of satellite imagery data and gathering information in GIS environment has lessened quality of the study the systematic data acquisition procedures used in the present study have helped in getting useful information about Ganga river dynamics. The detailed study has been carried out to bring into focus floodplain morphology dynamics, floodplain structure, channel geometry, meandering and sediment depositional characteristics of Ganga river system.

In the study of floodplain morphology dynamics, channel avulsion is a considerable complex response event, which modifies floodplain structure, channel geometry, meandering and sediment depositional characteristics of a river system (Keen-Zebert et al., 2012). To explain meandering-braiding complexities and floodplain formation a single mechanism can't be taken as perfect. In order to understand the meander character of modern channels, scientific analysis and explanation of many palaeo sequences of mud-silt-clay dominated facies is important (Keen-Zebert et al., 2012). The explanations for meandering has been done based on sedimentation in a braided (Leopold and Maddock, 1953), on autocyclic-stochastic movements (Wells and Dorr, 1987), instability of channel that is a sudden movement around a concave point (divergence point) and vertical accretion (shallow or deep inundation) including large breaches during a flood with a magnitude near to avulsion threshold (extrinsic or intrinsic) (Schumm, 1977). For the last six decades, in the tenet of fluvial geomorphology, several mathematical models have been proposed for the analysis of channel pattern especially for the identification of threshold between meandering-braided forms of a river. The channel pattern includes the empirical researches (Lane,1957) based on discharge-slope; discharge, slope and stream power based on Leopold and Wolman (1957); the physical interpretation of Begin (1981) based on flow shear stress and the physical and statistical analysis of Henderson, (1966) and Chitale (1973) based on bed material size and Leopold-Wolman analysis. Apart from these, many concepts of descriptive classification have also been proposed, mainly based on multi-channel form and sinuosity (Rust, 1978; Magdaleno and Fernández-Yust, 2011), river meandering and channel size analysis

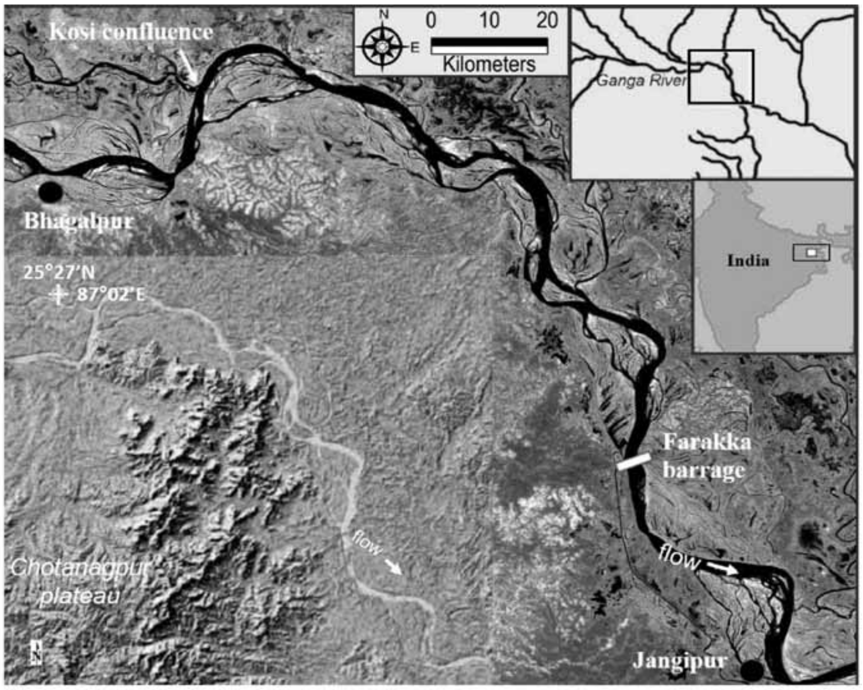

Figure 1. Location map of the study reach of the Ganga River.

(Williams, 1986). Others include channel bar forms (Brice, 1975), sedimentary controls and channel stability (Schumm, 1985) and floodplain and valley characteristics (Nanson and Croke, 1992; Alabyan and Chalov, 1998). Williams (1986) used an enlarged data set to (1) compare measured meander geometry to that predicted by the Langbein and Leopold (1966) theory, (2) examine the frequency distribution of the ratio radius of curvature/ channel width, and (3) derive 40 empirical equations (31 of which are original) involving meander and channel size features. He has further pointed out that the Langbein-Leopold sine-generated-curve theory for predicting radius of curvature agrees very well with the field data.

The study reach of the Ganga River is highly complex in terms of its meandering-braiding coexistence. A complex formation of channel meanders, channel braiding and ana -branching is a channel corridor complexity as well as a geomorphic asset. In order to demonstrate the meander-braiding complexities or single-multithread channel coexistence, it is necessary to find out the underlying causes and mechanics that shape the channels into single-multithread form (Knighton, 1998). It has been observed in the study reach, the meander portions of the channel are single thread and the braiding portions are multithread. Carson (1984) has pointed out two arguments that explain the meander-braiding complexity: i) braiding primarily depends on local shoaling of the thalweg rather than on the hydraulic threshold (e.g., stream power) and ii) it is worthless to find out a threshold for meandering and braiding. Moreover, the study by Nanson and Croke (1992) points out that the processes involved in floodplain formation range from a vast extension and diverse floodplain types. Such a range of flood plain processes support the need to building a specific model for each floodplain. The present study is mainly focused on the investigation of some geometric properties of the Ganga River at different axes in the considered reach.

Alea Yeasmin and Nazrul Islam (2011) carried out systematic studies to understand changing trend of channel pattern of the Ganges-Padma River. The study analyzes the changing trends of channel pattern of the Ganges-Padma River. A time series of satellite images in the period of 1973-2006 are compiled for analysis. It is believed that the Ganges-Padma River is a meandering river. But lately the Ganges-Padma has become a braided river due to high sediment transportation by Jamuna and deposition of Ganges-Padma River bed. For the purposes of study, the sinuosity ratio and braiding index were calculated in different time series. The analysis shows that the sinuosity ratio is increased over time. In 1973, it was 1.31 and in 1984, 1996, 2006 it was 1.33, 1.37, and 1.43, respectively. In 2006, though it was sinuous, since it is very close to 1.5 it indicates meandering. In case of braiding index, it has been observed that in 1973, the braiding index was 1.3 and in 1984, 1996, 2006 it was 1.43, 1.62, and 1.92, respectively.

I give below a detailed analysis of the study carried out by me.

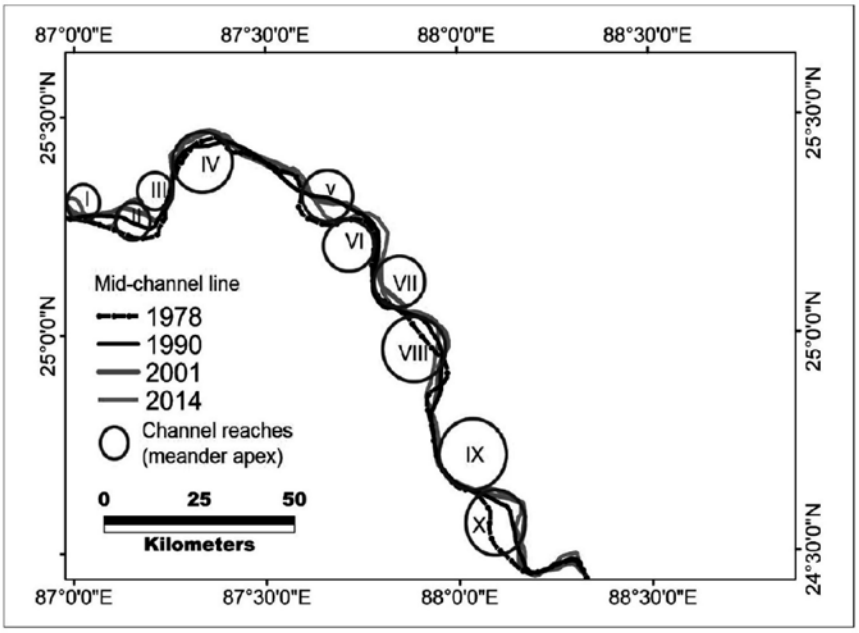

Figure 2. The position of mid-channel lines in 1978, 1990, 2001 and 2014. The circles are the meander apex or channel reaches (meandering axes).

Study Reach:

Out of ~2525 km of the flows of the river ~217 km stretch has been considered in this study. It is the middle-lower part of the river that ranges from Bhagalpur to Jangipur. The river drains up to the Kosi confluence in the north-east direction, then it flows in the east direction in Bihar. Finally, it flows in the south-east direction in West Bengal. The Ganga River bifurcates into two segments neat the edge of the Ganga-Brahmputra delta, one is the Hugly-Bhagirathi that drains in a southern direction joining the estuary of the Bay of Bengal. Another one is the Padma that drains through Bangladesh in the south-east direction to join the Brahmputra River and finally the estuary of the Bay of Bengal (Singh, 1971; Rudra 2010). The study reach is architectured by a basement high, two fault lines (the Rajmahal Fault and the Malda-Kishnaganj Fault), the Kosi confluence, the northern edge of Ganga-Brahmputra delta and Farakka barrage (Singh, 1971; Singh, 1996; Sinha and Ghosh, 2012) (Figure 1). The hydrology of the river in the study reach is extensively controlled by seasonal forces, the construction of Farakka barrage and annual-decadal flood events (Pal and Pani, 2016).

METHODOLOGY

The channel centreline of different years i.e., 1978, 1990, 2000 and 2014 has been taken into consideration to identify different axes. Landsat satellite images of the mentioned years have been used for the axis identification. Ten axes have been identified across the channel reach on the basis of Landsat images of different years (Figure 2). Figure 3 shows a detailed view of meandering geometry that has been incorporated in this study. However, following methods have been applied to explore geometric properties of the river in the study reach:

Braid-channel index (*Bfd*): The braid- channel ratio may be derived as (Friend and Sinha, 1993)

$$Bfd = L_{ctot} / L_{cmax} \qquad \text{............ (1)}$$

Where, Bfd is the braid-channel ratio, L_{ctot} is the total of the mid-channel length of all the channels in a reach and L_{cmax} is the length of the prime channel, in that reach. A high value shows multiplicity of the channel and high braidness where, a low value shows single flow of the channel.

Sinuosity index (P): It is a measure of the curvature of a channel. It can be formulated as (Friend and Sinha, 1993)

$$P = L_{cmax} / L_R \qquad \text{............ (2)}$$

Where, L_{cmax} is length of the primary channel in a reach and L_R is the straight line length of the channel for the same reach. A high value shows high meandering and a low value indicates the straightness.

Maximum asymmetry (z): It is a function of relative meander amplitude (r_e/W), relative bend-entry curvature (a/W) and inclination angle (ω). It can be defined as (Carson and Lapointe, 1983)

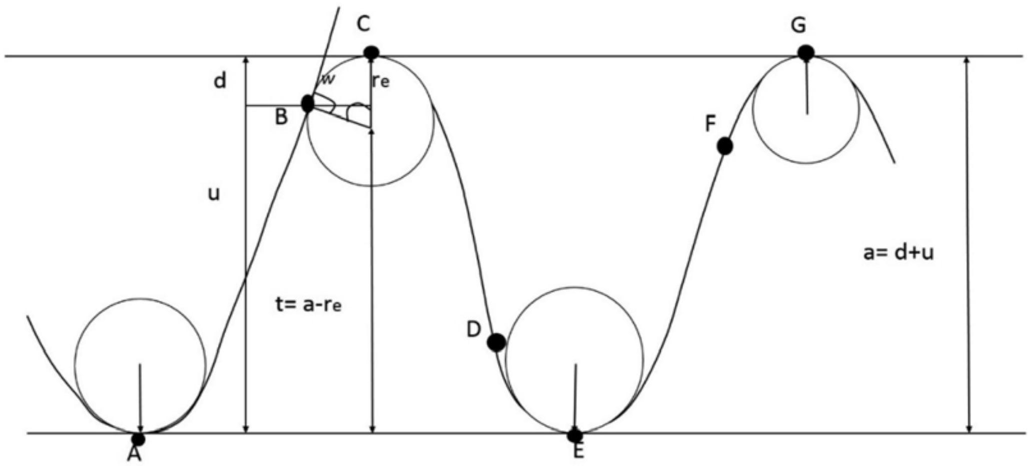

Figure 3. A view of simple geometry of meandering and its aspects (adopted from Carson and Lapointe, 1983).

$$z = 100\ (1-(r_e/a)(1-\cos\ \omega)) \quad ....\ (3)$$

Where, z is the maximum value of asymmetry or magnitude of delayed inflection asymmetry, r_e is the bend entry curvature or radius of curvature and r_e/a can be defined as

$$r_e/a\ =\ (r_e/w)\ /\ (a/w) \quad ....\ (4)$$

Where, a is the amplitude of meander trace or mean meander length and W is the channel width (Figure 3).

ANALYSES AND DISCUSSIONS:

The study reach of the river exists with a complex coexistence of the meandering-braided (expansion) and single thread forms (contraction). The channel where it meanders is also braided. The single thread portions across the reach are very small in length and most of them exist in the apex of some meanders. So, it is difficult to classify the channel into meander and braid form or a single thread. Hence, the use of discharge, slope and sediment size is not helpful to classify the channel into such forms. Figure 2 represents the position of the mid-channel lines in 1978, 1990, 2001 and 2014. The circles in the figure are the channel reaches where the channel has meandered. In the reach, there are ten meander apexes that have differences in various geomorphic characteristics.

Seven physical as well as mathematical parameters have been taken into consideration for the study: channel inflection angle (ω), meander wavelength (λ), relative meander amplitude or Channel width ratio (*a/W*), relative bend-entry curvature (*a/W*), braid-channel ratio (*Bfd*), sinuosity (*P*), maximum asymmetry or magnitude of delayed inflection asymmetry (*z*). All these factors have been measured and calculated with respect to the mid-channel lines (Figure 3 & 4).

The channel inflection angle (ω) is not same at the different meander apexes. It ranges from 40° to 110°. Apex III and IX have the highest degree of inflection viz. 110 and 105, respectively. The lowest value of channel inflection is for the axis VIII. Table 1 indicates that meander wavelength of the meander apex has also varied. It is maximum for the axis VIII (46.5) and minimum for III (11.2 km). The wavelength is lowest in the case of the axis III, because of the sudden change in the flow of the river in the north-east direction near Kahalgaon. It is so, as even at the axis III the maximum inflection angle exists (Figure 2). However, there exists no relationship between the inflection angles and the meander wavelengths. The relationship between the relative bend- entry curvature or channel width ratio (*a/W*) and relative bend curvature (r_e/W) is very strong and positive (R^2=0.9323) (Figure 4).

The relationship between bend-entry curvature and meander wavelength is positive along with the positive relationship between relative bend curvature and meander wavelength (Figure 4). All z-values indicate whether the traverses are convex (>55) or concave (< 45), down-valley structure (Carson and Lapointe, 1983). The value in between 45 and 55 indicates more or less the symmetric form of the traverse. The meander apex III, VII and IX have experienced convex-down-valley form and I, IV, V, VI, VIII and X have concave down-valley form. Only meander apex II has a little symmetric form of the traverse. Thus about 50% of the channel reaches is under the concave down-valley traverse.

The braid-channel ratio and the channel sinuosity index are probably the most important factors for the analysis and understanding of river morphology especially for meandering-braided channels. The study reach is highly complex in the context of the formation of meander and braid. The analysis suggests that the study reach planform does not maintain the conventional rules of the channel pattern classification proposed by Leopold and Wolman,

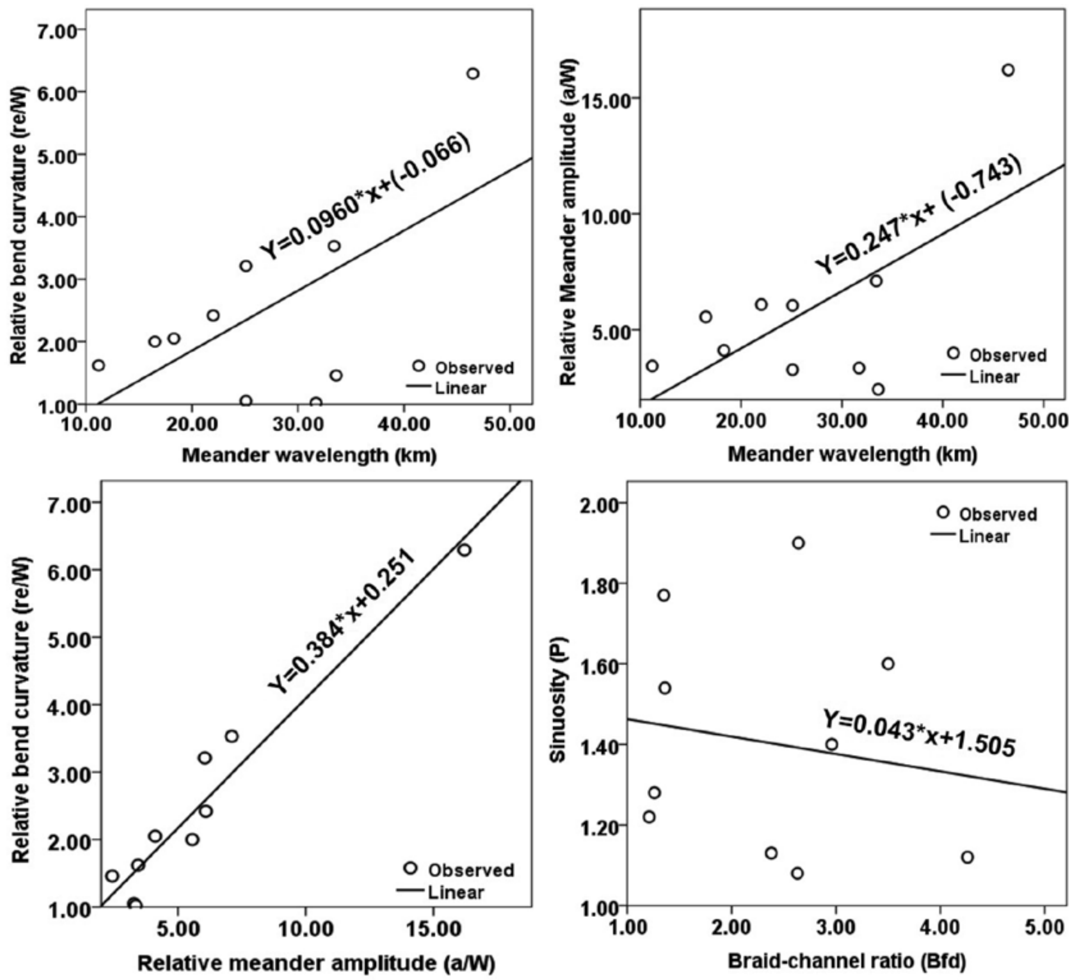

Figure 4. The four graphs indicate the linear relationships between a couple of variables viz. relative bend curvature and meander wavelength, relative meander amplitude and meander wavelength, relative bend curvature and relative meander amplitude & sinuosity and braid-channel ratio.

(1957).Visually it can easily be observed that the channel trough is tortuous and continuously flowing in a wave style. In the study reach, the channel's source is at Bhagalpur, where the trough is too broad because of point bars and channel bars. Then the channel trough narrows and becomes a single thread near Kahalgaon. After that the channel again becomes multi-threaded near Barari and maintains that pattern even beyond. There are six locations in the channel reach where the channel becomes multi-threaded. In between each two multi- threaded formations one can notice formation of a single thread. The study reach of the channel experiences meandering structure along with the single and multi-thread structure. It is mentioned earlier that significantly wherever the channel is braided the channel also meanders. The average sinuosity of the study reach is 1.48.The value is near to the threshold value of meandering (1.50 and more). In the study reach sinuosity ranges from 1.08 to 1.90 and braid-channel ratio ranges from 1.21 to 4.26. Hence, the channel in the study reach somewhere lies in between the sinuous-braided structure and the meander-braided structure. The apex III, IV, VIII, IX and X have both high channel sinuosity index and high braid-channel ratio. Another aspect is that both the sinuosity index and range of sinuosity are not very high compared to the braid-channel ratio and its range.

The result of planform geometry analysis of the study reach especially, the sinuosity index and braid channel ratio has a different scenario compared to earlier studies. The reason is that most of the former studies were based on temperate small to medium size rivers and the theories were largely developed based on the rivers with the temperate climatic condition. Hence, there is a huge difference in planform geometry of large tropical rivers and temperate rivers. In this study, statistically the relation between sinuosity and the braid-channel ratio is negative. However, the value is not significant (R^2=0.0249) (Figure 2). The planform structure of the rivers is controlled by many factors viz., underlying structural duality (the southern cratonic hard mass and the northern alluvial succession), discharge variability due to high seasonality in rainfall, yearly effect of flood events of different magnitude. This in turn makes the difference between the present study sinuosity index and braid-channel ratio theoretically approximate. The straightening in between the IX and X is due to the channel existence at the edge of Rajmahal Plateau on the right bank, the embankment construction near Farakka and the structural control on the channel trough due to two underlying faults of significant nature (the Rajmahal Fault and the Malda-Kishnaganj Fault) from Rajmahal to Jangipur. The other straight portion of the channel that lies in between the apex IV and V is probably controlled by underlying cratonic basement high that helps the channel to flow in the north-east direction.

CONCLUSIONS

There are numerous new models to explore the geometry of a channel; one or two dimensional models. But, it is difficult to fit either one or two dimensional models in case of large tropical rivers like Ganga because of its meander-braiding complexities. The study reach is highly ambiguous in terms of its meander-braiding pattern, which is shaped by underlying litho-structure, discharge variability and the construction of Farakka barrage. Present study is an attempt to understand the structural form of the channel in the reach with the help of some conventional methods that have been used herein. However, in order to explore the geometric properties of large tropical rivers, more scientific inquiries are needed. As significant monsoon variability is noticed due to global warming related ill effects, it is essential to monitor the entire stretch of Ganga River to take remedial measures to lessen any ill effects due to significant changes in the river morphology. Any artificial or natural obstructions along and across the river could result in flash floods affecting large number of villages and towns existing near the river banks.

ACKNOWLEDGEMENTS

The author would like to acknowledge the financial assistance received from the University Grants Commission (UGC), India. I am thankful to the anonymous reviewer for useful suggestions. I am grateful to the Chief Editor for significant suggestions, while carrying out final editing. This has helped in enhancing the quality of the manuscript.

Compliance with Ethical Standards

The author declare that he has no conflict of interest and adhere to copyright norms.

REFERENCES

Alabyan, A.M., and Chalov, R.S., 1998. Types of river channel patterns and their natural controls.Earth Surface Processes and Landforms, v.23, pp: 467-474.

Alea Yeasmin and Nazrul Islam., 2011. Changing trends of channel pattern of the Ganges-Padma river, M, Department of Geography and Environment, Jahangirnagar University, Dhaka, Bangladesh International Journal of Geomatics and Geosciences., v.2, no.2

Begin, Z., 1981. The relationship between flow shear stress and stream pattern. Journal of Hydrology, v.52, pp: 307-319.

Brice, J., 1975. Air photo interpretation of the form and behavior of alluvial rivers. st. Louis, MO: Final Report U.S. Army Research Office.

Carson, M., 1984. The meandering-braided river threshold: a reappraisal. Journal of Hydrology, v.73, pp: 315-334.

Carson, M., and Lapointe, M., 1983. The inherent asymmetry of river meander planform . Journal of geology, v.91, pp: 41-55.

Chitale, S., 1973. Theories and relationship of river channel patterns. Journal of Hydrology, v.19, pp: 285-308.

Derya Ozturk and Faik Ahmet Sesli., 2015. Determination of Temporal Changes in the Sinuosity and Braiding Characteristic of the Kizilirmak River, Turkey., Pol. J. Environ. Stud. v.24, no.5, pp: 2095-2112.

Friend, P.F., and Sinha, R., 1993. Braiding and meandering parameters. Geological Society Special Publication, v.75, pp: 105-111.

Henderson, F., 1966. Open Channel Flow. New York: Macmillan.

Keen-Zebert, A., Tooth, S., Rodnight, H., Duller, G.A., Roberts, H.M., and Grenfell, M., 2012. Late Quaternary Floodplain Reworking and the Preservation of Alluvial Floodplain Sedimentary Archavies in Confined and Unconfined River Valley in Eastern Interior of South Africa. Geomorphology, pp: 54-66.

Knighton, D., 1998. Fluvial Forms And Processes (1st ed.). New York: Arnold.

Lane, E., 1957. A study of the shape channels formed by natural streams flowing in erodible material. Omaha,NB: U.S. Army Eng. Division.

Langbein, W.B., and Leopold, L.B., 1966. River Meanders Theory of Minimum Variance. United States Government Printing Office, Washington, DC: U.S. Geological Survey.

Leopold, L.B., and Maddock, T., 1953. The hydraulic geometry of stream channels and some physiographic implications. United States Department of the Interior, pp: 1-57.

Leopold, L., and Wolman, M., 1957. River channels patterns: Braided, Meandering and straight. Washington, DC: U.S. Geological Survey.

Magdaleno, F., and Fernández-Yust, J., 2011. Meander dynamics in a changing river corridor. Geomorphology, pp: 197-207.

Nanson, G.C., and Croke, J.C., 1992. A genetic classification of floodplain. Geomorphology, v.4, pp: 459-486.

Pal, R., and Pani, P., 2016. Seasonality, barrage (Farakka) regulated hydrology and flood scenarios of the Ganga River: a study based on MNDWI and simple Gumbel model. Modeling Earth Systems and Environment, v.2, no.2, pp: 1-11.

Rudra, K., 2010. Banglar Nadikatha (Bengali). Kolkata: Sahitya Sanshad.

Rust, B. R., 1978. Depositional models for braided alluvium. In A. Miall (Ed.), Fluvial Sedimentology Alberta: Canadian Society of Petroleum Geologists., pp: 605-625.

Schumm, S., 1985. Patterns of alluvial rivers. Annual Review of Earth and Planetary Sciences, v.13, pp: 5-27.

Schumm, S.A., 1977. The fluvial system. New York: Wiley.

Singh, I.B., 1996. Geological Evolution of Ganga Plain- an overview. Journal of Palaeontological Society of India, v.41, pp: 99-137.

Singh, R., 1971. India: A Regional Geography. Varanasi: National Geographical Society of India.

Sinha, R., and Ghosh, S., 2012. Understanding dynamics of large rivers aided by satellite remote sensing: a case study from Lower Ganga plains, India. Geocarto International, pp: 207-219.

Wells, N.A., and Dorr, J.A., 1987. Shifting of Kosi River, northern India. Geology, v.15, no.3, pp: 204-207.

Williams, G.P., 1986. River meandering and channel size. Journal of Hydrology, v.88, pp: 147-164.

Received on: 2.9.16; Revised on: 13.1.17; Re-revised on: 5.3.17; Accepted on: 6.3.17

"It's coming home to roost over the next 50 years or so. It's not just climate change; it's sheer space, places to grow food for this enormous horde. Either we limit our population growth or the natural world will do it for us, and the natural world is doing it for us right now."

David Attenborough

(**Source:** https://www.brainyquote.com/quotes/keywords/climate_change.html)

J. Ind. Geophys. Union (May 2017)
v.21, no.3, pp: 198-206

Lutetium-Hafnium isotope evidence for the cogenesis of Neoarchean Veligallu and Gadwal greenstone belts, eastern Dharwar craton, India

Tarun C. Khanna
CSIR – National Geophysical Research Institute, Hyderabad-500 007, India
khannangri@ngri.res.in

**This research contribution is dedicated to the memory of Dr. Sayed Mahmood Naqvi (S.M. Naqvi). Dr. Naqvi was the proponent of geochemistry in NGRI, who has contributed immensely to the existing knowledge in the field of Archean geodynamics of the Dharwar craton, till his last breath on 4th September 2009. He is an everlasting source of inspiration to me.*

ABSTRACT
This research contribution elucidates the genetic link between the Veligallu and Gadwal greenstone belts that are located to the south and north respectively, of the Proterozoic Cuddapah basin in Eastern Dharwar Craton, India. The metavolcanic sequences in both these Neoarchean belts are characterised by an identical initial isotopic composition. Recent study indicates field and petrological similarities, identical nature of magmatism and most significantly, the corresponding metavolcanic rocks from these two belts relate to the same initial $^{176}Hf/^{177}Hf$ isotope composition. Therefore, it is inferred that these two greenstone terranes form part of a linear N-S trending Neoarchaean arc system, which is extensively obscured by the sedimentary cover of the Proterozoic Cuddapah basin, subsequent to post-accretionary geodynamic processes in the eastern Dharwar craton, India.

Key words: Lutetium-Hafnium, Veligallu, Gadwal, Greenstone belt, Dharwar craton, India.

INTRODUCTION

Lutetium-Hafnium isotope studies of juvenile magmatic rocks, in the recent past, have provided important constraints on the nature of magmatism and crustal growth processes in the Precambrian volcanic terranes (e.g. Blichert-Toft and Arndt, 1999; Polat and Munker, 2004; Hoffmann et al., 2010; Khanna et al., 2014). Unlike the Sm-Nd isotopic system, which is otherwise a very sensitive indicator of crustal recycling or assimilation during magmatic emplacement and post magmatic metamorphic processes that may cause ambiguity in the initial $^{143}Nd/^{144}Nd$ isotopic composition of the analysed bulk-rock samples, Vervoort and Blichert-Toft (1999) have evidently shown that the Lu-Hf isotope system is extremely robust and unperturbedly preserves the record of initial isotopic composition, even when the rocks are intensely deformed and metamorphosed under amphibolite facie conditions.

Khanna et al., (2014), presented the combined Hf-Nd isotope determinations in the bulk-rock metavolcanic samples from Gadwal greenstone belt. Recently, Khanna et al., (2016a) have presented the Lu-Hf isotope systematics of the metavolcanic rocks from the Veligallu greenstone belt.

The data has been compiled from the above published work and shown in Table 1. A comparative re-examination of the Lu-Hf isotope systematics for the corresponding metavolcanic rocks from these two belts has presented an important revelation. Through a revisit of these two greenstone belts from an isotopic perspective, I present the initial $^{176}Hf/^{177}Hf$ isotope composition for the corresponding metavolcanic sequences in these greenstone belts and thus, propose their evolution from a common mantle source at ~2.7 Ga.

For a detailed account of the geology, geochemistry, petrogenesis, and isotopic aspects of the Veligallu and Gadwal greenstone belts the reader is referred to Srinivasan (1990); Manikyamba et al., (2005, 2007); Manikyamba and Khanna (2007); Khanna (2007, 2013); Khanna et al., (2014, 2015, 2016a).

Regional Geology

The Dharwar proto-continent is subdivided into three distinct cratonic blocks: the western Dharwar craton, the eastern Dharwar craton, and the southern granulite terrane (Swami Nath and Ramakrishnan, 1981). The NNW-SSE trending shear zone extending along the eastern margin of the Chitradurga greenstone belt (Naqvi and Rogers, 1987) is considered as a marker that separates the eastern and western blocks. The western and eastern blocks of the Dharwar craton comprise laterally extensive and linearly arcuate Mesoarchean and Neoarchean greenstone terranes surrounded by younger granitoids. Basically, the greenstone belts located in the eastern Dharwar craton (EDC) are comparatively linear in appearance, mostly

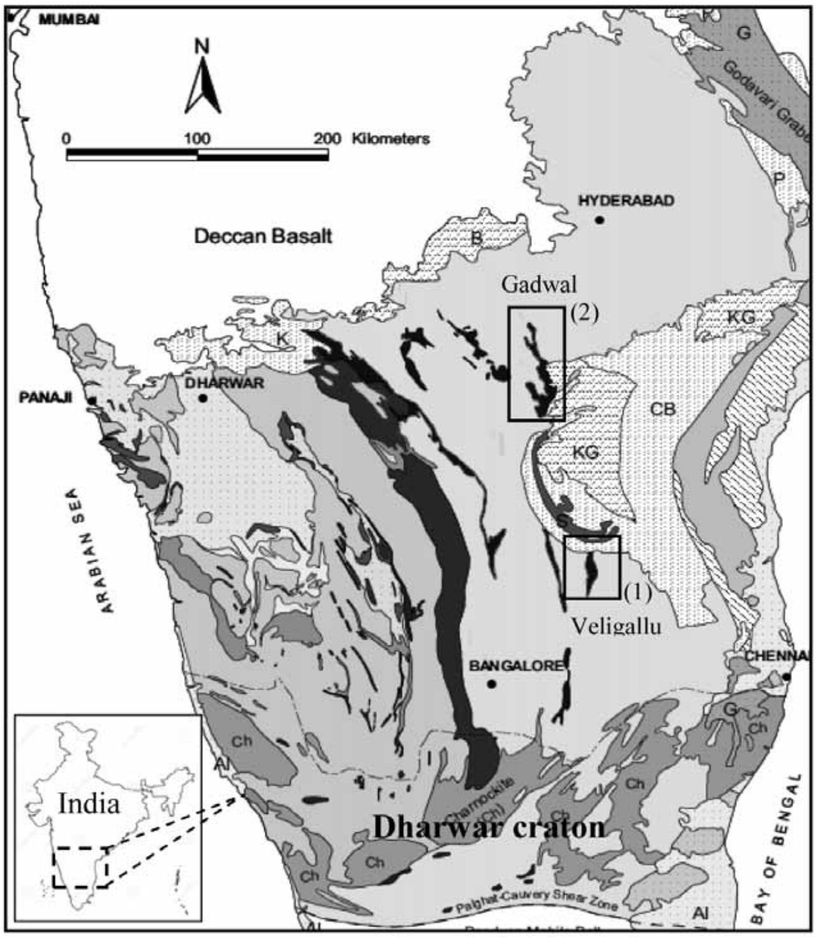

Figure 1. Generalized geological map of Dharwar craton, adapted from project Vasundhara of Geological Survey of India Records, 1994. Gadwal and Veligallu greenstone belts are also labeled and highlighted in rectangular boxes.

characterized by a north–south disposition, which are predominantly composed of metavolcanic rocks and minor metasedimentary components. The focus of this study are the Veligallu and Gadwal greenstone belts that are located on the southern and northern margins of the Proterozoic Cuddapah basin (Nagaraja Rao et al., 1987), in EDC, India (Figure 1).

The Veligallu greenstone belt (Figure 1) broadly exhibits N-S trend with an approximate strike length of ~ 60 km, and a maximum width of ~ 6 km in the central part (Srinivasan, 1990). The volcano-sedimentary sequence was subjected to greenschist to lower amphibolite grade metamorphism. The metamorphism of the volcanic units is presumed to be synchronous with the first generation (F1) folds preserved in the rocks (Ramam and Murty, 1997). The metavolcanic lithologies in the Veligallu belt are constituted of boninite-type ultramafics, basalt, high Mg-andesite and adakite suite of rocks that are associated with banded iron formations (BIFs) and metasediments (Khanna et al., 2015). The metaultramafic igneous rocks with distinctive boninite-like geochemical attributes, occur as discontinuously interlayered conformable bands paralleling the mafic volcanic rocks in the Veligallu belt. The metavolcanic rocks in the Veligallu belt yielded a Lu-Hf isochron age of 2696 ± 54 Ma (Khanna et al., 2016a).

The Gadwal belt (Figure 1) follows N–S trend in the southern part and NNW-SSE in the north, imparting an arcuate shape. The belt has an approximate strike length of ~ 90 km with a maximum width of ~ 5 km, as observed in the central part (Srinivasan, 1990). The rocks have been metamorphosed under greenschist to lower amphibolite facies conditions. The north-central part of the belt is composed primarily of basalts of both tholeiitic and calc-alkaline affinity (Khanna, 2013), and a geochemically distinctive group of boninitic rocks (Manikyamba et al., 2005). Dacites and rhyolites are also present in the north-central parts of the belt. Some of these felsic rocks are characterized by Phanerozoic adakite-like geochemical attributes (Manikyamba et al., 2007).The metavolcanic rocks in the Gadwal belt yielded identical Lu-Hf and Sm-Nd ages of 2700 ± 24 Ma and 2701 ± 28 Ma, respectively (Khanna et al., 2014).

Table 1. Bulk-rock Lu-HF isotope data for the corresponding metavolcanics in the Veligallu and Gadwal schist belts, eastern Dharwar craton, India.

Location / rock type	Sample No.	$^{176}Lu/^{177}Hf$	$^{176}Hf/^{177}Hf$ (± 2σ)
Veligallu			
basalt	TVK-67	0.0516	0.283870 ± 08
	TVK-68	0.0426	0.283435 ± 10
	TVK-72	0.0431	0.283423 ± 13
	TVK-74	0.0318	0.282865 ± 08
	TVK-77	0.0357	0.283047 ± 12
	TVK-81	0.0381	0.283192 ± 05
	TVK-87	0.0420	0.283398 ± 07
	TVK-137	0.0275	0.282580 ± 06
	TVK-155	0.0604	0.284252 ± 15
	TVK-156	0.0422	0.283328 ± 14
boninitic rocks	TVKR-2	0.0287	0.282679 ± 07
	TVKR-4	0.0356	0.283022 ± 14
	TVKR-12	0.0323	0.282814 ± 09
	TVKR-17	0.0345	0.282989 ± 06
	TVKR-20	0.0349	0.282942 ± 10
adakitic rocks	TVK-46	0.0029	0.281318 ± 08
	TVK-47	0.0024	0.281323 ± 04
	TVK-78	0.0024	0.281314 ± 05
Gadwal			
basalt	G-38	0.0273	0.282639 ± 06
	GWL-48	0.0292	0.282835 ± 06
	G-46	0.0356	0.283010 ± 05
	G-58	0.0325	0.282874 ± 05
	G-33	0.0284	0.282665 ± 06
	G-35	0.0298	0.282771 ± 08
boninitic rocks	TCK-35	0.1100	0.286863 ± 10
	TCK-36	0.1126	0.287112 ± 08
	TCK-40	0.1240	0.287505 ± 13
	TCK-43	0.1098	0.286957 ± 08
	TCK-44	0.0973	0.286207 ± 12
	G-21	0.0414	0.283345 ± 08
	G-22	0.0597	0.284277 ± 06
	G-23	0.0521	0.283842 ± 08
adakitic rocks	G-69	0.0068	0.281521 ± 04
	G-72	0.0054	0.281433 ± 04

Analytical Techniques

For bulk-rock geochemistry and Lu-Hf isotopes, the rocks were powdered manually using an agate mortar and pestle. An aliquot of the same sample was used for major and trace element analysis at CSIR – National Geophysical Research Institute, India. The major element oxides were analyzed using pressed powder pellets, on a Philips MagiX PRO PW2440; microprocessor controlled, wavelength dispersive sequential XRF. The relative standard deviation for the major element oxides is < 3% (Krishna et al., 2007; 2016). For the determination of trace elements including large ion lithophile elements (LILE), high field strength elements (HFSE) and rare earth elements (REE), 50 mg of finely ground sample powder was digested in a freshly prepared mixture of ultrapure grade acids (HF +HNO_3) taken in 3:1 ratio in screw top Teflon "Savillex" vessels, and heated on a hot plate at 160°C. The samples were analyzed by high resolution inductively coupled plasma mass spectrometry (HR-ICP-MS; Nu Instruments Attom®, UK). The detailed procedures relating to sample dissolution, analytical methodology and instrument parameters are described in Khanna et al., (2016b).

Lutetium and Hf concentrations and Hf isotopes were determined for a total number of 34 metavolcanic rock samples consisting of a combined subset of 13 boninitic rocks [$8_{(Gadwal)}$ + $5_{(Veligallu)}$], 16 basalts [$6_{(Gadwal)}$ + $10_{(Veligallu)}$] and 5 adakites [$2_{(Gadwal)}$ + $3_{(Veligallu)}$] (Table 1), at the Center for Elemental Mass Spectrometry (CEMS), Department of Earth and Ocean Sciences, University of South Carolina, USA. A detailed description of the analytical methodology is given in Khanna et al., (2014, 2016a). In summary,

Table 2. Comparisons between the ~2.7 Ga Veligallu and Gadwal greenstone belts, eastern Dharwar craton (EDC), India.

S. No.	Qualified component	Veligallu greenstone belt	Reference	Gadwal greenstone belt	Reference
1.	Location	South of Cuddapah Basin, eastern Dharwar craton	Srinivasan (1990)	North of Cuddapah Basin, eastern Dharwar craton	Srinivasan (1990)
2.	Structural disposition	North-South	Srinivasan (1990)	North-South	Srinivasan (1990)
3.	Deformation	3 generation folds (F1, F2 and F3)	Srinivasan (1990); Ramam and Murty (1997)	3 generation folds (F1, F2 and F3)	Srinivasan (1990); Ramam and Murty (1997)
4.	Metamorphic grade	Greenschist to amphibolite facies	Srinivasan (1990)	Greenschist to amphibolite facies	Srinivasan (1990)
5.	Foliation	NNE-SSW, sub-vertical foliation	Srinivasan (1990)	NNW-SSE, sub-vertical foliation	Srinivasan (1990)
6.	Volcanic units	Ultramafic (boninitic); Basalt – high-Mg-andesite – adakite	Khanna et al., (2015; 2016a)	Boninite-adakite; Basalt-andesite-rhyolite	Manikyamba et al., (2005, 2007); Manikyamba and Khanna (2007); Khanna (2007; 2013)
7.	Sedimentary units	Banded Iron Formations (prominent ridges); chromian muscovite quartzite*	Srinivasan (1990); Ramam and Murty (1997); *Khanna, T. C. (unpublished dataset)	Banded Iron Formation (thin lenses); devoid of clastic or non-clastic sediments.	Srinivasan (1990); Ramam and Murty (1997)
8.	Intrusive unit & age	mafic dikes, gabbro, pyroxenite, and granitoids	Srinivasan (1990); Ramam and Murty (1997)	Dolerite dikes, basaltic alkaline dikes (~2.2 Ga), and granitoids	Khanna et al., (2013; 2016b); Venkateshwarlu and Khanna (2015)
9.	Age of the schist belt & Radiometric dating method	2697 ± 5 Ma; 2696 ± 54 Ma; bulk-rock Lu-Hf.	Jayananda et al., (2013); Khanna et al., (2016a)	2586 ± 7 Ma; SIMS zircon U-Pb. 2700 ± 24 Ma, Lu-Hf; and 2701 ± 28, Sm-Nd. (bulk-rock)	Jayananda et al., (2013); Khanna et al., (2014)
10.	Nature of magmatism	Intraoceanic, subduction zone magmatism	Khanna et al., (2015);	Intraoceanic, subduction zone magmatism	Manikyamba et al., (2005, 2007); Manikyamba and Khanna (2007); Khanna (2007)
11.	Geodynamic setting & concluding evidence	Back-arc setting; Petrogenesis of basalts.	Khanna et al., (2015)	Back-arc setting; Petrogenesis of basalts.	Khanna (2013)

100–150 mg of sample powder were digested in steel jacketed Parr Teflon bombs using $HF–HNO_3$ mixtures. The samples were then picked up in 10 ml of 1 M HNO_3 to ensure a visibly clear solution. 10-15% of that solution was aliquoted quantitatively in a separate Teflon beaker and spiked with mixed ^{176}Lu-^{179}Hf tracers for parent-daughter determination by isotope dilution following the method described in Khanna et al., (2014). Hafnium isotopes as well as Hf and Lu isotope dilution ratio measurements were determined on the Thermo Finnigan NEPTUNE MC-ICP-MS with the PLUS upgrade installed. The sample solutions were introduced with a 100 ul self-aspirating Teflon nebulizer (ESI, USA) coupled to an APEX-Q (ESI, USA) system using a Jet-sampler cone and X-skimmer cone configuration. Isochrons were calculated with the ISOPLOT program (Ludwig, 2001), using the decay constants $\lambda^{176}{}_{Lu} = 1.867 \times 10^{-11}$. The initial isotope compositions were calculated using the chondritic values: $^{176}Hf/^{177}Hf = 0.282785$, $^{176}Lu/^{177}Hf = 0.0336$ (Bouvier et al., 2008).

DISCUSSION

The Veligallu and Gadwal greenstone belts predominantly constitute of metavolcanic rocks with subordinate

Table 3. Representative geochemical mean composition of the metavolcanic rocks in the Veligallu and Gadwal green stone belts, eastern Dharwar craton, India.

	Veligallu [(1)]			Gadwal [(2)]		
	basalt	boninitic rocks	adakitic rocks	basalt	boninitic rocks	adakitic rocks
SiO_2	49.41	50.23	73.04	52.69	48.74	65.64
TiO_2	1.10	0.22	0.19	0.81	0.28	0.50
Al_2O_3	12.30	5.92	14.30	13.62	10.33	14.96
Fe_2O_3	15.26	7.95	2.45	11.82	11.64	6.08
MnO	0.20	0.13	0.03	0.16	0.15	0.08
MgO	9.32	30.22	0.72	7.32	18.74	2.48
CaO	9.87	5.14	2.57	10.82	9.32	5.14
Na_2O	1.75	0.10	4.53	2.42	0.61	3.71
K_2O	0.68	0.05	2.12	0.25	0.15	1.10
P_2O_5	0.12	0.03	0.05	0.10	0.03	0.15
Mg#	55	89	36	55	77	44
Cr	197	3346	19	115	2008	15
Ni	122	802	24	107	839	6
Rb	27	2	52	15	59	58
Sr	117	7	120	180	34	259
Cs	1.4	0.2	0.6	2	7	11
Ba	124	14	306	80	39	236
Sc	42	27	3.01	29	43	9
V	332	135	0.90	186	94	128
Ta	0.19	--	0.63	--	0.05	0.68
Nb	3.03	0.89	6.22	3.19	0.79	7.27
Zr	64	21	163	59	17	153
Hf	1.76	0.61	3.73	1.70	0.44	3.40
Th	0.37	0.54	4.30	0.73	0.27	9.18
U	0.14	0.22	1.58	0.24	0.14	2.11
Y	27	7	6	26	13	15
La	4.10	1.94	18.75	5.23	2.00	25.62
Ce	10.78	4.03	32.35	12.84	4.11	46.59
Pr	1.67	0.57	3.17	1.91	0.56	4.77
Nd	8.18	2.52	11.21	8.65	2.44	18.34
Sm	2.65	0.74	1.95	2.68	0.69	3.58
Eu	0.99	0.25	0.65	0.92	0.29	1.11
Gd	3.42	0.92	1.57	3.34	1.09	2.94
Tb	0.64	0.17	0.21	0.63	0.26	0.46
Dy	4.28	1.15	0.89	4.23	1.87	2.22
Ho	0.95	0.26	0.16	0.95	0.49	0.39
Er	2.61	0.74	0.46	2.64	1.44	1.24
Tm	0.40	0.12	0.07	0.42	0.47	0.19
Yb	2.74	0.81	0.44	2.81	1.49	1.21
Lu	0.43	0.13	0.07	0.43	0.24	0.19

Data sources: (1) Khanna et al. (2015, 2016a);
(2) Manikyamba et al. (2005, 2007); Khanna (2007, 2013); Manikyamba and Khanna (2007)

metasediments (Srinivasan, 1990). Basalt-andesite-rhyolite series along with boninite-adakite geochemical variants in these Neoarchean belts indicate subduction zone magmatism (Srinivasan, 1990; Manikyamba and Khanna, 2007). Low incidence of gold mineralization has been recorded in both these Neoarchean greenstone belts of the EDC (Sesha Sai et al., 2001; Sahoo et al., 2009). Veligallu and Gadwal greenstone belts are located at the southern, and northern parts of the Cuddapah basin along its western margin, respectively (Figure 1). The following comparative aspects between the two belts reveal significant similarities. These aspects are concisely presented in Table 2, and certain subtle features are comparatively discussed below.

The basalts are tholeiitic in composition (FeO*/MgO ~ 1.46, SiO_2 ~ 51 wt. %; Miyashiro, 1974). They have a mean uniform narrow range in their SiO_2 (49 – 53 wt. %), MgO (7.3 – 9.3 wt. %), Fe_2O_3 (12 – 15 wt. %), and TiO_2 (0.81 – 1.10 wt. %), and identical Mg# (55) (Table 3). On

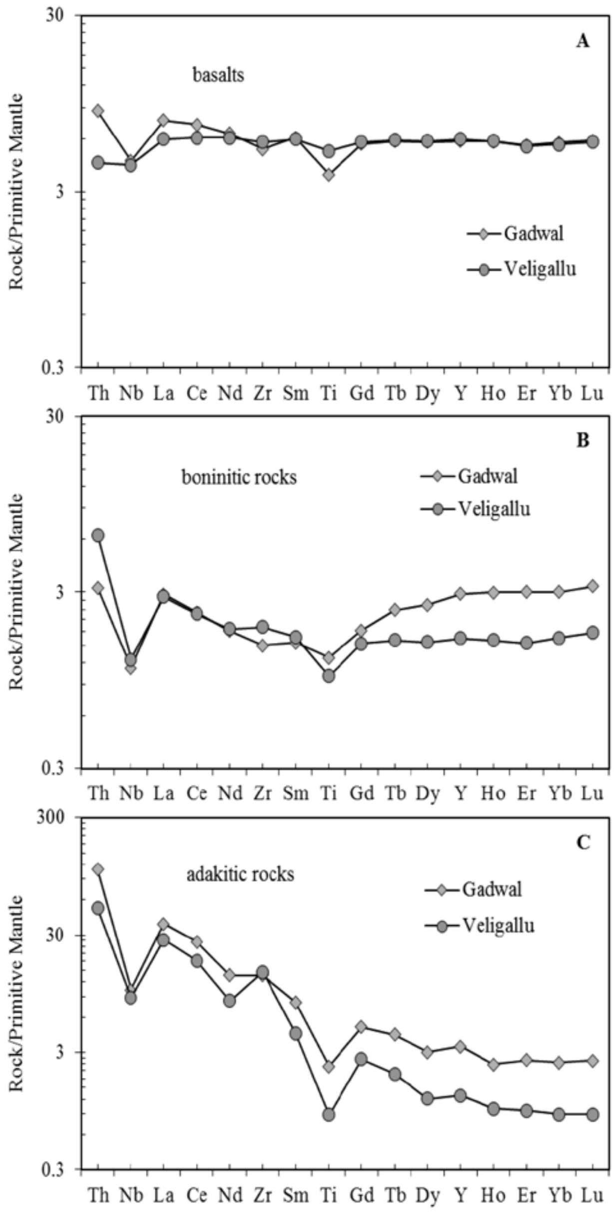

Figure 2. Primitive mantle normalized trace and rare earth element compositions of the corresponding metavolcanic rocks from the Veligallu and Gadwal greenstone belts. Normalized values are from Sun and McDonough (1989).

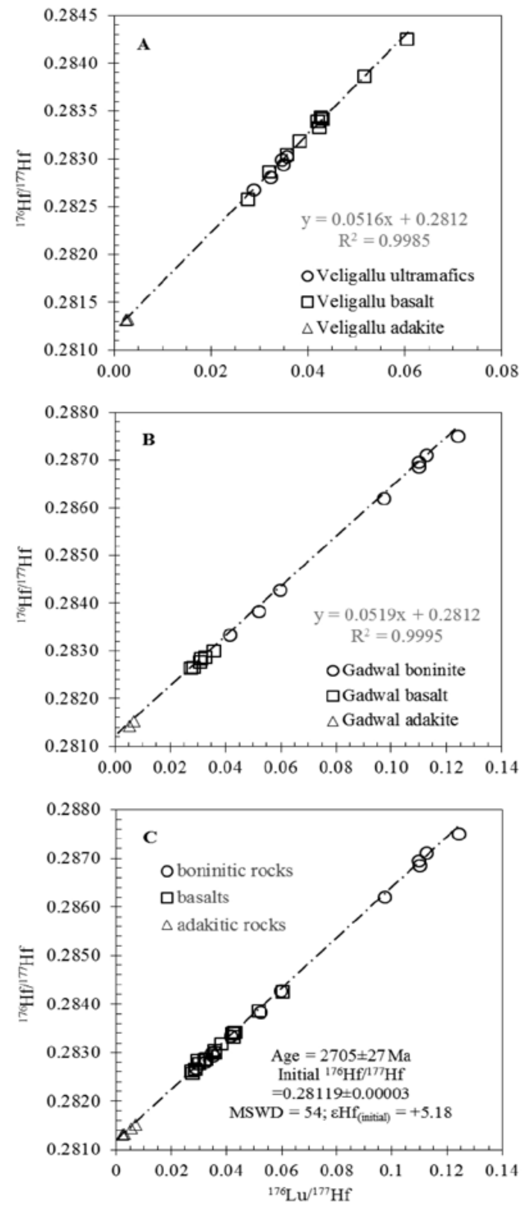

Figure 3. $^{176}Lu/^{177}Hf$ versus $^{176}Hf/^{177}Hf$ bivariate diagrams for the corresponding metavolcanic rocks in the (A) Veligallu belt, and (B) Gadwal belt. Note the identical intercept defined by these rocks. (C) Isochron derived for the entire sample population as shown in (A) and (B), and data given in Table 1.

a primitive mantle normalized trace element variation diagram (Figure 2A), the basalts, collectively as a group, display flat rare earth element patterns with negative Nb [$(Nb/La)_{pm} < 1$)] and Ti [$(Ti/Gd)_{pm} < 1$)] anomalies. To first order, except for the slight differences in the magnitude of depletion in Nb and Ti, the high field strength element abundances (Nb, Zr, Hf and Y; Table 3) and the normalized REE patterns are remarkably identical to each other.

Unlike the basalts, the boninitic rocks are characterized by a broad range in their mean geochemical compositions (Table 3). For example, the MgO contents and Mg# significantly vary from ~18 to ~30 wt. %, and 77 to 89, respectively, over a narrow range of SiO_2 = 48.7 to 50.2 wt. %. Although, they are characterized by low TiO_2 (~0.25 wt. %) with higher than chondritic Al_2O_3/TiO_2 (> 22; Sun and McDonough, 1989) ratios with identical Nb and Ti anomalies on a primitive mantle normalized trace element variation diagram (Figure 2B), the high MgO and Mg# in the Veligallu samples compared to those sampled in the Gadwal sector, suggests that the Gadwal boninitic rocks are comparatively more evolved. Conversely, the Veligallu adakitic rocks are characterized by higher contents of SiO_2 and Na_2O, and significantly lower concentrations in their TiO_2, Fe_2O_3, MgO, Mg#, Y and Yb (Table 3); and thus, on this basis appear to be relatively more evolved compared to those reported from the Gadwal sector. Accordingly, on a primitive mantle-normalized trace element variation diagram (Figure 2C) they display identical negative Nb and Ti anomalies, and contrasting positive Zr spikes.

Khanna et al., (2016a) have shown that the Veligallu basalts and the boninite-like ultramafics are cogenetic in nature, and that the ultramafics represent cumulates derived from the associated basaltic melt instantaneously after their separation from the mantle source (e.g. Szilas et al., 2015). Similar petrogenetic model is applicable for the Gadwal basalt – boninite association. In the $^{176}Lu/^{177}Hf$ versus $^{176}Hf/^{177}Hf$ bivariate diagram, the Veligallu metavolcanics describe a consistently linear trend with an intercept of 0.2812 (Figure 3A) on the y-axis. The intercept is identical to the one described by the corresponding metavolcanic rock sequence in the Gadwal sector (Figure 3B). This necessarily indicates that besides the geochemical attributes, the volcanic sequences in the two belts have the same initial isotopic composition, and hence it provides a compelling evidence for their derivation from a common mantle source. Collectively, the volcanics yield an age of 2705 ± 27 Ma with an initial $^{176}Hf/^{177}Hf = 0.28119 \pm 03$ and $\varepsilon Hf_{(i)} = +5.18$ (Figure 3C). The positive initial isotopic compositions obtained for the Veligallu – Gadwal metavolcanics is consistent with their derivation from a depleted mantle source relative to chondritic mantle at ~2.7 Ga.

CONCLUSIONS

Geochemical compositions determined for the metavolcanic rocks in the Veligallu and Gadwal greenstone belts indicate identical trace and rare earth element attributes. (2) the boninitic rocks, in these two belts, are spatially associated with the arc basalts; (3) the arc basalt and boninite-like ultramafic suite represents corresponding melt and derivative cumulate; (4) based on the trace element attributes of the corresponding basalt sequences in the individual belts, a palaeo-back arc tectonic setting has been proposed (Khanna, 2013; Khanna et al., 2015); (5) the metavolcanic sequences in the Veligallu and Gadwal belts are characterized by an identical initial $^{176}Hf/^{177}Hf$ isotopic composition, which provides a compelling evidence of cogenesis from a common mantle source; (6) therefore, it is proposed that these two greenstone belts form part of a linear N-S trending Neoarchean arc system, which is obscured by the sedimentary cover of the Proterozoic Cuddapah Basin.

ACKNOWLEDGEMENTS

I am thankful to Dr. V.M. Tiwari, Director, NGRI, for his permission to publish this work. The Department of Science and Technology, India is thankfully acknowledged for funding the projects SR/FTP/ES-7/2012, and SR/BY/A-03/09. Drs. C. Manikyamba, D.V. Subba Rao, M. Ram Mohan, A. Keshav Krishna, Gene M. Yogodzinski, and Michael Bizimis are profusely thanked for their intellectual encouragement. I am thankful to Dr. K. N. Srinivasan, and Dr. V. V. Sesha Sai for reviewing and editing the manuscript. The reviewers' suggestions enhanced the quality of the manuscript. I sincerely thank the Chief Editor for his continued support, guidance and encouragement.

Compliance with ethical Standards

The author declare that he has no conflict of interest and adhere to copyright norms.

REFERENCES

Blichert-Toft, J., and Arndt, N.T., 1999. Hf isotope compositions of Komatiites. Earth and Planetary Science Letters, v.171, pp: 439–451.

Bouvier, A., Vervoort, J.D., and Patchett, P.J., 2008. The Lu–Hf and Sm–Nd isotopic composition of CHUR: constraints from unequilibrated chondrites and implications for the bulk composition of terrestrial planets.Earthand Planetary Science Letters, v.273, pp: 48–57.

Hoffmann, E.J., Munker, C., Polat, A., Konig, S., Mezger, K., and Rosing, M.T., 2010. Highly depleted Hadean mantle reservoirs in the sources of early Archean arc-like rocks, Isua supracrustal belt, southern West Greenland. Geochimica et Cosmochimica Acta, v.74, pp: 7236–7260.

Jayananda, M., Peucat, J.-J., Chardon, D., Krishna Rao, B., Fanning, C.M., and Corfu, F., 2013. Neoarchean greenstone volcanism and continental growth, Dharwar craton, southern India: Constraints from SIMS U–Pb zircon geochronology and Nd isotopes. Precambrian Research, v.227, pp: 55–76.

Khanna, T.C., 2007. Geochemistry and tectonic setting of metavolcanic rocks of Gadwal greenstone belt [Ph.D. Thesis]: Osmania University, pp: 297.

Khanna, T.C., 2013. Geochemical evidence for a paired Arc – Back-arc association in the Neoarchean Gadwal greenstone belt, eastern Dharwar craton, India. Current Science, v.104, pp: 632–640.

Khanna, T.C., Bizimis, M., Yogodzinski, G.M., and Mallick, S., 2014. Hafnium–neodymium isotope systematics of the 2.7 Ga Gadwal greenstone terrane, Eastern Dharwar craton, India: implications for the evolution of the Archean depleted mantle.Geochimica et Cosmochimica Acta, v.127, pp: 10–24.

Khanna, T.C., Sesha Sai, V.V., Bizimis, M., and Krishna, A.K., 2015. Petrogenesis of Basalt – high-Mg Andesite – Adakite in the Neoarchean Veligallu Greenstone Terrane: Geochemical evidence for a rifted back-arc crust in the eastern Dharwar craton, India. Precambrian Research, v.258, pp: 260–277.

Khanna, T.C., Sesha Sai, V.V., Bizimis, M., and Krishna, A.K., 2016a. Petrogenesis of ultramafics in the Neoarchean Veligallu greenstone terrane, eastern Dharwar craton, India: Constraints from bulk-rock geochemistry and Lu-Hf isotopes. Precambrian Research, doi: 10.1016/j.precamres.2016.09.020.

Khanna, T.C., Babu, E.V.S.S.K., Zhao, G.C., Satyanarayanan, M., Keshav Krishna, A., and Sawant, S.S., 2016b. Geochemistry and petrogenesis of mafic alkaline dike(s) to the east of Gadwal greenstone terrane: Implications for OIB – type magmatism in parts of the eastern Dharwar craton, India. Journal of the Indian Geophysical Union, v.20, no.1, pp: 49–62.

Krishna, A.K., Murthy, N.N., and Govil, P.K., 2007. Multi-element analysis of soils by wavelength-dispersive X-ray fluorescence spectrometry. Atomic Spectroscopy, v.28, pp: 202–214.

Krishna, A.K., Khanna, T.C., and Rama Mohan, K., 2016. Rapid quantitative determination of major and trace elements in silicate rocks and soils employing fused glass discs using wavelength dispersive X-ray fluorescence spectrometry. Spectrochimica Acta Part B, v.122, pp: 165–171.

Ludwig, K., 2001. User's manual for Isoplot/Ex Version 2.49, A Geochronological toolkit for Microsoft Excel, Berkeley Geochronology Center. Spec. Publ. 1a.

Manikyamba, C., and Khanna, T.C., 2007. Crustal growth processes as illustrated by the Neoarchaean intraoceanic magmatism from Gadwal greenstone belt, Eastern Dharwar Craton, India. Gondwana Research, v.11, pp: 476–491.

Manikyamba, C., Naqvi, S.M., Subba Rao, D.V., Ram Mohan, M., Khanna, T.C., Rao, T.G., and Reddy, G.L.N., 2005. Boninites from the Neoarchaean Gadwal Greenstone belt, Eastern Dharwar Craton, India: implications for Archaean subduction processes. Earth and Planetary Science Letters, v.230, pp: 65–83.

Manikyamba, C., Kerrich, R., Khanna, T.C., and Subba Rao, D.V., 2007. Geochemistry of adakites and rhyolites from Gadwal greenstone belt, India: implications on their tectonic setting. Canadian Journal of Earth Science, v.44, pp: 1517–1535.

Nagaraja Rao, B.K., Rajurkar, S.T., Ramalingaswamy, G., and Ravindra Babu, B., 1987. Stratigraphy, structure and evolution of the Cuddapah basin. In: Radhakrishna, B.P. (Ed.), Purana Basins of Peninsular India (Middle to Late Proterozoic), Geological Society of India Memoirs, v.6, pp: 33-86.

Naqvi, S.M., and Rogers, J.G.W., 1987. Precambrian Geology of India. Oxford University Press, New York, pp: 223.

Polat, A., and Munker, C., 2004. Hf–Nd isotope evidence for contemporaneous subduction processes in the source of late Archean arc lavas from the Superior Province, Canada. Chemical Geology, v.213, pp: 403–429.

Ramam, P.K., and Murty, V.N., 1997. Geology of Andhra Pradesh. Geological Society of India publication, pp: 245.

Sahoo, P., Subba Rao, K., and Anasuya, R., 2009. Investigation for gold mineralisation in the northern part of the Veligallu greenstone belt, Chitoor district, A.P. Unpub. Prog. Rep. GSI 2004-06.

Sesha Sai, V.V., Krishan Rao, P.V., Ananda Murthy, S., Bhattacharjee, S., and Sreeramachandra Rao, K., 2001. Incidence of Gold mineralisation in Gadwal Schist Belt, Andhra Pradesh. GSI Special Publication No.58, pp: 239-243.

Srinivasan, K.N., 1990. Geology of the Veligallu and Gadwal schist belts. Geological Survey of India Records, v.5, pp: 123.

Sun, S-S., and McDonough, W.F., 1989. Chemical and isotopic systematics of oceanic basalts: implications for mantle compositions and processes. In: Saunders, A.D., Norry, M.J., (Eds.) Magmatism in Ocean Basins. Geol. Soc. [London] Sp. Pub., v.42, pp: 313–345.

Swami Nath, J., and Ramakrishnan, M., 1981. The early Precambrian supracrustals of southern Karnataka. Memoir Geological Survey of India, v.112, pp: 350.

Szilas, K., Kelemen, P.B., and Rosing, M.T., 2015. The petrogenesis of ultramafic rocks in the > 3.7 Ga Isua supracrustals belt, southern West Greenland: Geochemical evidence for two distinct magmatic cumulate trends. Gondwana research, v.28, pp: 565–580.

Venkateshwarlu, M., and Khanna, T.C., 2015. Paleomagnetism and rock magnetism of Gadwal "Dike 2", eastern Dharwar craton, India. Jour. Indian Geophys. Union, v.19, no.4, pp: 447–453.

Vervoort, J.D., and Blichert-Toft, J., 1999. Evolution of the depleted mantle: Hf isotope evidence from juvenile rocks through time. Geochimica et Cosmochimica Acta, v.63, pp: 533–556.

Received on: 29.9.16; Revised on: 16.11.16; Accepted on: 24.11.16

Yellowstone's Last Super-eruption

Geologists suggest that mixing of magma melt pockets could have caused the explosion a little more than 600,000 years ago. Yellowstone National Park is renowned for more than just its hot springs and Old Faithful. The area is famous in the volcanology community for being the site of three explosive super eruptions, the last of which was 631,000 years ago.

During that eruption, approximately 1000 cubic km of rock, dust, and volcanic ash blasted into the sky. Debris rained across the continental United States, spanning a rough triangle that stretches from today's Canadian border down to California and over to Louisiana. In places, ash reached more than a meter thick. Hannah Shamloo, and Christy Till, examined two crystals of feldspar that they found embedded in the tuff. These crystals, called phenocrysts, form as magma cools slowly beneath the volcano. Temperature information locked in a phenocryst's outer rims can be extracted using a technique called feldspar thermometry. The technique relies on the fact that certain minerals vary their compositions in known ways as temperatures change. Thus, scientists can work backward from the exact compositions of minerals present in these outer rims to estimate the surrounding temperature when the crystal rim formed. The duo found signatures in the rims that point to an increase in temperature and uptick in the element barium in the magma just before the eruption. (**Citation:** Woodward, A. (2017), Pinpointing the trigger behind Yellowstone's last supereruption, *Eos, 98,* doi:10.1029/2017EO065953.

J. Ind. Geophys. Union (May 2017)
v.21, no.3, pp: 207-213

Textural Analysis of Coastal Sands from Ramakrishna Beach - Bhimunipatnam tract (Visakhapatnam) East Coast of India

B. Suvarna[1], C. H. Posendra Mohan[2] and V. Sunitha*[1]
[1]Department of Geology, Yogi Vemana University, 516003, Kadapa A.P, India
[2]Department of Geology, Andhra University, Visakhapatnam-530003, A.P, India
*Corresponding Author: vangala_sunitha@yahoo.com

ABSTRACT
This paper presents textural analyses; study of Particle-size distribution parameters, Mean size (M_Z), Standard Deviation (σ), Skewness (Sk) and Kurtosis (K_G) pertaining to beach sands of Ramakrishna beach–Bhimunipatnam tract, East coast of Visakhapatnam, Andhra Pradesh. As part of this study, detailed textural characteristics of 23 representative samples from nine traverses of coastal sediments in different environments (Backshore, Foreshore, Dune, Berm) which lies between 17°46′-17°54′ latitudes and 83°21′-83°27′ longitudes have been carried out. By treating with sieves of different size, the samples for textural analyses have been divided into nine (18,25,35,45,60,80,120,170,230) fractions. Statistical studies indicate that the coastal sediment average values are mean size (0.55 to 2.34), Standard Deviation (0.42 to 0.99), Skewness (- 0.53 to .27) and Kurtosis (- 0.41 to 1.64). Scatter Plots are used to know the interrelation ship and geological significance of the size parameters. Frequency distribution curves and scatter plots drawn between different grain size parameters clearly establish that the nature of the sediments is dominantly unimodal of which, the dominant constituent is medium sand in various microenvironments i.e. backshore, foreshore, dune and Berm.

Key words: Textural analysis, Backshore, Foreshore, Dune, Berm, East Coast.

INTRODUCTION

Particle-size distributions (PSDs) are fundamental physical properties of soil and are typically presented as the percentage of the total dry weight of soil occupied by a given size fraction. This property is commonly used for soil classification and for the estimation of some hydraulic properties (Campbell and Shiozawa, 1992).

Grain size distribution is an important parameter that has been widely used by sedimentologists to elucidate transport dynamics. Sediment texture refers to the shape, size and three-dimensional arrangement of the particles that make up sediment. The grain size distribution is affected by the nature of source material, distance from the source and shoreline, topography and transport mechanisms and the mechanical processes involving prolonged action of the waves.

Hence, grain size analysis provides important on various sedimentological conditions (Mahadevan and Anjaneyulu, 1954; Folk and ward, 1957; Carver 1971; Friedman, 1961, 1967; Ramasastry and Myrland, 1959; Ramamohan Rao et al., 1982; Bull, 1962; Bhat et al., 2002; Jagannadha Rao and Krishna Rao,1984; Jagannadha Rao, et al., 2013; Dhanunjaya Rao et al., 1989; Reddy and Malathi 2002; Mohan and Rajamanickam, 1998; Mohan, 2000; Nageswara Rao et al., 2005; Rajesh et al., 2007; Ergine et al., 2007; Ramanathan et al., 2009; Rajasekhara Reddy and Karunakarudu, 2011; Ganesh et al., 2013; Karunakarudu et al., 2013). Further, the study of grain size characteristics are valuable to understand the source for the evolution of coastal sand environments. Role of transporting and depositional agents such as rivers, rivulets, streams, waves and currents, sea level oscillations, shoreline configuration, winds, etc. and aspects like the distance from the shoreline, distance from the source material, nature of the source material and topography of the area influence the grain size characters (Bangaku Naidu et al., 2016). Earlier, many attempts have been made by several sedimentologists (Udden, 1914; Mason and Folk, 1958; Friedman, 1961, 1967)

Sahu, 1964; Veerayya and Varadachari, 1975; Ramamohan Rao et al., 1982; Jagannadha Rao and Krishna Rao, 1984; Dhanunjaya Rao et al., 1989; Frihy et al., 1995,2002; Hanamgond and Chavidi, 1997; Mohan and Rajamanickam, 1998; Reddy and Malathi 2002; Nageswara Rao et al., 2005; Rajasekhara Reddy and Karunakarudu, 2009; Jagannadha Rao et al., 2016; examined variations in grain size characteristics of different beach environments in east coast and established the relationships between slope angle and mean grain size, for Pudimadaka and Pentakota beaches and concluded that the slope angle increases with increase in grain size. Grain size data was used to understand the micro level variations in the depositional environments along the north of Pondicherry and Ennore coasts by Mohan and Rajamanickam (1998) who concluded that the dune samples represent unimodal and others show bimodal to polymodal source of influence. Mohan, (2000) studied the Quaternary land forms to evaluate the variation

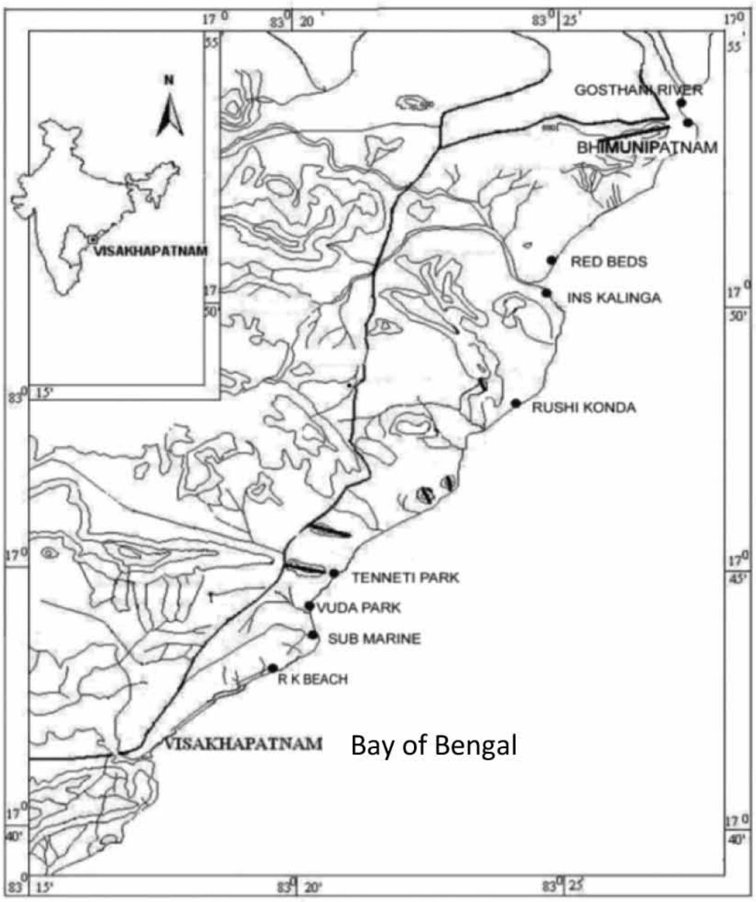

Figure 1. Sample locations of the study area Ramakrishna beach (R.K. Beach) to Bhimunipatnam.

in the distribution of grain size and depositional processes along the coastal sub-environments, along the coast between Vedaranyam and Rameshwaram, Tamil Nadu.

Mahadevan and Anjaneyulu (1954); Mahadevan and Nageswara Rao (1950) compared the grain size distribution between the beach and sand dredged sands from the entrance of the harbor channel of Visakhapatnam, east coast of Andhra Pradesh. Perhaps this was the first report of the beach sands granulometry from the Indian subcontinent. Later, Sastry et al., (1979) examined configuration changes and variation in grain size parameters to understand the erosional and depositional processes along Visakhapatnam Bhimunipatnam coast and noticed accretion from January to August and erosion during September and December. Chandramohan et al., (1981) studied the erosional and depositional environments at Visakhapatnam beach and observed erosion during South west monsoon and deposition during North East monsoon (calm weather period). The present study deals with the grain size distribution of coastal sands between Ramakrishna Beach to Bhimili confluence with an objective to understand sediment depositional environments and the depositional patterns of the sediments in the study area.

Study Area

The area under investigation lies between latitudes N 17^0 46′ and N $17^0$54′ and longitudes E 83^0 21′and E 83^0 27′ covering parts of the Survey of India toposheet No: 65 O/6. The area from Ramakrishna Beach to Bhimili is situated to the south of Visakhapatnam, Andhra Pradesh, India (Figure 1). Ramakrishna Beach-Bhimili tract appears like a Basin, and it is bounded by Kailasa, Yaradaand Narvahill ranges on North, South, West, respectively and East by Bay of Bengal. It has an undulating topography with a height of 4 to 50 m above MSL (excluding hills).

Geology and Geomorphology of the Study area

The study area is characterized by the Garnet-sillimanite biotite gneiss (khondalites), hypersthene granites (charnockite), garnetiferous granite (leptynite) of the Precambrian Eastern Ghat Granulite Belt (EGMB), Quartzite and pegmatite are other rock types that occur as bedded and banded as well as massive Formations. This area covered with denudational hills of range between 30 to 594m Kailasa and Yarada are extending nearly east to west, and thus deviate from the NE-SW trend of Eastern Ghats. The geomorphic features resulted from coastal and landward processes (Jagannadha Rao et al., 2012). The sediments are the prominent features and attain a height of 30 meters above the sea level. The drainage pattern of the study area is controlled mainly by the Gosthani River.

Materials and Methods

A total of 23 sediment samples are collected by pushing down a PVC tube (60 mm dia) along 9 Traverses from Ramakrishna Beach to Bhimili in different microenvironments, i.e. dunes, back shore, fore shore and berm. A representative portion of the sediments weighing 100 gm from the bulk sediment samples and are separated by coning and quartering procedure. 100 gm of sample is soaked in distilled water to dissolve the salts, then in H_2O_2 to remove carbonates and in HCl to remove shell material for 12 hours, respectively. After that the wet sediment is dried in oven with110^{0}c.The dry samples is placed in the uppermost sieve in a set of stacked sieves. The samples are subjected to grain size analysis by standard Ro-Tap sieve shaker at ½ Φ intervals of ASTM meshes (Hegde et al., 2006).

Sieve analysis

Sieving is commonly used in determining the grain size distribution of sand. For sieving analysis we are using ASTM (American Society of Testing Materials) meshes. The dry sample is placed in the upper most sieve in a set of stacked sieves. The stack of sieves arranged in order so that the coarsest sieve at the top with finer ones below is placed in Ro-Tap sieve shaker (the mesh numbers are 18, 25, 35, 45, 60, 80, 120, 170, 230, -230 respectively) after 10-15 minutes of shaking the sand that has collected on each sieve and the pan is removed and weighed From those we had found the weight percentage of each fraction from the sample and then cumulative weight percentage of the sample. The cumulative weight percentages were plotted on probability arithmetic graphs. Thus obtained Φ5, Φ16, Φ25, Φ50, Φ75, Φ84, Φ95 values. These values are used to compute the textural parameters like mean size (Mz), Standard Deviation (Sd), Skewness (Sk1), and Kurtosis (KG) according to the formula of Folk and Ward (1957).

RESULTS AND DISCUSSIONS

Textural Studies

The data generated from the grain size analysis data was used to compute textural parameters like graphic mean size, graphic standard deviation, graphic skewness and graphic kurtosis according to the formulae of Folk and Ward (1957), all the statistical analysis data shown in (Table1).

In Backshore environments, the standard deviation varies from (0.44Φ to 0.74Φ) with mean size (1.02Φ to 2.3Φ). The skewness and kurtosis are varies from (-0.48Φ to 0.23Φ), (0.79Φ to 1.60Φ). In Berm environment, the standard deviation varies from (0.40Φ to 0.98Φ) with mean size 1.3Φ the skewness and kurtosis are varies from (-0.18Φ to 0.15Φ), (0.48Φ to 0.68Φ). In the Fore shore environment, the standard deviation varies from (0.56Φ to 0.99Φ) with mean size 1.25Φ the skewness and kurtosis are varies from (-0.53Φ to 0.57Φ), (0.41Φ to 1.36Φ).

Scatter plots between certain parameters are also helpful to interpret the energy conditions, transportation, mode of deposition etc. Passega (1957); Visher (1969); Martins (1965); Folk and Ward (1957) and others described that these trends and interrelationship exhibited in the scatter plots might indicate the mode of deposition and in turn aid identifying the environments. However, Mason and Folk (1958); Friedman (1961) claimed to establish the differentiation between Aeolian, beach and river sediments based on these Scatter plots.

The Scatter plot between Mean size VS Standard deviation (Figure 2a) of the present samples shows the clustering of values near the extreme end of right limb of inverted V-shaped established trend of (Hough, 1942; Inman, 1949, 1953; Griffiths, 1951; Folk and Ward, 1957; Folk, 1959; Walger, 1961 and Hubert, 1961; Seralathan and Padmalal, 1994). The nature of the sediments is dominantly unimodal of which, the dominant constituent is medium sand. The silt is subordinate, making the admixture moderately sorted. The Scatter plot between Mean size and Skewness (Figure 2b) clearly brings out the values, some areas are positively skewed area and some areas are negatively Skewed (Folk and Ward, 1957). It further indicates a unimodal nature of sediments with higher percentage of medium sand and subordinate silt. The relation between Mean size VS Kurtosis (Figure 2c) values indicates a dominance of platykurtic category followed by mesokurtic. The plot between Standard deviation VS Skewness (Figure 2d) shows moderately sorted and positively and negatively skewed sediments. The plot between Standard deviation VS kurtosis (Figure 2e) shows that the majority of samples are of platy to mesokurtic nature, moderately sorted and of medium sand size. Plots of skewness VS kurtosis (Figure 2f) are effective tool in ascertaining the textural aspects and interpreting the genesis of sediments as reflected in the normality of their size distribution.

According to Duane (1964) and Cronan (1972) negatively skewed grain size curves are indicative of areas of erosion or non–deposition, where as positively skewed curves indicated deposition. The results indicate most of

Table 1. Statistical analysis of beach sands of different micro-environments of study area, (1, 2, 3, 4, 5,6,7,8, &9) are the station numbers. Mean size, standard deviation, skewness and kurtosis of all micro-environment samples is in (phi) value.

Location	S. No	Environment	Mean size	Standard deviation	Skewness	Kurtosis
RKB	1	Fore Shore	1.02	0.82	-0.14	0.41
SM	2	Fore Shore	1.25	0.99	-0.12	0.62
VP	3	Fore Shore	0.55	0.59	0.57	0.65
TP	4	Fore Shore	1.24	0.59	-0.39	1.23
RS	5	Fore Shore	1.77	0.71	0.02	1.01
INS	6	Fore Shore	1.75	0.60	0.01	1.32
RB	7	Fore Shore	2.34	0.59	-0.53	1.36
GR	8	Fore Shore	1.27	0.80	0.01	0.89
BHI	9	Fore Shore	2.2	0.56	0.12	0.87
R.KB	1	Back Shore	1.84	0.54	0.18	0.85
SM	2	Back Shore	1.75	0.74	-0.19	0.93
VP	3	Back Shore	1.02	0.56	-0.33	0.96
TP	4	Back Shore	1.95	0.49	0.11	0.88
RS	5	Back Shore	2.08	0.62	-0.14	0.79
INS	6	Back Shore	2.3	0.50	-0.10	0.87
RB	7	Back Shore	1.92	0.45	0.23	1.50
GR	8	Back Shore	1.52	0.59	-0.48	1.64
BHI	9	Back Shore	2.04	0.44	0.07	1.21
RK	1	Berm	1.64	0.42	0.15	0.48
SM	2	Berm	1.30	0.98	-0.18	0.55
VP	3	Berm	0.88	0.70	-0.18	0.68
INS	1	Dune	2.28	0.48	0.16	0.97
RB	2	Dune	2.05	0.55	0.27	0.82

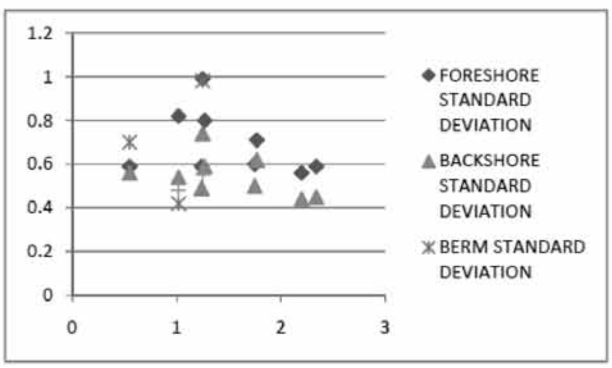

Figure2(a). Mean size vs Standard Deviation.

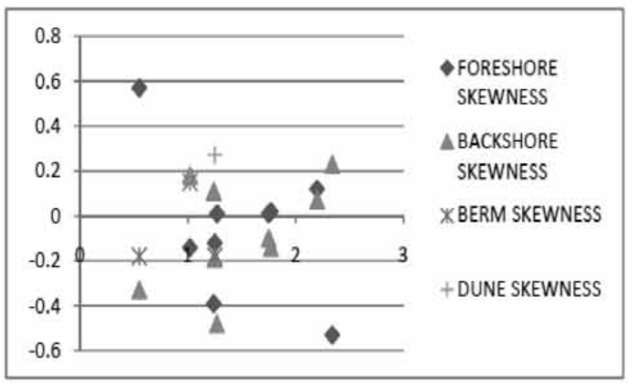

Figure 2(b). Mean size vs Skewness

the sediments are well deposited. Some negatively skewed sediments indicate non-deposition. Therefore the positive skewness of these dements indicate the grains are medium to fine grained.

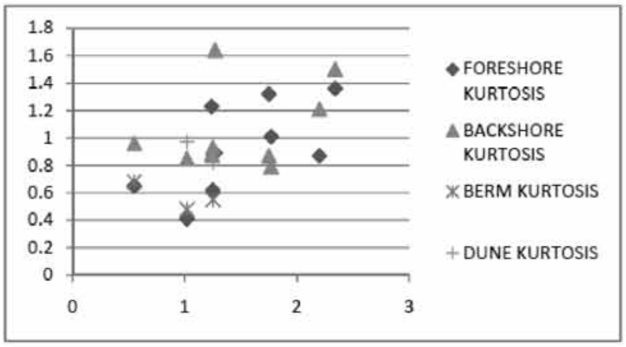

Figure 2(c). Mean size vs Kurtosis

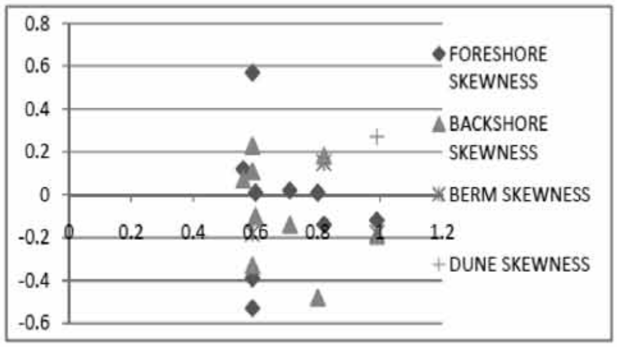

Figure 2(d). Standard Deviation vs Skewness

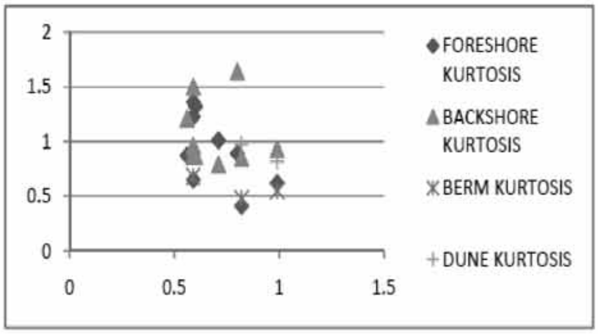

Figure 2(e). Standard Deviation vs Kurtosis

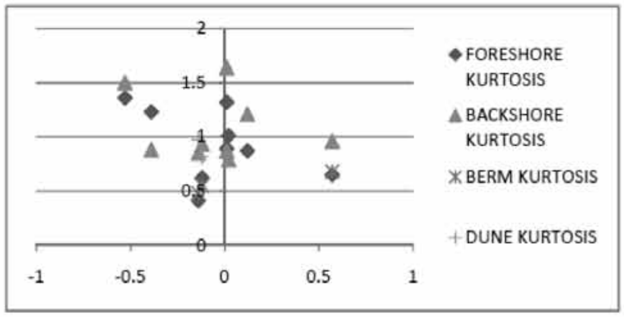

Figure 2(f). Skewness vs Kurtosis

Figure 2. (a, b, c, d, e, f) Scatter Plots.

CONCLUSIONS

Textural analyses data of the coastal sand from Ramakrishna Beach - Bhimunipatnam tract, Visakhapatnam east coast, reveal that the source of the beach sediments are is from the adjoining hill ranges made of granulite facies of rocks that are part of the Precambrian Eastern Ghat Granulite Belt (EGMB). This area covers two important hill ranges one is Kailasa Ranges another one is Yarada Ranges. The altitude of these is hills range between 30m to 594m above mean sea level. Frequency distribution curves and scatter plots drawn between different grain size parameters clearly establish that the nature of the sediments is dominantly unimodal of which, the dominant constituent is medium sand in various microenvironments i.e. backshore, foreshore, dune and Berm. The sands of the dune environment are fine and very fine- grained, dominantly well sorted followed by moderately sorted populations of positively skewed and Platykurtic nature. In back shore environment, fine and very fine sands area abundant than medium grain sands. In berm area the sediments are fine sands and negatively skewed sands, platykurtic. The foreshore regions were covered with fine and very fine sands and these are equally populated by well sorted and moderately sorted nature, negatively skewed, leptokurtic to platykurtic sands.

ACKNOWLEDGEMENTS

Authors are thankful to Dr.V.V.Sesha Sai, GSI, Hyderabad, for useful suggestions in reviewing the manuscript and apt editing. We thank the Chief Editor for his valuable support and encouragement.

Compliance with ethical Standards

The authors declare that they have no conflict of interest and adhere to copyright norms.

REFERENCES

Bangaku Naidu, K., Reddy, K.S.N., Ravi Sekhar, Ch., Ganapati Rao, P., and Murali Krishna, K.N., 2016. Grain Size Distribution of Coastal Sands between Gosthani and Champavathi Rivers Confluence, East Coast of India, Andhra Pradesh. J. Ind. Geophys Union, v.20, no.3, pp: 351-361.

Bhat, M.S., Chavadi,V.C., and Hegde, V.S., 2002. Morphological and textural characteristics of Kudle beach, Karnataka, central west coast of India. Jour.Geol. Soc. India, v.59, pp: 125-131.

Bull, W.B., 1962. Relation of textural patterns of depositional environment of Alluvial fan deposits. Jour. Sed. Pet, v.32, pp: 211-216.

Campbell, G.S., and Shiozawa, S., 1992. Prediction of hydraulic properties of soils using particle-size distribution and bulk density data, in Proceedings of the International Workshop on Indirect Methods for Estimating Hydraulic Properties of Unsaturated Soils, edited by M. T. van Genuchten et al., Univ. of Calif., Riverside, pp: 317– 328.

Carver, R.W., 1971. Procedures in sedimentary petrology. John wiles, New York, pp: 458.

Chandramohan, P., Narasimha Rao, T.V., and Panakala Rao, D., 1981. Studies on the beach changes at Visakhapatnam, Mahasagar - Bulletin of Nat. Inst. Oceanography, v.14, no.2, pp: 105-115.

Cronan, D.S., 1972. Skewness and kurtosis in polymodal sediments from the Irish Sea. Jour. Sed. Pet., v.42, no.1, pp: 102-106.

Dhanunjaya Rao, G., Krishnaiah Settey, B., and Rami Naidu, Ch., 1989. Heavy mineral content and textural characteristics of coastal sands in the Krishna-Godavari, Gosthani – Champavathi, and Penna river deltas of Andhra Pradesh, India: a comparative study. Journal of Atomic Mineral Science (Joams), Earfam., v.2.

Duane, D.B., 1964. Significance of skewness in Recent sediments, western Pamlico Sound, North Carolina. Jour. Sed. Pet., v.34, no.4, pp: 864-874.

Ergine, M., Seref Keskin, Umaran Dogan, A., Yusuf, K.K., and Zehra Karakas., 2007. Grain Size and heavy mineral distribution as related to hinterland and environmental condition for modern beach sediments from the Gulf of Antalya and Finke, Eastern Mediterranean. Mar. Geol., v.240, pp: 185-196.

Folk, R.L., and Ward, W.C., 1957. Brazos River Bar: A study in the significance of grain-size parameters. Jour. Sed. Pet., v.27, pp: 3-26.

Folk, R.L., 1959. Interaction of source and environment in controlling plots of size versus sorting. Program of Dallas Meeting-Soc. Econ. Paleontologists Mineralogis Fs, pp: 67-68.

Frihy, O.E., Lofty, M.F., and Komar, P.D., 1995. Spatial variation in heavy minerals and patterns of sediment sorting along the Nile Delta, Egypt. Sed. Geol., v.97, pp: 33-41.

Frihy, O.E., Badr, A.M., and Hassan, M.S., 2002. Sedimentation processes at the navigation channel of the Damietta harbor on the Northeastern Nile Delta coast of Egypt. Journal of Coastal Research, v.18, no.3, pp: 459–469.

Friedman, G.M., 1961. Distinction between dune, beach and river sands from their textural characteristics. Jour. Sed. Pet., v.27 pp: 3-26.

Friedman, G.M., 1967. Dynamic processes and statistical parameters compared for size frequency distribution of beach and river sands. Jour. Sed. Pet., v.37, pp: 327-354.

Ganesh, B., Naidu, A.G.S.S., Jagannadha Rao, M., Karunakarudu, T., and Avataram, P., 2013. Studies on textural characteristics of sediments from Gosthani river estuary- Bhimunipatnam, A.P., East Coast of India. Jour. Ind. Geophys. Union., v.17, no.2, pp: 139-151.

Griffiths, J.C., 1951. Size versus sorting in some Caribbean sediments. The Journal of Geology, v.59, no.3, pp: 211-243.

Hanamgond, P.T., and Chavadi, V.C., 1997. Sediment Movement and depositional environment of Kawada Bay beaches, Uttara Kannada district, West coast of India. Jour. Geol. Soc. of India., v.56, pp: 193-200.

Hegde, V.S., Shalini, G., and Gosavi Kanchanagouri, D., 2006. Provenance of heavy minerals with special reference to ilmenite of the Honnavar beach, Central west coast of India. Curr. Sci., v.91, pp: 644-648.

Hough, J.L., 1942. Sediments of Cape Cod Bay, Massachusetts. J. Sediment, Petrol., v.12, pp: 10-30.

Hubert, J.F., 1961. A course in statistical geology (geometries): Jour. Geol. Education, v.9, no.2, pp: 57-61.

Inman, D.L., 1949. Sorting sediments in the light of fluid mechanics. Jour. Sed. Petrol., v.19, pp: 10-30.

Inman, D.L., 1953. Areal and seasonal variations in beach and nearshore sediments at La Jolla, California. Beach Erosion Board, Office Chief Eng., Tech. Mem., No. 39.

Jagannadha Rao, M., Greeshma, A.G., Sudha Rani, B., Mallikarjuna Rao, M., and Raju, U.P.N., 2016. Origin and Occurrence of calcretes from Red sediments of Visakhapatnam-Bhimunipatnam coast, East Coast of India J. Ind. Geophys. Union., v.20, no.2, pp: 249-253.

Jagannadha Rao, M., and Krishna Rao, J.S.R., 1984. Textural and mineralogical studies on red sediments of Visakhapatnam Bhimunipatnam coast. Geo views, v.12, no.2, pp: 57-64.

Jagannadha Rao, M., Greeshma, A.G., Avatharam, P., Anil, N.C., and Karunakarudu, T., 2012. Studies on Coastal Geomorphology along Visakhapatnam Bhimunipatnam coast, East Coast of India. J.Ind.Geophys.Union, v.16, no.4, pp: 179-187.

Jagannadha Rao, M., Greeshma Gireesh, A.G., Avatharam, P., Anil, N.C., and Karunakarudu, T., 2013. Studies on Coastal Geomorphology along Visakhapatnam to Bhimunipatnam, East Coast of India J. Ind. Geophys. Union, v.16, no.4, pp: 179-187.

Karunakarudu, T., Jagannadha Rao, M., Ganesh, B., Avataram, P., and Naidu, A.G.S.S., 2013. Studies on textural characteristics of ErraKalva River, west Godavari District, Andhra Pradesh, East Coast of India. International Journal of Geomatics and Geosciences., v.4, no.2, pp: 280-295.

Mahadevan, C., and Nageswarao, B., 1950. Grain size characters in Visakhapatnam coast. Current Science, v.19, pp: 48-49.

Mahadevan, C., and Anjaneyalu, B.J.N.S.R., 1954. Studies on dredged sands off Visakhapatnam Harbour area. Andhra Univ Mem Oceanogra, v.1, pp: 51–56.

Martins, L.R., 1965. Significance of skewness and kurtosis inenvironmental interpretation. Jour. Sed. Petrol., v.35, pp: 768-770.

Mason, C.C., and Folk, R.L., 1958. Differentiation of beach, dune and aeolian flat environments by size analysis. Mustang Island, Texas. Jour. Sed. Petrol., v.28, pp: 211-226.

Mohan, P.M., and Rajamanickam, G.V., 1998. Depositional environment: Inferred from grain size along the coast of Tamil Nadu. Jour. Geo. Soc. of. India., v.52, pp: 95-102.

Mohan, P.M., 2000. Sediment transport mechanism in the Vellar Estuary, east coast of India. Ind. Jour. Mar. Sci., v.29, no.1, pp: 27-31.

Nageswara Rao, N., Suryam, R.K., and Ranga Rao, V., 2005. Depositional environment inferred from grain size parameters of the beach sediments between False Devi Point to Kottapatnam, Andhra Pradesh Coast. Jour. Geo. Soc. of. India., v.65, pp: 317-324.

Passega, R., 1957. Textural characteristics of clastic deposition. Bull. Amer. Assoc. Petrol. Geol., v.41, no.9, pp: 1952-1984.

Rajasekhara Reddy, D., and Karunakarudu, T., 2011. Textural characteristics of the sediments of Mahanadi River, East Coast of India. Jour. Ind. Assoc. of Sed., v.30, no.2, pp: 73-85.

Rajasekhara Reddy, D., and Karunakarudu, T., 2009. Textural characteristics of the sediments of Mahanadi Delta, East Coast of India. Jour. Ind. Assoc. of. Sed., v.30, no.1, pp: 73-85.

Rajesh, E., Anbarsu, K., and Rajamanickam, G.V., 2007. Grain size distribution of silica sands in and around Marakkanam Coast of Tamil Nadu. Jour. Geo. Soc. of. India., v.69, pp: 1361-1368.

Ramanathan, A.L., Rajkumar, K., Jayjit Majumdar., Gurmeet Singh., Behera, P.N., Santhara, S.C., and Chidambaram, S., 2009. Textural characteristics of the surface sediments of a tropical mangrove Sundarban ecosystem India. Indian journal of marine sciences., v.38, no.4, pp: 397-403.

Ramamohan Rao, T., Shanmukha Rao, Ch., and Sanyasi Rao, K., 1982. Textural Analysis and Mineralogy of the BlackSand Deposits of Visakhapatnam-Bhimunipatnam Coast, Andhra Pradesh, India. Jour. Geo. Soc. of. India., v.23, pp: 284-289.

Ramasastry, A.A., and Myrland, P., 1959. Distribution of temperature, salinity and density in the Arabian Sea along the south Malabar coast (South India) during the post-monsoon season. Indian J. Fish., v.6, pp: 223-255.

Reddy, D.R., and Malathi, V., 2002. Occurrence of kyanite in the nearshore sediments of north coastal Andhra Pradesh and its implication. Journal of the Geological Society of India, v.60, no.3, pp: 329-331.

Sastry, M.V.A., Acharyya, S.K., Shah, S.C., Satsangi, P.P., Ghosh, S.C., and Singh, G., 1979. Classification of Indian Gondwana sequence – A Reappraisal. Fourth Int. Gondwana Symp., v.2, pp: 502-509.

Sahu, B.K., 1964. Depositional mechanism from the size analysis of clastic sediments. Jour. Sed. Pet., v.34, pp: 73-83.

Seralathan, P., and Padmalal, D., 1994. Textural studies of surficial sediments of Muvattupvzha River and central vembanad estuary, Kerala. Jour. Geo. Soc. of. India., v.43, no.2, pp: 179-190.

Udden, J.A., 1914. Mechanical Composition of Clastic Sediments. Geol. Soc. Amer. Bull., v.25, pp: 655-744.

Veerayya, M., and Varadachari, V.V.R., 1975. Depositional environments costal sediments of Calangute, Goa. Sedimentary Geology, v.14, pp: 63-74.

Visher, G.S., 1969. Grain Size distribution and depositional processes. Jour. Sed. Pet., v.39, pp: 1074-1106.

Walger, E., 1961. Die Korngrossenverteilung von Einzellagen Sandiger Sedimente undihre Geneti-scheBedeutung. Geol. Rundschazc, v.51, pp: 494-507.

Received on: 24.8.16; Revised on: 16.1.17; Accepted on: 20.1.17

"The most important thing about global warming is this. Whether humans are responsible for the bulk of climate change is going to be left to the scientists, but it's all of our responsibility to leave this planet in better shape for the future generations than we found it".

Mike Huckabee

(**Source:** https://www.brainyquote.com/quotes/keywords/climate_change.html)

J. Ind. Geophys. Union (May 2017)
v.21, no.3, pp: 214-222

A morphological study of low latitude ionosphere and its implication in identifying earthquake precursors

Devbrat Pundhir*[1,3], Birbal Singh[1], O. P. Singh[2] and Saral Kumar Gupta[3]
[1]Department of Electronics & Communication Engineering, Raja Balwant Singh Engineering Technical Campus, Bichpuri, Agra, India-283105
[2]Department of Physics, Raja Balwant Singh Engineering Technical Campus, Bichpuri, Agra, India-283105
[3]Department of Physics, Banasthali Vidyapith, Banasthali, Rajasthan, India-304022
*Corresponding Author: devbratpundhir@gmail.com

ABSTRACT
The low latitude ionosphere is highly variable because of the existence of equatorial ionization anomaly (EIA) and irregularities like spread-F and sporadic E. The GPS-TEC data have been analyzed from 01 January to 31 December 2007 (Period-I) and then from 01 January to 31 December, 2011 (Period-II) during low and high solar activity periods respectively. The results are validated with the recent ionospheric model IRI-2012 and we found a very good agreement in trend. However, IRI model indicated larger values of diurnal variations for both the periods. We have found a strong correlation ($\approx$ 0.98) between IRI and TEC data during each of the three seasons (winter, summer, and equinox) for both periods except for winter season ($\approx$ 0.85) of period-I. The TEC values are larger during equinox and smaller during winter season which may be attributed to solar activity. The peak GPS-TEC values are found in the range of 15-25 TECU and 25-30 TECU during the first and second periods respectively. To examine the effect of magnetic storms on TEC data, monthly correlation coefficients have been calculated between $\sum$Kp and TEC for period-II but it was very poor. A few specific cases of magnetic storms have shown their delayed effect on the TEC data at low latitude Agra station, 1-4 days after the occurrence of event. Therefore, TEC anomalies attributed to earthquakes have to be examined in the light of anomalies caused by the above factors.

Key words: GPS-TEC, morphological study, low latitude, IRI-2012 model, Earthquakes.

INTRODUCTION

The low latitude ionosphere is also influenced by the geophysical phenomena like solar flares, magnetic storms and various anthropogenic sources like nuclear explosions, volcanic activities, dust storms, and seismic activities (Pulinets and Davidenko, 2014) in addition to the EIA spread-F and sporadic E. These factors bring out substantial variation in the structure and dynamics of the low latitude ionosphere. In view of the occasional existence of the ionization anomalies produced by these factors, it is sometimes difficult to identify the anomalies produced by the seismic events. Hence, a morphological study of the low latitude ionosphere is essential so that anomalies produced by earthquakes may be clearly identified and separated from those produced by other sources.

Globally, a number of researchers have studied the morphological features of the ionosphere using GPS based TEC measurements and found very interesting and valuable results (Warnant, 2000; Wu et al., 2008, 2012; Natali and Meza, 2011; Akala et al., 2013; Huy et al., 2014). In India, due to existence of the EIA, researchers have studied the low latitude ionosphere extensively using GPS based TEC measurements and also compared their results with ionospheric IRI models (Gupta and Singh, 2000; Bhuyan and Borah, 2007; Bagiya et al., 2009; Chauhan and Singh, 2010; Mukherjee et al., 2010; Kumar et al., 2012; Prasad et al., 2012; Sharma et al., 2012; Chakraborty et al., 2014; Karia et al., 2015; Rathore et al., 2015). Recently, the GPS-TEC studies have achieved a great success in predicting the behavior of the ionosphere and also proved to be very useful to detect the effects of solar events (Lastovicka, 2002; Dashora et al., 2009; Trivedi et al., 2011, 2013; Xu et al., 2012; Adebiyi et al., 2014). The morphological studies by Rama Rao et al., (2006a) investigated the temporal and spatial variations of TEC data taken from the Indian GPS network during the period of low solar activity of 2004-2005. The diurnal variation in TEC in the equatorial ionization anomaly (EIA) region shows its maximum value between 13:00 and 16:00 LT and the day minimum between 05:00 and 06:00 LT at all the observing stations from the equator to the EIA crest region. The seasonal variations of TEC have shown maximum during the equinox months and minimum during the summer. Prasad et al., (2012) have also studied the variations of TEC at four Indian GPS stations during the year 2004. The higher and lower TEC values are found during equinoctial and summer months respectively and a significant day-to-day variability was also observed. The variations are higher at the anomaly crest locations and lesser at the equatorial stations which are supported well by IRI-2007 model over the four Indian GPS stations. The variations with solar activity indices (SSN, F10.7 and EUV) have shown a good correlation during equinoctial months and a poor correlation during summer months. In spite of many reports available in literature on the morphological study of GPS-TEC over low latitudes during low and high solar activity periods, no attempts have been made to examine the influence of seismic activities and segregate them from general morphological features. The purpose of the present work is to identify earthquake precursors from the complex morphological variation in the low latitude ionosphere, a new attempt made in this area.

Experimental setup

The experimental setup of TEC measurements has been installed at Seismo-electromagnetics and Space Research Laboratory (SESRL) of R.B.S. Engineering Technical Campus, Bichpuri, Agra (Formerly R.B.S. College Agra) by our earlier group (Chauhan et al., 2012). Bichpuri is located 12 km west of Agra city in a rural area where electrical and electromagnetic noises are very low and round the clock observations have been taken since 2006. The related equipment from Silicon Valley, U.S.A. includes GPS antenna (Novatel's Model GPS702), receiver (Novatel's Euro Pak 3-M), connecting cables and relevant software (novatel.com). GPS receiver can be operated at two ultra-high frequencies L1 = 1575.42 MHz and L2 = 1227.6 MHz and we can receive 11 GPS satellite signals at these frequencies. It measures phase and amplitude at 50-Hz rate and code/carrier divergence at 1 Hz rate for each satellite being tracked and computes TEC from combined frequencies by pseudo range and carrier phase measurements. The primary purpose of the GPS receiver is to collect ionospheric scintillation and TEC data for all visible satellites.

Method of Analysis

The analysis procedure is to convert slant-TEC (STEC) into vertical-TEC (VTEC) by multiplying with a suitable mapping function as given by (Mannucci et al., 1993);

$$S(E) = \frac{1}{\cos z} = \left[1 - \left(\frac{R_E \times \cos(E)}{R_E + h_s}\right)^2\right]^{-0.5} \quad \text{..... 1}$$

where R_E is the mean radius of the earth in km, h_s, the ionosphere (effective) height above the earth's surface, z, the zenith angle and E, the elevation angle in degrees. The effective ionospheric height of 350 km is used for determination of IPP locations (Rama Rao et al., 2006b). Since TEC variation may be affected by multipath, troposcatter and water vapor at low elevation angles (Rama Rao et al., 2006b), values of TEC are taken at higher elevation angles (50°).

In this paper, the results of analysis of TEC data for two years from 01 January-31 December, 2007 (period-I) and 01 January-31 December, 2011 (period-II) recorded at the low latitude GPS station Agra, India during low and high solar activity periods are presented. The study of diurnal and seasonal variations of TEC data indicated significant variations from low to high solar activity periods. The results are also compared with recent ionospheric model IRI-2012 and we find a very good agreement in trends (strong correlation) but IRI model overestimates during each of the three seasons (winter, summer and equinox) for both the periods. The effects of magnetic storms have also been examined on TEC data which are found to cause a significant change. The data of ∑Kp, solar flux (F10.7 cm) indices and IRI-2012 model are taken from the NASA website of http://omniweb.gsfc.nasa.gov/form/dx1.html and http://omniweb.gsfc.nasa.gov/vitmo/iri2012_vitmo.html respectively. This paper suggested that morphological study of GPS-TEC data must be taken into account while examining the earthquake induced TEC anomalies.

The correlation coefficient has also been calculated between GPS-TEC and IRI-TEC and then GPS-TEC and ∑Kp respectively by using following equation;

$$\text{Correlation Coefficient} = \frac{N\sum xy - (\sum x)(\sum y)}{\sqrt{[N(\sum x^2) - (\sum x)^2][N\sum y^2 - (\sum y)^2]}} \quad \text{.....2}$$

where x and y are two samples, and N is the number of pairs. ∑Kp index quantifies the disturbances in the horizontal component of the earth's magnetic field recorded at magnetic observatories located around the globe. It has been widely used in ionospheric and atmospheric studies for the examination of magnetic storm. It records in three hours interval over magnetic observatories and the final data are found by averaging the data recorded over all the observatories. This data is available on the websites of Kyoto, Japan and NASA, USA for public access.

RESULTS

Diurnal variations

The four contour diagrams shown in Figure 1 depict the average monthly variations of TEC data for each period from 01 January-31 December, 2007 and 01 January-31 December, 2011 at our Agra station and the same variations with IRI-2012 model. Here, one TEC unit (1TECU) is ≈ 10^{16} electrons per meter^2. The diurnal pattern of VTEC increases during sunrise to an afternoon maximum and then decreases to a minimum just before sunset.

The usual features of low latitude ionosphere as appeared in diurnal variation of TEC data like VTEC values show a minimum during morning hours and gradually increase with the time of the day attaining a maximum in the afternoon and again decrease steadily

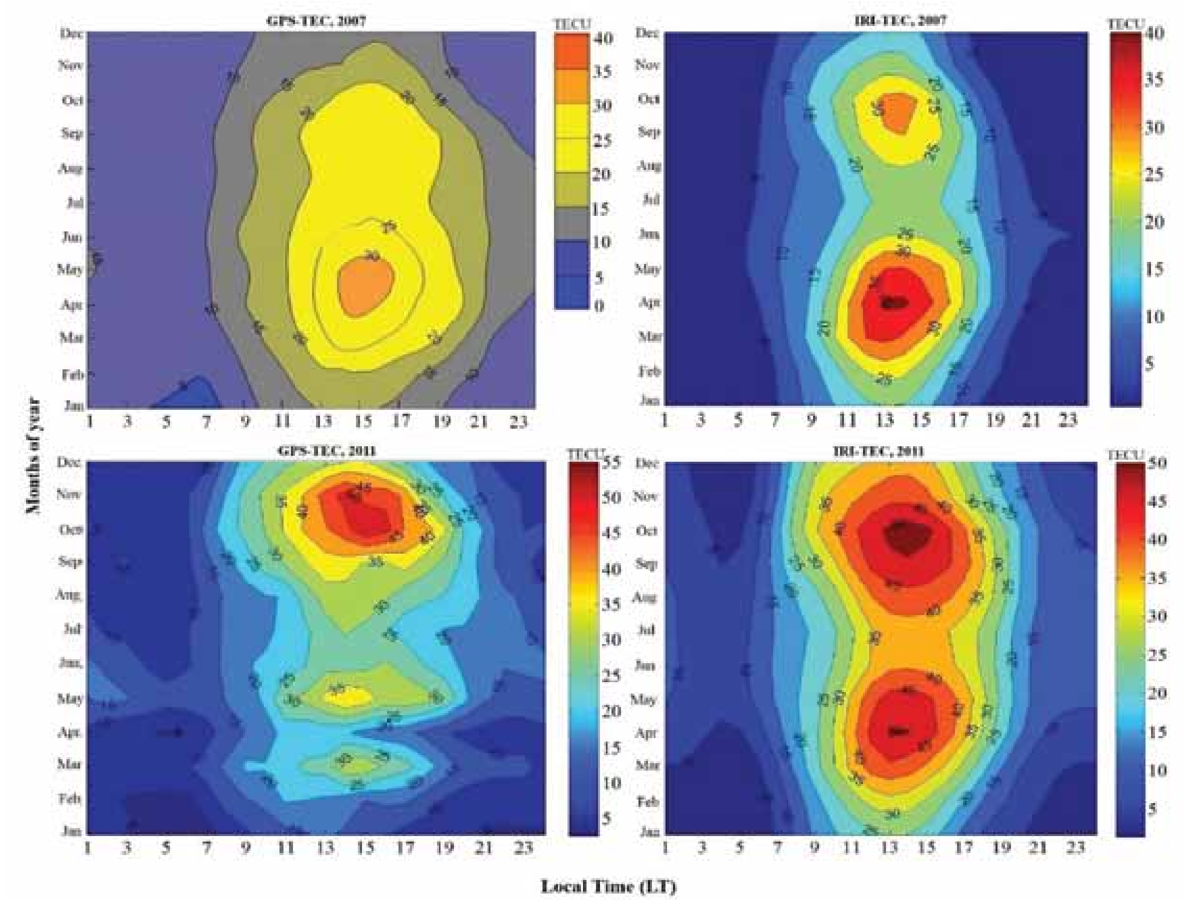

Figure 1. Upper panel (left) shows the contour plot of average monthly GPS-TEC variations during period-I (2007) over a low latitude station, Agra, India and the upper panel (right) presents the IRI-2012 model TEC data variations over the same station and for the same period. The lower panel shows the same variations as above but for the period-II (2011).

after sunset. These features are similar to those obtained by earlier workers (Mukherjee et al., 2010; Kumar et al., 2012; Sharma et al., 2012). The peak value of the VTEC lies between 14:00 and 16:00 hrs. These plots show the monthly variations of VTEC, mostly during the mid-day to morning hours which are helpful in forecasting and navigation (Bagiya et al., 2009; Rama Rao et al., 2006a). The monthly variations of VTEC at Agra may be attributed to the changes in the intensity of the arriving solar radiations (Natali and Meza, 2011; Akala et al., 2013). The highest GPS-TEC values are found in equinoctial month of April ($\approx$ 30 TECU) for period-I also supported by corresponding IRI-TEC variation. The highest GPS-TEC values for period-II are also found in equinoctial months of November and October ($\approx$ 45-50 TECU). Here, it can be noticed that IRI-TEC variations are almost similar to our results during both the periods except that IRI model shows $\approx$ 5 TECU higher values of TEC as compared to our data for equinoctial months for period-I. So it may be concluded here that TEC values are enhanced in equinox than in winter and summer season.

Seasonal Variations

The seasonal variations of TEC and their comparison with IRI model are shown in Figures 2 and 3. Here, the three seasons are considered i.e. summer, equinox, and winter. The months of April, May, June, and July are taken in summer solstice. The average of TEC data is taken for the months of March, April, and September, October corresponding to two equinoxes. Another combination of months of November, December, January, and February, corresponds to winter solstice. In these figures, the upper panels show the variation of TEC data in each of three seasons (winter, summer, and equinox) and the same variations with seasonal IRI-TEC shown by solid and dotted lines respectively and the lower panels present the correlation plot between GPS-TEC and IRI-TEC for the two periods. The peak GPS-TEC values are found in the range of 15-25 TECU for all the seasons. Here, the IRI model overestimates during peak hours and underestimates during morning and afternoon hours in case of winter and equinox season. It underestimates during morning

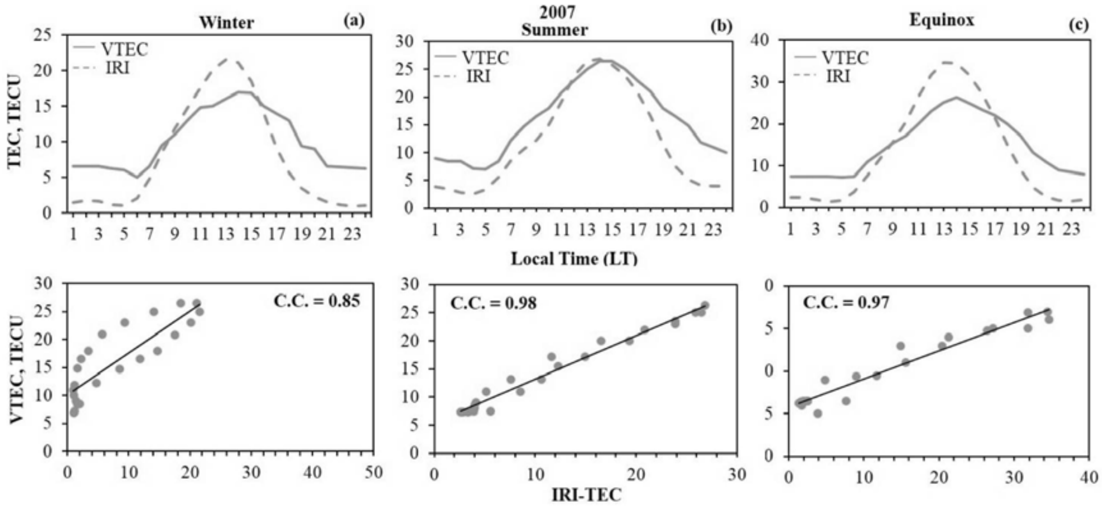

Figure 2. Upper panel presents the variation of GPS-TEC and IRI-TEC by solid and dotted lines during each of the three seasons (winter, summer and equinox) respectively for the period-I (2007). The lower panel shows the correlation plots between VTEC and IRI-TEC for the same as above.

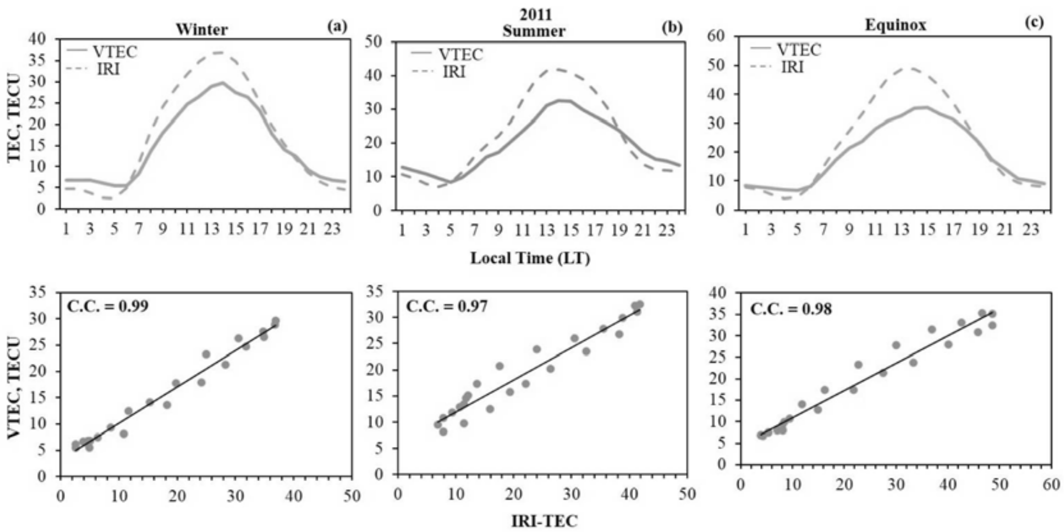

Figure 3. Shows the same as Figure 2 but for the period-II (2011).

and afternoon hours in summer season. To validate our results, the correlation coefficients are calculated between GPS-TEC and ionospheric IRI-2012 model TEC data for each of the three seasons which shows a strong correlation ($\approx$ 0.98) between them except for winter where it is 0.85 during period-I.

In Figure 3, one can see that the TEC values are higher in period-II as compared to that in period-I. It may be because of the direct effect of solar activity. The peak TEC values lie in the interval of 25-30 TECU. From this figure, it can be seen that IRI model overestimates in this period also but shows a strong correlation $\approx$ 0.98 for all the seasons. One more interesting point is a change in TEC values from period-I to period-II. So these changes may be interpreted in the light of solar activity (discussed in solar activity dependence and geomagnetic storm effect). The GPS-TEC and IRI-TEC show higher values during equinoxes and lower values in winter relative to those in summer for both the periods. These results are similar to the findings of earlier workers (Kumar et al., 2012; Sharma et al., 2012). The mechanisms which are related to these variations are described later. This study is consistent with the studies of other low latitude stations in the vicinity of our station. For example, Sharma et al., (2012) have investigated the TEC variations over Delhi (beyond the EIA region and closer to Agra) in addition to Trivandrum equatorial station during low and high solar activity and found similar variations.

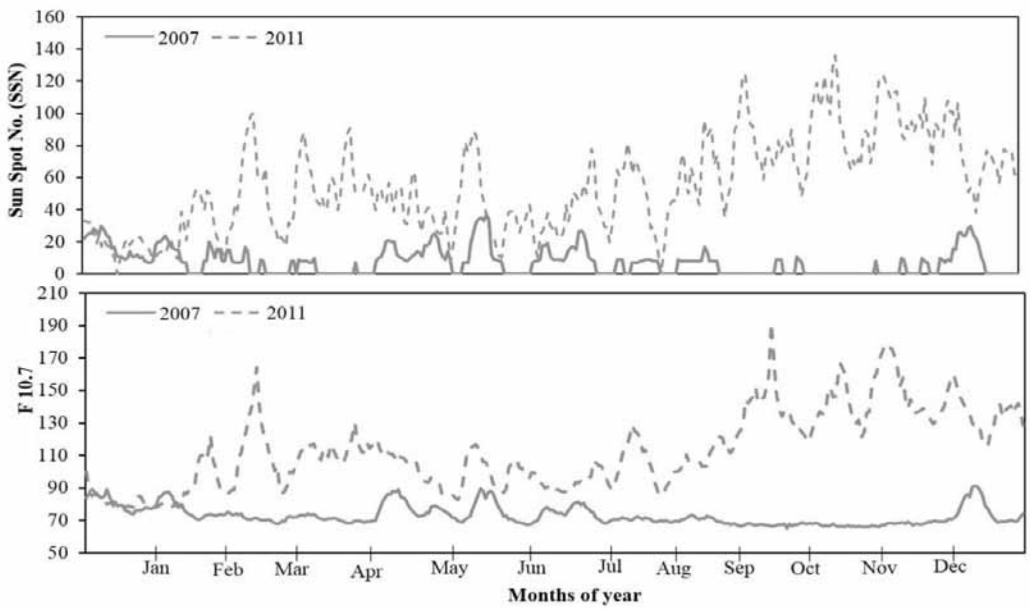

Figure 4. Upper panel shows the variations of Sun Spot Numbers (SSNs) for the period-I (2007) and period-II (2011) by solid and dotted lines respectively. The lower panel shows the variations of F10.7 flux for the same periods.

Solar activity dependence and geomagnetic storm effect

To see the effect of solar activity on TEC data during the period under consideration, sun spot numbers (SSNs) and solar flux F10.7 indices are plotted for period-I and period-II by solid and dotted lines respectively (Figure 4). The upper panel of this figure shows the variation of SSN which is almost quiet for period-I but shows large variations for period-II in equinoctial months. As it may be seen here, the maximum values of SSN are $\approx$ 30 and $\approx$ 140 during period-I and period-II respectively. The lower panel of this figure shows the variation of solar flux F10.7 during both the periods. We can clearly see that the maximum values of solar flux F10.7 are $\approx$ 90 for period-I and $\approx$ 190 for period-II. Here, a large change in maximum values of solar activity parameters can be seen between the two periods. It confirms that the solar activity affects the TEC data largely during period-II in comparison to period-I.

To see the effect of geomagnetic storms on the TEC data at our Agra station, we examined the correlation between the monthly TEC variations and geomagnetic activities for which the correlation coefficient between TEC data and $\sum$Kp index is calculated for each month of year 2011. The results are shown in Figure 5. Here, it is noted that values of correlation coefficients are very poor for the period under consideration, so we can say that geomagnetic activity does not affect the TEC data largely.

While the monthly correlation does not produce a satisfactory result, four cases of magnetic storms are selected to see the effect of magnetic storm on TEC data such as those occurred on 06 August, 27 September, 25 October and on 01 November, 2011. On these days, $\sum$Kp index values are high compared to the values on normal days. For the first case, the VTEC variations (upper panel) and corresponding $\sum$Kp index (lower panel) are plotted for the period of 03 August to 16 August 2011 in Figure 6a. It can be seen that the enhancement in VTEC data occurs on 07 August, one day after the occurrence of a magnetic storm. In the second case, the period of 25 September to 08 October 2011 is considered and plotted in the same way corresponding to this period. One can notice in Figure 6b that $\sum$Kp index values (lower panel) are > 30 between 26-29 September, whereas the major enhancements occur in TEC data during 2-3 October (5-6 days after). Similarly, two other cases of VTEC variations in relation to magnetic storms during 23 October-05 November are shown in Figure 6c. In the lower panel of this figure, it can be seen that $\sum$Kp values are high ($\geq$ 30) on 25 October and 01 November. The enhancements occur in the data corresponding to these two moderate magnetic storms during 1-4 days after the occurrence of these storms. However, it is well known that geomagnetic storm can produce large perturbations in the ionospheric F-region in the form of enhancements and depletions in the electron density during periods of positive and negative phases of a magnetic storm, respectively.

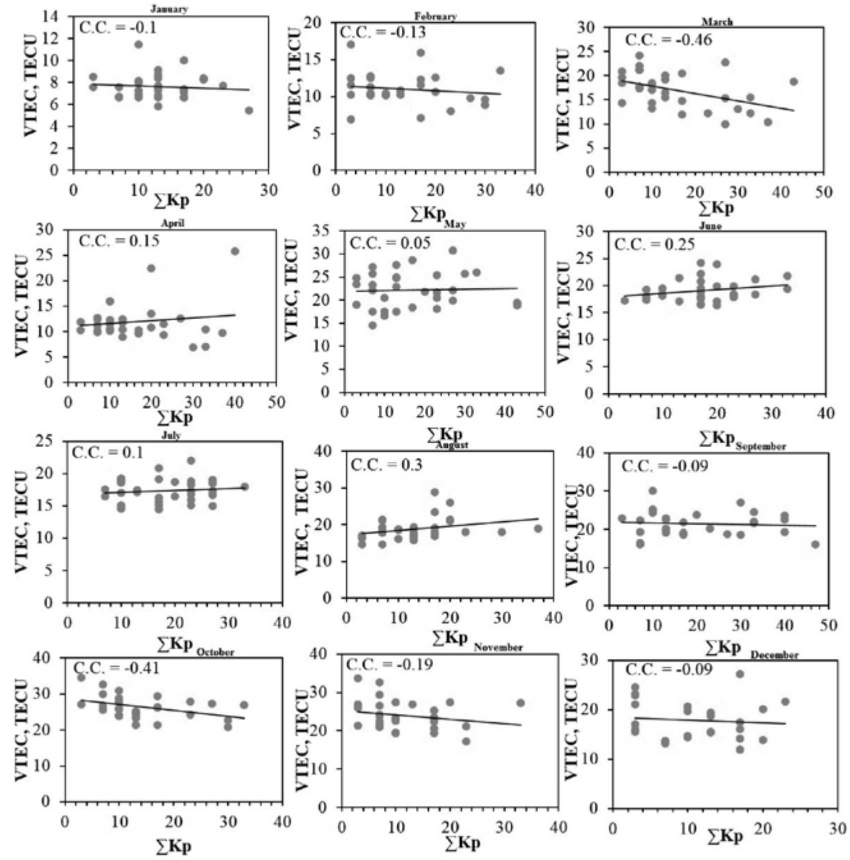

Figure 5. The correlation plots between VTEC and geomagnetic activity factor (∑ Kp index) during the period-II (2011).

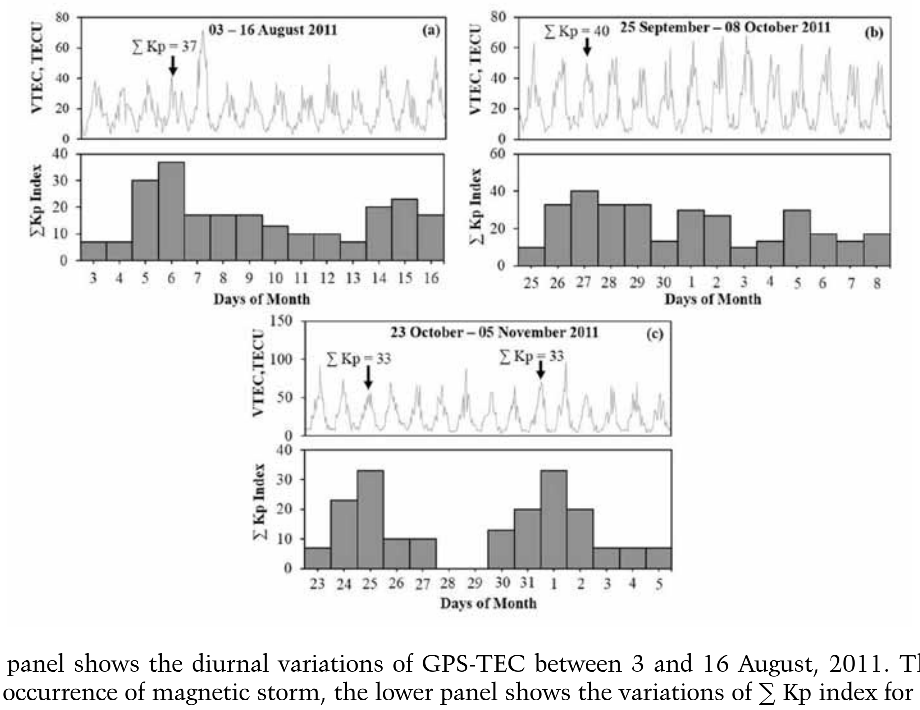

Figure 6. (a) Upper panel shows the diurnal variations of GPS-TEC between 3 and 16 August, 2011. The downward arrow indicates the day of occurrence of magnetic storm, the lower panel shows the variations of ∑ Kp index for the same period. (b) the same variations as Figure 6a but for the period of 25 September-08 October, 2011. (c) same variations as Figure 6a but for the period of 23 October-05 November, 2011.

Table 1. Main points of the interpretation of results.

S. N.	Type of variation	Quiet Period (2007)	High Solar Activity period (2011)
1.	General variation	In summer, the TEC values are high (≈ 30 TECU).	In both summer and equinox TEC values are high (≈ 40 and 50 TECU respectively).
2.	Solar activity variation (a) Sunspot Numbers	In summer TEC (≈ 35 TECU) is relatively higher than other months of seasons.	TEC is much higher (≈45-50 TECU) during equinoctial months.
	(b) F10.7 cm	Similar to the above	Similar to the above
3.	Magnetic storms (moderate)	-----	TEC enhanced 1-4 days after the occurrence of event.

Summary of the results

The results obtained from the analysis of the GPS-TEC data over Agra during low and high solar activity periods are summarized in the Table 1.

Analysis of the results for interpreting earthquake induced TEC anomalies

From the summary of the results presented above, it is clear that TEC values vary significantly with seasons and solar activity i.e. during quiet periods TEC shows enhancement in summer, while during disturbed periods it shows enhancements in equinoxes also. A particular point to be noted is that TEC shows anomalously enhanced values after a few days of occurrence of magnetic storms. Several workers have reported rise in TEC a few days before the occurrence of earthquakes (Dabas et al., 2007; Chauhan et al., 2012; Singh et al., 2012). In order to authenticate such results, it is necessary to examine the variation in TEC with respect to season and solar activity so that it will not lead to wrong conclusion.

Now, it is necessary to justify the GPS-TEC variations using possible mechanisms. The rise in TEC data can be attributed to solar extreme UV ionization coupled with the upward vertical E × B drift. Our station is located in the equatorial ionization anomaly region in which two crests in the ionospheric electron density often show a minimum nearby magnetic dips 15^0 north and south respectively (Appleton, 1946). In this study, we find that the GPS-TEC and IRI-TEC show higher values during equinoxes and lower values in winter relative to those in summer for both the study periods. Here, it may be noticed that the large difference in magnitude of VTEC exists between period-I and period-II because of the low to high solar activity period. Generally, during the daytime, the equator is hotter than the North and South poles which causes meridional wind flow towards the poles from the equator. The flow of meridional wind changes the neutral composition and O/N_2 decreases at equatorial stations. This decrease in O/N_2 ratio, which is maximum during the equinox months, will result in higher electron density. Hence equinox VTEC will be highest (Bagiya et al., 2009; Kumar et al., 2012).

Solar activity affects the magnetospheric dynamics, and influences the plasma density distribution within the ionosphere. The variations of ionospheric VTEC with solar activity can be studied, using solar flux F10.7 cm and SSN which are the useful indicators of solar activity relevant for ionospheric effects. The F10.7 cm flux may be defined as the radio power of sun at a frequency of 2800 MHz commonly measured in solar flux unit (1 sfu = 10^{-22} Wm^{-2} Hz^{-1}). Generally, the ionization level varies to higher values during a high solar activity period and lower values during a low solar activity period. SSN is a temporary phenomenon but it is very important to define the solar activity effect. The changes in the TEC data variations at our station are attributed to the changes in the solar activity period which is confirmed by the variations of solar activity factors (F10.7 and SSN) which matches well with the earlier studies.

The rise in TEC data during the periods of magnetic storms may be attributed to the delayed effects of the induced electric field penetrating the low latitude ionosphere and magnetosphere (Jain and Singh, 1977; Rastogi and Klobuchar 1990; Lakshmi et al., 1983, 1997; Jain et al., 2010). Basically, two main factors may affect the ionosphere during a magnetic storm: First is thermospheric heating mainly caused by storm-induced thermospheric winds (Danilov and Lastovicka 2001), which results at low latitudes, ionization level increase short of any noteworthy changes in the ratio of atom to molecule (Fuller-Rowell et al., 1994). Second is the penetration of an eastward electric field to low latitudes which results in the enhancements of the fountain effect and the EIA poleward. The enhanced fountain effect is responsible for the enhancements in TEC data measured at low latitudes.

There are numerous reports showing TEC anomalies a few days prior to the occurrence of earthquakes. It has been suggested that earthquake induced electric fields penetrate the ionosphere and cause such anomalies. However, the TEC anomalies occur with season and magnetic storms also. It is very useful to examine TEC variations carefully.

CONCLUSIONS

The GPS-TEC data have been analyzed at a low latitude station Agra, India for two periods i.e. from 01 January-31 December, 2007 and 01 January-31 December, 2011 corresponding to low and high solar activity periods respectively. The diurnal and seasonal TEC variations have been studied for both the periods of observation. The effect of solar activity has been examined in terms of sun spot numbers and F10.7 flux variation whose maximum values are 30 and 90 for period-I and 140 and 190 for period-II respectively. The maximum values of GPS-TEC have been found during equinox (30 and 50 TECU) and minimum in winter (5 and 15 TECU) during period-I and period-II. A strong correlation (≈ 0.98) between GPS-TEC and IRI-2012 model have been found for each season except winter season (≈ 0.85) of period-I. Hence, it may be concluded that the TEC value will be maximum during equinox season which may be attributed to solar activity for each period. The monthly correlation between $\sum$Kp and GPS-TEC was not found to be so good but in four specific cases of magnetic storms, TEC increases, 1-4 days after the occurrence of the events. Finally, it is concluded that TEC anomalies attributed to earthquakes must be examined in the light of anomalies caused by the factors which have considered in this paper.

ACKNOWLEDGEMENTS

Authors are thankful to Ministry of Earth Sciences, Government of India, New Delhi for financial support in the form of major research project. Authors are also thankful to Omniweb NASA for the data of solar flux (F10.7 cm) and $\sum$Kp indices and IRI-2012 model. The authors also thankful to Dr. Vemuri Satya Srinivas and Dr. M.R.K. Prabhakar Rao for useful suggestions to enhance the quality of the manuscript. Authors thank Dr. M.R.K. Prabhakar Rao for apt editing. Authors are highly grateful to the Chief Editor for unequivocal support.

Compliance with ethical Standards

The authors declare that they have no conflict of interest and adhere to copyright norms.

REFERENCES

Adebiyi, S.J., Adimula, I.A., and Oladipo, O.A., 2014. Seasonal variations of GPS derived TEC at three different latitudes of the southern hemisphere during geomagnetic storms, Adv. Space Res., v.53, pp: 1246–1254.

Akala, A.O., Seemala, G.K., Doherty, P.H., Valladares, C.E., Carrano, C.S., Espinoza, J., and Oluyo, S., 2013. Comparison of equatorial GPS-TEC observations over an African station and an American station during the minimum and ascending phases of solar cycle 24, Ann. Geophys., v.31, pp: 2085–2096.

Appleton, E.V., 1946. Two Anomalies in the Ionosphere. Naturedoi: 10.1038/157691a0., v.157, pp: 691.

Bagiya, M.S., Joshi, H.P., Iyer, K.N., Aggarwal, M., Ravindran, S., and Pathan, B.M., 2009. TEC variations during low solar activity period (2005–2007) near the Equatorial Ionospheric Anomaly Crest region in India, Ann. Geophys., v.27, pp: 1047–1057.

Bhuyan, P.K., and Borah, R.R., 2007. TEC derived from GPS network in India and comparison with the IRI, Adv. Space Res., v.39, pp: 830–840.

Chakraborty, M., Kumar, S., De, B.K., and Guha, A., 2014. Latitudinal characteristics of GPS derived ionospheric TEC: a comparative study with IRI 2012 model, Ann. Geophysics, A0539, v.57, no.5.

Chauhan, V., and Singh, O.P., 2010. A morphological study of GPS-TEC data at Agra and their comparison with the IRI model, Adv. in Space Res., v.46, pp: 280-290.

Chauhan, V., Singh, O.P., Pandey, U., Singh, B., Arora, B. R., Rawat, G., Pathan, B.M., Sinha, A.K., Sharma, A.K., and Patil, A.V., 2012. A search for precursors of earthquakes from multi-station ULF observations and TEC measurements in India, Ind. J. Rad. & Space Phys, v.41, pp: 543 -556.

Dabas, R.S., Das, R.M., Sharma, K., and Pillai, K.G.M., 2007. Ionospheric pre-cursors observed over low latitudes during some of the recent major earthquakes, J. Atmos. Solar Terr. Phys., v.69, no.15, pp: 1813–1824.

Danilov, A.D., and Lastovicka, J., 2001. Effects of geomagnetic storms on the ionosphere and atmosphere. Int. J. Geomagn. Aeron., v.2, pp: 209–224.

Dashora, N., Sharma, S., Dabas, R.S., Alex, S., and Pandey, R., 2009. Large enhancements in low latitude total electron content during 15 May 2005 geomagnetic storm in Indian zone, Ann. Geophys., v.27, pp: 1803–1820.

Fuller-Rowell, T.J., Codrescu, M.V., Moffett, R.J., and Quegan, S., 1994. Response of the thermosphere and ionosphere to geomagnetic storms. J. Geophys. Res., v.99, pp: 3893–3914.

Gupta, J.K., and Singh, L., 2000. Long term ionospheric electron content variations over Delhi, Ann. Geophys., v.18, pp: 1635–1644.

Huy, M. Le., Amory-Mazaudier, C., Fleury, R., Bourdillon, A., Lassudrie-Duchesne, P., Tran Thi, L., Nguyen Chien, T., Nguyen Ha and Vila, P., 2014, Time variations of the total electron content in the Southeast Asian equatorial ionization anomaly for the period 2006-2011, Adv. Space Res., v.54, pp: 355-368.

Jain, A., Tiwari, S., Jain, S., and Gwal, A.K., 2010. Study of TEC response during severe geomagnetic storms near the crest of the equatorial ionization anomaly. Ind. J. Radio Space Phys., v.39, pp: 11–24.

Jain, S.K., and Singh, B., 1977. Vertical motions of the low and equatorial-latitude F2 layers during prolonged and isolated magnetic storms, J. Geophys. Res., v.82, pp: 723-726.

Karia, S.P., Patel, N.C., and Pathak, K.N., 2015. Comparison of GPS based TEC measurements with the IRI-2012 Model for the period of low to moderate solar activity (2009-2012) at the crest of equatorial anomaly in Indian region, Adv. Space Res., v.55, no.8, pp: 1965-1975.

Kumar, S., Priyadarshi, S., Krishna, S.G., and Singh, A.K., 2012. GPS-TEC variations during low solar activity period (2007-2009) at Indian low latitude stations, Astrophys & Space Sci., v.339, pp: 165–178.

Lakshmi, D.R., Reddy, B.M., and Sastri, S., 1983. A prediction model for equatorial low latitude HF communication parameters during magnetic disturbances, Ind. J. Radio Space Phys., v.12, pp: 1-18.

Lakshmi, D.R., Veenadhari, B., Dabas, R.S., and Reddy, B.M., 1997. Sudden post-midnight decreases in equatorial in F-region electron densities associated with severe magnetic storms, Ann. Geophysicae, v.15, pp: 306-313.

Lastovicka, J., 2002. Monitoring and forecasting of ionospheric space weather-effects of geomagnetic storms, J. Atmos. and Solar-Terr. Phys., v.64, no.5–6, pp: 697–705.

Mannucci, A.J., Wilson, B.D., and Edwards, C.D., 1993. A new method for monitoring the earth's ionosphere total electron content using the GPS global network, in Proceedings of ION GPS-93 (Institute of Navigation), pp: 1323-1332.

Mukherjee, S., Sarkar, S., Purohit, P.K., and Gwal, A.K., 2010. Seasonal variation of total electron content at crest of equatorial anomaly station during low solar activity conditions, Adv. Space Res., v.46, pp: 291–295.

Natali, M.P., and Meza, A., 2011. Annual and semiannual variations of vertical total electron content during high solar activity based on GPS observations, Ann. Geophys., v.29, pp: 865–873.

Prasad, S.N.V.S., Rama Rao, P.V.S., Prasad, D.S.V.V.D., Venkatesh, K., and Niranjan, K., 2012. On the variabilities of the Total Electron Content (TEC) over the Indian low latitude sector, Adv. Space Res., v.49, pp: 898-913.

Pulinets, S.A., and Davidenko, D., 2014. Ionospheric precursors of earthquakes and Global Electric Circuit", Adv. in Space Res., v.53, no.5, pp: 709-723.

Rama Rao, P.V.S., Gopi Krishna, S., Niranjan, K., and Prasad, D.S.V.V.D., 2006a. Temporal and spatial variations in TEC using simultaneous measurements from the Indian GPS network of receivers during the low solar activity period of 2004–2005, Ann. Geophys., v.24, pp: 3279–3292.

Rama Rao, P.V.S., Niranjan, K., Prasad, D.S.V.V.D., Gopi Krishna, S., and Uma, G., 2006b. On the validity of the ionospheric pierce point (IPP) altitude of 350 km in the equatorial and low latitude sector. Ann. Geophys., v.24, pp: 2159–2168.

Rastogi, R.G., and Klobuchar, J.A., 1990. Ionospheric electron content within the equatorial anomaly belt. J. Geophys. Res., v.95, pp: 19045.

Rathore, V.S., Kumar, S., and Singh, A.K., 2015. A statistical comparison of IRI TEC prediction with GPS TEC measurement over Varanasi, India, J. Atmos. Solar-Terr. Phys., v.124, pp: 1-9.

Sharma, K., Dabas, R.S., and Ravindran, S., 2012. Study of total electron content variations over equatorial and low latitude ionosphere during extreme solar minimum, Astrophys Space Sci., v.341, pp: 277–286.

Singh, A.K., Kumar, S., Singh, R., and Singh, A.K., 2012. Pre-Earthquake Ionospheric Anomalies Observed using Ground Based Multi-Instruments", Int. J. Adv. Earth Sci., v.1, no.1, pp: 13-19.

Trivedi, R., Jain, A., Jain, S., and Gwal, A.K., 2011. Study of TEC changes during geomagnetic storms occurred near the crest of the equatorial ionospheric ionization anomaly in the Indian sector, Adv. Space Res., v.48, pp: 1617-1630.

Trivedi, R., Jain, S., Jain, A., and Gwal, A.K., 2013. Solar and magnetic control on night time enhancement in TEC near the crest of the Equatorial Ionization Anomaly, Adv. Space Res., v.51, pp: 61-68.

Warnant, R., 2000. The increase of ionospheric activity as measured by GPS, Earth Planets Space, v.52, pp: 1055–1060.

Wu, C.C., Liou, K., Shan, S.J., and Tseng, C.L., 2008. Variation of ionospheric total electron content in Taiwan region of the equatorial anomaly from 1994–2003. Adv. Space Res., v.41, pp: 611–616.

Wu, Y.W., Liu, R.Y., Zhang, B.C., Wu, Z.S., Ping, J.S., Liu, J.M., and Hu, Z.J., 2012. Variations of the ionospheric TEC using simultaneous measurements from the China Crustal Movement Observation Network, Ann. Geophys., v.30, pp: 1423–1433.

Xu, Z., Weimin, W., Nan, Z., Xiaofei, S., and Haotian, Z., 2012. Variability study of ionospheric total electron content at crest of equatorial anomaly in China from 1997 to 2007, Adv. Space Res., v.50, pp: 70–76.

Received on: 9.9.16; Revised on: 16.11.16; Re-revised on: 8.2.17; Accepted on: 19.2.17

"By the time we see that climate change is really bad, your ability to fix it is extremely limited... The carbon gets up there, but the heating effect is delayed. And then the effect of that heat on the species and ecosystem is delayed. That means that even when you turn virtuous, things are actually going to get worse for quite a while".

Bill Gates

(**Source:** https://www.brainyquote.com/quotes/keywords/climate_change.html)

J. Ind. Geophys. Union (May 2017)
v.21, no.3, pp: 223-229

Analysis of trends in extreme precipitation events over Western Himalaya Region: intensity and duration wise study

M. S. Shekhar*[1], Usha Devi[1], Surendar Paul[2], G. P. Singh[3] and Amreek Singh[1]

[1]Snow and Avalanche Study Establishment, Research and Development Centre, Sector 37, Chandigarh - 160036, India
[2] India Meteorological Department, Chandigarh - 160036, India
[3]Department of Geophysics, Institute of Science, Banaras Hindu University, Varanasi-221005, India
*Corresponding Author: sudhanshu@sase.drdo.in

ABSTRACT

The impact of climate change on precipitation has received a great deal of attention by scholars worldwide. Efforts have been made in this study to find out trends in terms of intensity and duration of precipitation for different altitudes and ranges in Western Himalaya region representing Jammu & Kashmir and Himachal Pradesh. In terms of intensity, precipitation has been classified as Low, Medium and Heavy. Durations of precipitation are classified as prolonged dry days (PDD), short dry days (SDD), prolonged wet days (PWD) and short wet days (SWD). Analysis indicates significant positive trends for low and heavy precipitation events and negative for medium precipitation events in Pir-Panjal range. For Shamshawari and Great Himalaya ranges, there is no significant trend for low, medium and heavy precipitation events. In terms of altitude, significant positive trends in low precipitation events have been observed for lower and middle altitudes and no significant trend has been found for medium and heavy precipitation events for other altitudes. In terms of duration, PDD/SDD shows significant increasing/decreasing trends for all ranges and altitudes. PWD and SWD show decreasing and increasing trends alternatively but not significant for all ranges and altitudes. For this study, the widely accepted Mann-Kendall test was run at 0.1, 0.05, 0.01 and 0.001 significance levels on time series data for the time period, 1991 to 2016.

Key words: Precipitation events, Dry and Wet days, Mann-Kendall test, Tele-connections, Western Himalaya.

INTRODUCTION

Report in Intergovernmental Panel on Climate Change (IPCC): "Changes in Climate Extremes and their Impact on the Natural Physical Environment" indicates that the changing climate leads to changes in the frequency, intensity, spatial extent, duration and timing of weather and climate extremes, and can result in the unprecedented extremes (Field et al., 2012). The report also describes that in the 21st century the frequency of heavy precipitations from total rainfall will increase over many areas of the globe. This is particularly the case in high latitudes and tropical regions and in winter in the northern mid-latitudes. The Himalaya region contains the most extensive and rugged high altitude areas on the earth. In the Indian subcontinent context, Himalayas govern the climate and weather system. Northwest India receives enormous amount of snow during winter due to a synoptic weather system called Western Disturbance (WD) and monsoon phenomenon during summer time. Some WDs produce well-distributed and large amounts of precipitation over the Himalayan region, while others pass across this area without causing precipitation (Malurkar, 1947). Several studies have been undertaken by researchers to see the trends of extreme events all over India. Significant trends in the occurrences of heavy rainfall events during the summer monsoon season have been studied by Rakhecha and Soman, 1994. Das (2002) studied the frequency of WDs in the pre-monsoon season, as well as its relation with monsoon rainfall and its advancement over Northwest India. Their study found a significant decreasing trend in the frequency of WDs during May. Using observations and reconstructions from tree rings, pre-monsoon and summer cooling have been reported in some portions of the Western Himalaya (Yadav et al., 2004). And overall annual temperatures in the Himalayas have recorded significant increase in the last century (Pant and Borgaonkar, 1984; Sharma and Ganju, 2000; Bhutiyani et al., 2007).

Bhutiyani et al., (2008) conducted trend analyses on discharge data from rivers in the Northwest Himalaya and found that a number of high magnitude flood events had increased in this region in the last three decades. Dash et al., (2009) studied the changes in the characteristics of rainfall events in India. Their results show that the frequencies of moderate and low rainy days considered over the entire country had significantly decreased in the last half century. Due to extremely intricate topography and altitude-dependent climate, mountain region is highly vulnerable to extreme rainfall events and cloudbursts. These sharp weather fluctuations cause sudden short term as well as long term flood / outbursts in this orographic region (Nandargi and Dhar, 2011). Cloudbursts and associated flash floods are the regular and frequent disasters in Himalaya region (Thayyen et al., 2013). Kedarnath

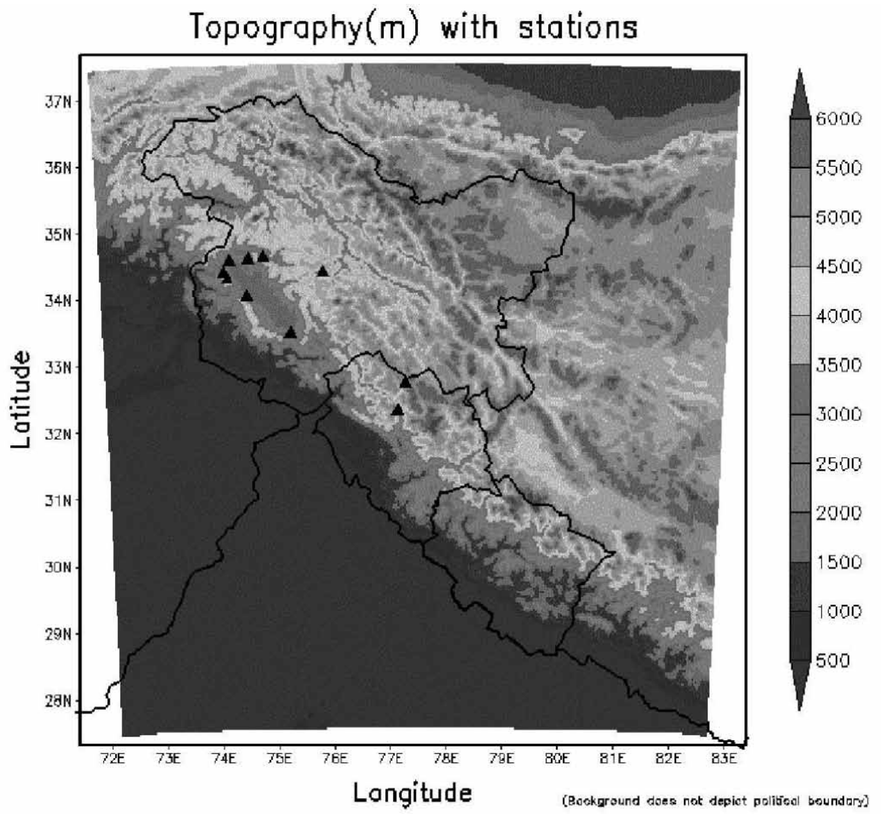

Figure 1. Location of the 10 meteorological stations considered for the present study.

disaster (June 2013), Rudraprayag cloudburst (September 2012), Manali cloudburst (July 2011) are a few of the major cloudburst events notable for causing great damages to human lives and infrastructure. Therefore study of changes in the spatial and temporal distributions of extreme precipitation events over Western Himalaya has great relevance in the context of planning, policy formulation and global warming.

Though several studies were carried out by earlier researchers to find out significant trends in precipitation over the Western Himalaya, this is the first attempt to analyze trends in intensity of precipitation depending upon number of occurrences and durations, altitude and range wise in Western Himalayan region representing Jammu & Kashmir and Himachal Pradesh. An attempt is also made in this study to link/relate the influences of global features via El Niño and North Atlantic Oscillation (NAO) Index with precipitation events in the area selected for the study.

DATA AND METHODOLOGY

Data

Daily precipitation data for winter season (Nov–April) for the period (1992–2016) of 10 stations over Western Himalaya region (Figure 1) maintained by Snow and Avalanche Study Establishment (SASE), Defence Research and Development Organization (DRDO) has been taken up for the present study. In order to study the intensity and duration of extreme precipitation events in terms of ranges and altitudes, Western Himalaya has been divided into 3 ranges i.e. Pir-Panjal, Shamshawari and Great Himalaya as was already done in Shekhar et al.,(2014) and 3 altitudes as Lower (2400- 2800 meter), Middle (2800-3200 meter) and Higher altitudes (3200-3800 meter). There is no basis for division of altitudes except to include at least 3-4 stations per every altitude range.

Methodology

The present study deals with examination of trends in the frequency of extreme precipitation events over Western Himalaya region in terms of their intensity and duration. In terms of intensity, the maximum number of the occurrence of the precipitation events is considered. Similarly in terms of duration, continuous precipitation with intensity $\geq$2.5 mm/day for < (less than) or $\geq$ (more and equal) 4 consecutive days are defined as Short Wet Days (SWD) or Prolonged Wet Days (PWD). Similarly, continuous precipitation with intensity <2.5 mm/day for < (less than) or $\geq$ (more and equal) 4 consecutive days are considered as Short Dry Days (SDD) or Prolonged Dry Days (PDD)

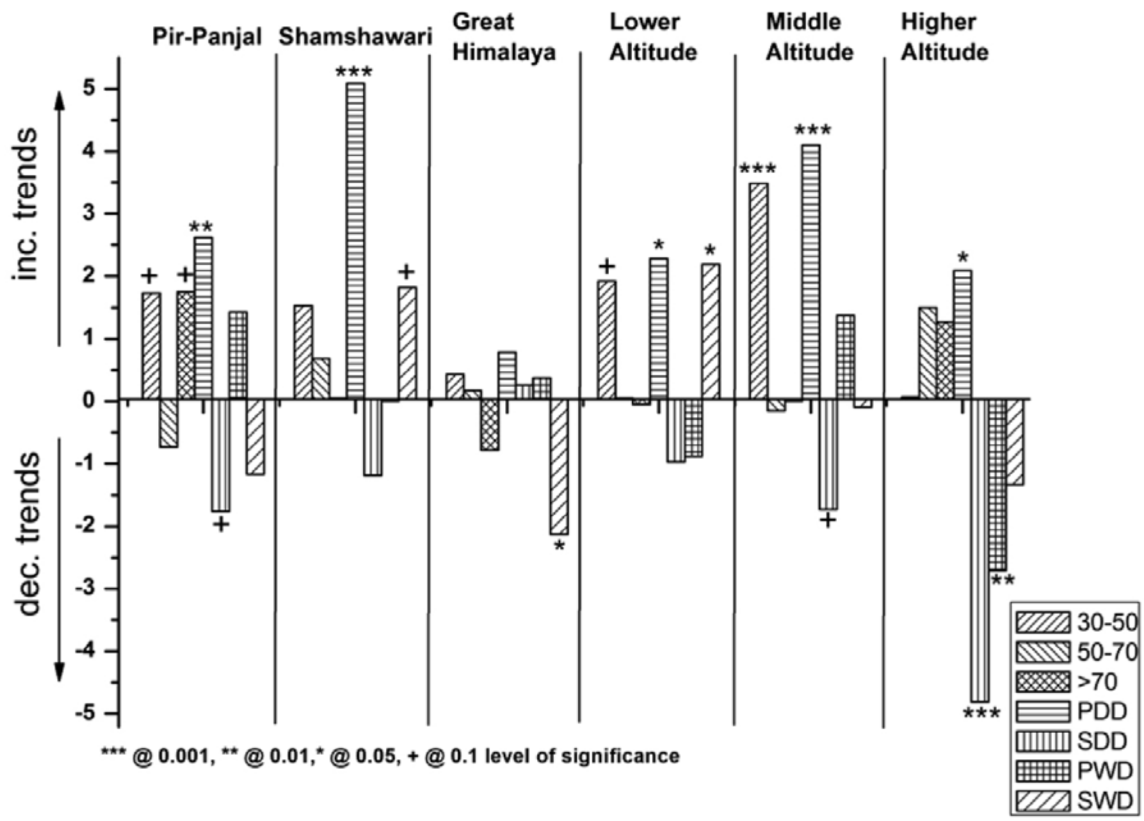

Figure 2. Mann-Kendall trends of ranges and altitudes in terms of intensity and duration for all extreme precipitation events 30-50 mm, 50-70 mm, >70 mm, PDD, SDD, PWD and SWD.

(Dash et al., 2009). This study pertains to winter season only as maximum precipitation observed only in this season in Western Himalaya region. Prevalent practice in IMD is to use rainfall data of 5 consecutive days for the average of precipitation. In this study we have used 4 consecutive days as the minimum duration of long precipitation events.

The intensity of precipitation between 30-50(mm), 50-70(mm) and >70(mm) are considered as low, medium and heavy precipitation events respectively. In this study the calculations of trend statistics were carried out by using Mann-Kendall schemes and tested at 0.1, 0.05, 0.01 and 0.001 levels of significance as can be seen in Figure 2. The Mann-Kendall (MK) is a nonparametric technique for detecting trends in meteorological time series (Gemmer et al., 2011).

RESULTS AND DISCUSSION

Trend analysis, as shown in Figure 3, indicates that the frequency of precipitation events over Western Himalaya region in terms of their intensity in Pir-Panjal range has increasing trend in case of low and heavy precipitation events at 0.1 level of significance. There is however, no significant trend in Shamshawari and Great Himalaya ranges. In medium precipitation events decreasing trends are observed in Pir-Panjal range and increasing trends in Shamshawari and Great Himalaya but these are not significant. In case of lower and middle altitudes, the low precipitation events show increasing trends at 0.1 and 0.001 levels of significance respectively. No trends have been observed for medium and heavy precipitation events. In terms of intensity, no significant trends have been observed in higher altitude.

Study of precipitation events in terms of duration show that there is increasing trend in case of PDD in Pir-Panjal and Shamshawari range at 0.05 and 0.001 significance levels respectively but no significant increasing trend for PDD in case of Great Himalaya. All the three altitudes have positive trends for PDD. SDD indicates decreasing trends for all altitudes and ranges except Great Himalaya as shown in Figure 4. PWD shows positive trends for all ranges but not significant and mixed trends have been observed for all altitudes (Figure 4). SWD has alternately decreasing and increasing trends for all ranges and altitudes.

Teleconnection studies

Walker circulation is the vast loop of winds that influence the precipitation in Himalayan region which varies during El-Nino and La-Nina oscillations. As per ncdc.

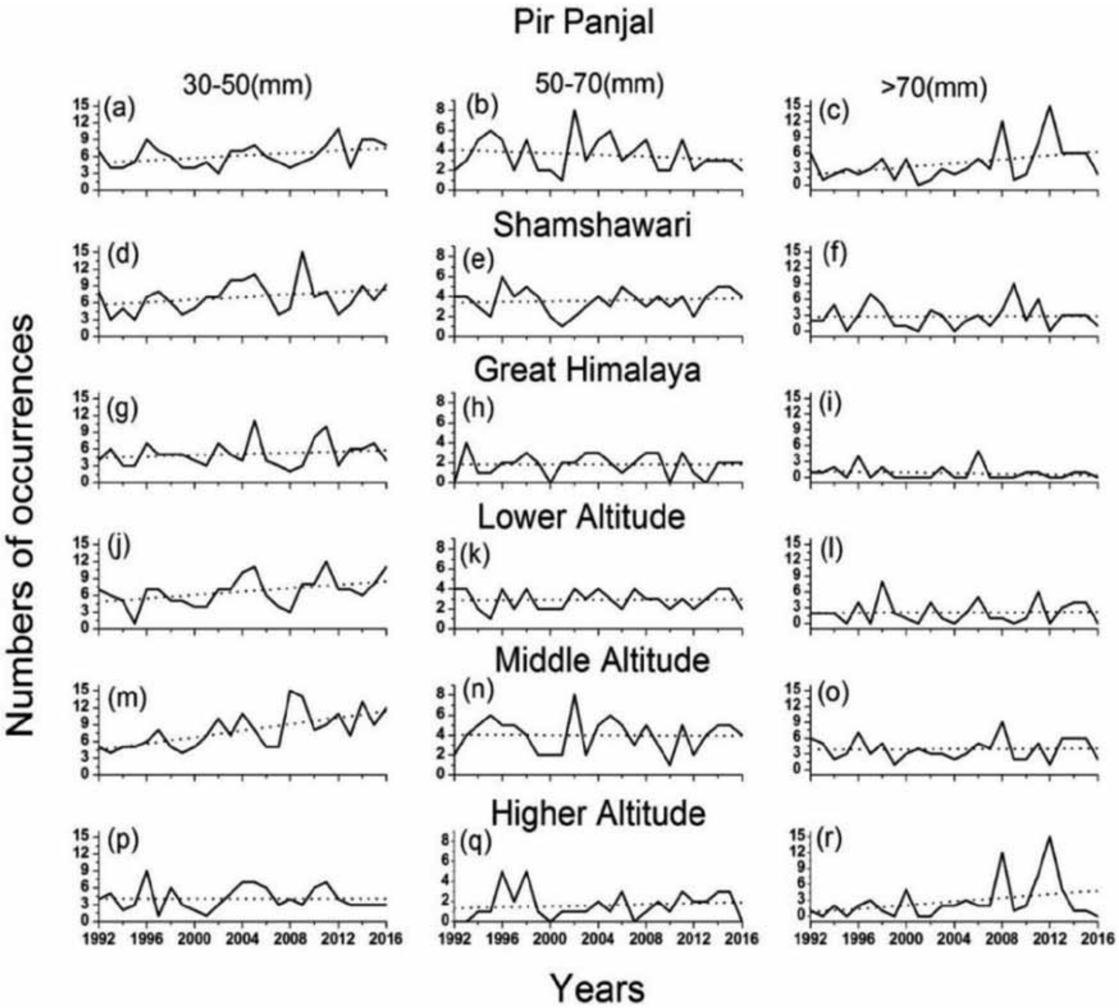

Figure 3. Time series of the numbers of occurrences for 30-50mm (1st column), 50-70mm (2nd column) and >70mm (3rd column) during winter season. Sets of plots (a), (b), (c) represents Pir-Panjal, (d), (e), (f) represents Shamshawari, (g), (h), (i) represents Great Himalaya, (j), (k), (l) represents Lower Altitude, (m), (n), (o) represents Middle Altitude and (p), (q), (r) represents High Altitude over Western Himalaya. In each subplot a linear trend line is represented by dashed line.

noaa.gov, ENSO is a periodic fluctuation in sea surface temperature (El-Nino) and the air pressure of the overlying atmospheric (Southern Oscillation) across the equatorial Pacific Ocean. A permanent low and high-pressure system over Iceland (Icelandic low) and the Azores (The Azores High) respectively controls the strength and direction of westerly winds which bring precipitation in Himalayan region. The relative strengths and the positions of these systems vary from year to year and the variation is known as North Atlantic Oscillation (NAO). Details can be found in www.plumbot.com. Relation of El-Nino and NAO with winter precipitation over Western Himalaya is shown in Figure 5.

Positive correlation of low and medium precipitation events and negative correlation for heavy precipitation events with El-Nino have been observed for all ranges except Great Himalaya which indicates positive correlation for low and heavy precipitation events and negative with medium precipitation events. In terms of duration, all precipitation events show positive correlation with El-Nino except PWD which indicates negative correlation for all ranges.

In terms of altitudes, lower altitude has a positive correlation with all duration and intensity precipitation events except PWD which shows negative correlation with El-Nino. In middle altitude, precipitation events show negative correlations in terms of intensity and positive in terms of duration except for PWD. No clear correlation for higher altitude precipitation events has been observed with El-Nino. NAO has positive correlation with low and medium precipitation events and negative correlation with heavy precipitation events for all ranges except Pir-Panjal which indicate negative correlation for medium precipitation events and positive for heavy precipitation

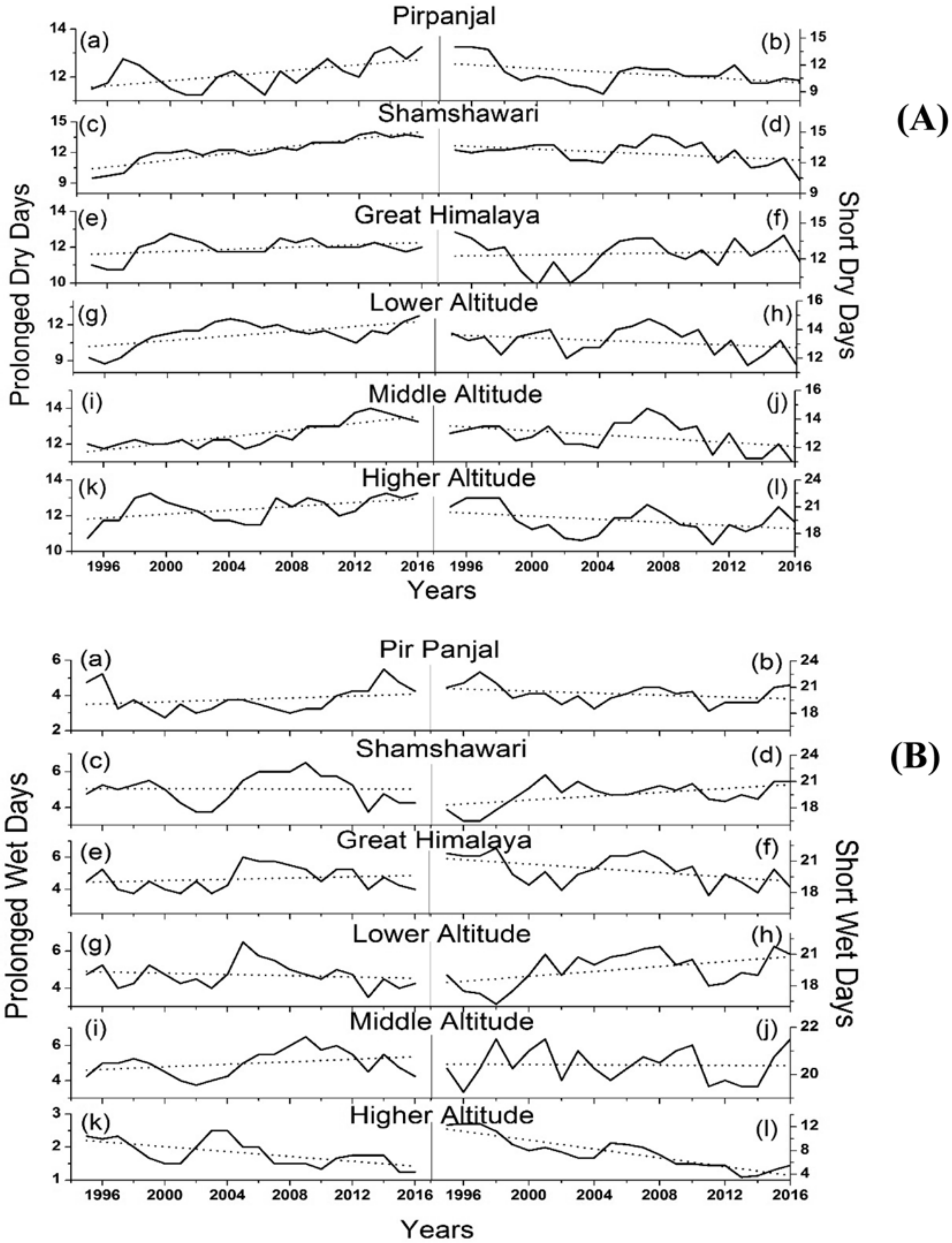

Figure 4. Time series of the numbers of (A) PDD/SDD and (B) PWD/SWD. Left/Right panels depict PDD/SDD and PWD/SWD respectively, in the winter season for (a and b) Pir-Panjal, (c and d) Shamshawari, (e and f) Great Himalaya, (g and h) Lower Altitude, (i and j) Middle Altitude and (k and l) High Altitude over Western Himalaya. In each subplot a linear trend line is represented by dashed line.

events. Positive correlation of ranges with NAO has been observed for all precipitation events in terms of duration except SDD. In terms of altitudes, positive correlation has been observed for lower altitude for all intensity and duration precipitation events except heavy and SDD. In middle altitude, positive correlation has been observed for all intensity and duration precipitation events except SDD and PWD. Similarly higher altitude shows positive relation for all intensity and duration precipitation events except low intensity events and SWD.

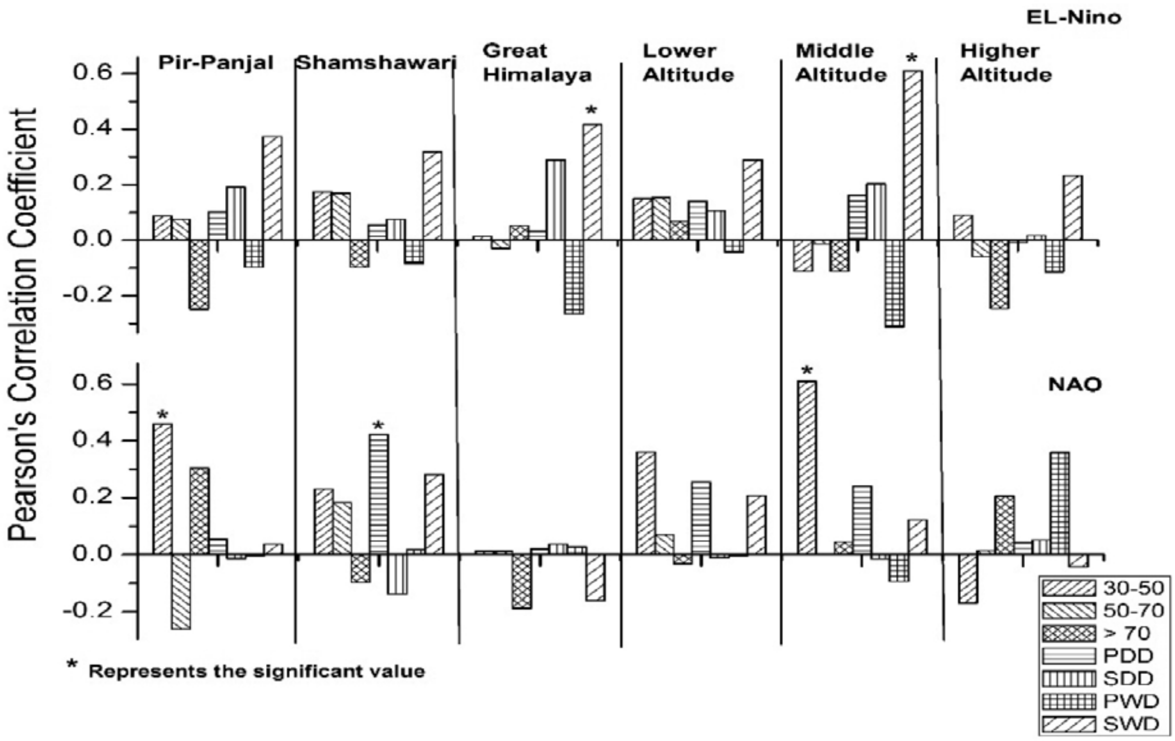

Figure 5. Pearson's correlation coefficient of El-nino and NAO with observed winter precipitation over Western Himalaya region.

CONCLUSIONS

Based on the study of intensity and duration for seasonal precipitation over the Western Himalaya region, following conclusions can be drawn. In terms of intensity, the low precipitation events indicate increasing trends for all ranges and altitudes over Western Himalaya. The medium precipitation events show over all negative trends for all ranges and altitudes except higher altitude where positive trend has been observed but not significant. Heavy precipitation events indicate significant increasing trend in Pir-Panjal range and no clear trend has been observed for other ranges and altitudes. PDD/SDD shows significantly increasing/decreasing trends for all ranges and altitudes in Western Himalaya region which indicate that rainy days have decreased and duration of dry spell has increased over the Western Himalaya region. PWD do not indicate any clear trend for all ranges and altitudes. SWD indicates alternately decreasing and increasing trend in all ranges and altitudes. No significant correlation has been observed of precipitation events in terms of intensity with El-Nino. SWD shows positive correlation with El-Nino for all ranges and altitudes but significant only for Great Himalaya and Middle altitude. NAO has positive correlation with low precipitation events for all ranges and altitudes except Great Himalaya and no clear correlation has been observed for other precipitation events.

ACKNOWLEDGEMENTS

Authors are thankful to Director SASE (DRDO) for providing the necessary support and guidance to complete this work. Thanks to all the internet sources from which information has been gathered. Contribution made by Mr. Narasimha Rao, SRF, Hazard Assessment and Forecasting Division (HAFD) for preparing graphs is duly acknowledged. Thanks are due to Dr. Jagabandhu Panda for constructive review and suggestions. They also thank Prof. B. V. S. Murty for editing the manuscript. We thank the Chief Editor for the support and guidance.

Compliance with Ethical Standards

The authors declare that they have no conflict of interest and adhere to copyright norms.

REFERENCES

Bhutiyani, M.R., Kale, V.S., and Pawar, N.J., 2007. Long-term trends in maximum, minimum and mean annual air temperatures across the North-Western Himalaya during the 20th Century, Climatic Change, v.85, pp: 159–177.

Bhutiyani, M.R., Kale V.S., and Pawar N.J., 2008. Changing stream flow patterns in the rivers of Northwest Himalaya: Implications of global warming in the 20th century, Curr. Sci. India, v.95, pp: 703-708.

Das, S., 2002. Evaluation and verification of MM5 forecasts over Indian region. 12th PSU/NCAR Mesoscale Model Users Workshop, 24-25 June, Boulder, Co., pp: 77-81.

Dash, S.K., Kulkarni, M.A., Mohanty, U.C., and Prasad, K., 2009. Changes in the characteristics of rain events in India, Geophys. J. Res., D10109, doi: 10.1029/2008JD010572., v.114.

Field, C.B., Barros, V., Stocker, T.F., Qin, D., Dokken, D.J,. Ebi, K.L., Mastrandrea, M.D., Mach, K.J., Plattner, G.K., Allen, S.K., Tignor, M., and Midgley, P.M., IPCC, 2012. Managing the Risks of Extreme Events and Disasters to Advance Climate Change Adaptation, A Special Report of Working Groups I and II of the Intergovernmental Panel on Climate Change, Cambridge University Press, Cambridge, UK, and New York, NY, USA, pp: 582.

Gemmer, M., Fischer, T., Jiang, T., Su, B., and Liu, L.L., 2011. Trends in precipitation extremes in the Zhujiang River basin, South China, J. Clim., http://dx.doi.org/10.1175/2010JCLI3717.1., v.24, pp: 750–761.

Malurkar, S.L., 1947. Abnormally dry and wet western disturbances over north India, Curr. Sci. India, v.16, no.5, pp: 139-140.

Nandargi, S., and Dhar, O.N., 2011. Extreme Rainfall events over the Himalayas between 1871 and 2007, Hydrological Sciences Journal – Journal des Sciences Hydrologiques, DOI: 10.1080/02626667.2011.595373., v.56, no.6, pp: 930-945.

Pant, G.B., and Borgaonkar, H.P., 1984. Climate of the hill regions of Uttar Pradesh, Himalayan Research and Development v.3, pp: 13–20.

Rakhecha, P.R., and Soman, M.K., 1994. Trends in the Annual Extreme Rainfall Events of 1 to 3 Days Duration over India, Theoretical and Applied Climatology, v.48, no.4, pp: 227–237.

Sharma, S.S., and Ganju, A., 2000. Complexities of avalanche forecasting in Western Himalaya – an overview, Journal of CRST, v.31, no.2, pp: 95–102.

Shekhar, M.S., Kumar, S.M., Joshi, P., and Ganju, A., 2014. Mountain Weather Research and Forecasting over Western and Central Himalaya by using Mesoscale Models, International Journal of Earth and Atmospheric Sciences, v.1, no.2, pp: 71-84.

Thayyen, R.J., Dimri, A.P., Kumar, P., and Agnihotri, G., 2013. Study of cloudburst and flash floods around Leh, India, during August 4–6, 2010, Natural Hazards. DOI: 10.1007/s11069-012-0464-2., v.65, no.3, pp: 2175–2204.

Yadav, R.R., Park, Won-Kyu, Singh, J., and Dubey, B., 2004. Do the Western Himalaya defy global warming? Geophysical Research Letters, v.31, pp: L17201.

Received on: 23.9.16; Revised on: 24.11.16; Re-revised on :19.12.16 Accepted on: 20.1.17

EARTH'S INNER CORE DOESN'T MELT

Scientists have found out why the inner core of our Globe remains solid, despite being hotter than the Sun. Researchers at KTH Royal Institute of Technology in Sweden, found to be reinserted due to that on the edge of the Inner Core; pieces of crystal structure continuously melt and diffuse, only to be re-inserted due to the superhigh overall pressure akin to "shuffling deck of cards".

This energy distribution cycle keeps the monocrystalline inner core stable and solid. Spinning within the Earth's molten core is a crystal ball, nearly the size of our Moon - composed actually of a mass formation of almost pure crystallized iron. Understanding this strange and unobservable feature of the planet we live on, depends on knowing the atomic structure of these crystals - something the scientists have been trying to do for years.

(**Source:** "Fact of the Matter": INNER MATTERS : Indian Express, Bhubaneswar Edition of Monday the 20th February 2017, Page14).

J. Ind. Geophys. Union (May 2017)
v.21, no.3, pp: 230-235

A study of Cyclonic Storms of the South Indian Ocean And Indian Summer Monsoon Rainfall

P. Chandrasekhara Rao*[1], Vishal. S. Thorat[2], Vrishali V. Kulkarni[1] and P.H. Raghavendra Rao[1]
[1]India Meteorological Department, Pune, India
[2]Junior Research Fellow, India Meteorological Department, Pune, India
*Corresponding Author: pcsraoimd@gmail.com

ABSTRACT
Coastal regions of the globe that have potential threat from the storms are studied well, but mid-oceanic storms which rarely approach the coast are not paid adequate attention. One such region is the South Indian Ocean (SIO) basin, where more than 15 storms form every year. Over 80% of these do not impact countries either in the West basin or those in the East basin but die out in the ocean itself. However they are likely to show considerable effect on the Indian summer monsoon rainfall. Hence, in this study an attempt is made to find the correlation of these storms with the Indian Summer Monsoon Rainfall (ISMR). Also, the effect of El-Nino Southern Oscillation (ENSO) on the genesis of storms is studied. During El-nino episodes, storms of the SIO get shifted to the Western part with the ultimate result of less rainfall over India. Storm activity gets significantly reduced in the Eastern part of SIO during El-nino. It is found that the correlation coefficient is -0.37 for the West SIO storms and all India rainfall during El-Nino years. Correlation coefficient of -0.15 is obtained for the West SIO storms and 0.26 for East SIO storms with the June all India summer monsoon rainfall.

Key words: South Indian Ocean, Indian Summer Monsoon Rainfall, El Nino, La Nina, Storms

INTRODUCTION

Tropical cyclones form in equatorial regions, where sea surface temperatures (SSTs) exceed 26-27°C, but rarely within less than 4°-5° from the Equator, some literatures have listed several other conditions favoring genesis, such as (i) large values of low level relative vorticity, (ii) weak vertical and horizontal wind shear, (iii) conditional instability through a deep atmospheric layer, (iv) large relative humidity in the lower and middle troposphere, all of which are fulfilled within the Inter-Tropical Convergence Zone (ITCZ), and (v) a deep oceanic mixed layer (Alberto et al., 2009). A rapidly rotating storm system with a low-pressure center, strong winds, and a spiral arrangement of thunderstorms and heavy rain is recognized as tropical cyclone (Kumar and Kumar, 2013). It is referred to by names such as hurricane in the Northeast Pacific or in North Atlantic, typhoon in North-Western Pacific, and tropical cyclone in the Indian ocean.

About one-third of world petroleum supplies and over half of sea-trade in crude oil pass through South-West Indian Ocean waters (Chang-Seng and Jury, 2010a). Sudden cyclogenesis and storm surges increase the risk of marine environmental hazards and coastline erosion, particularly for island nations such as Mauritius, Reunion and Madagascar (Chang-Seng and Jury, 2010a). More often, meridional pulses of the Indian Monsoon create periods of cyclonic vorticity and Tropical Cyclone development around 10°S (Chang-Seng and Jury 2010b).

Each basin has different time periods of storm formation. Pacific and Atlantic basins have maximum storms during the northern hemisphere summer season. In the North Indian Ocean cyclones are in maximum number during pre- and post- monsoon seasons. In South Indian Ocean (SIO), tropical cyclone activity begins in late October and ends in May with its peak from late January to early March. Cyclones that form in the west of the SIO can affect Mauritius, Mozambique, Madagascar, Tanzania and Kenya, where as those in the east of SIO can affect Australia and Indonesia (Rao et al., 2012)

Cyclones are of different categories depending on the intensity, which is measured in terms of the prevailing wind speeds. There are seven categories of cyclones in the South Indian Ocean, tropical disturbance (< 27 kt), tropical depression (28 - 33 kt), moderate tropical storm (34 – 47kt), severe tropical storm (48 - 63 kt), tropical cyclone (64 - 89 kt), intense tropical cyclone (90 – 115 kt), very intense tropical cyclone (> 115 kt) (WMO/ESCAP Panel on Tropical Cyclones, 2015). For any region, storms that can affect the coasts are well monitored and studied but the storms that occur in the middle of the ocean are rarely considered in the study of rainfall over the land. Mid-oceanic storms can play an important role in the transfer of heat from one region to another. Since heat potential associated with the storm is considerably large, it can affect the weather patterns and the amount of rainfall. The effect of storms forming in the SIO on the Southwest Monsoon is discussed here.

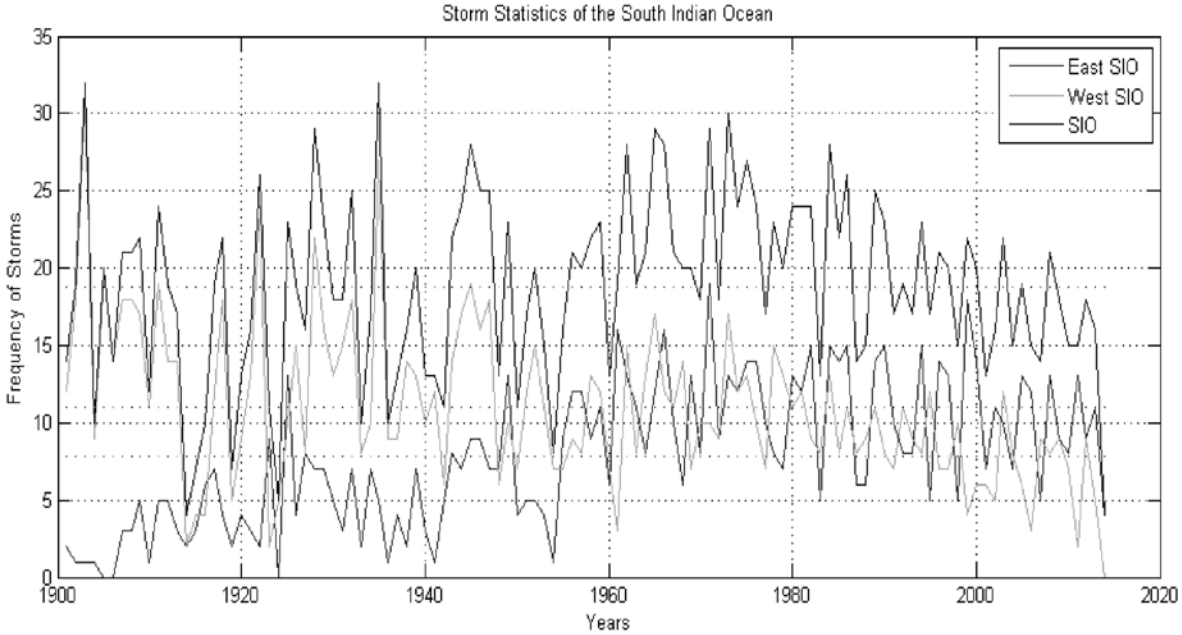

Figure 1. Frequency of Occurrences of Storms of the South Indian Ocean.

DATA AND METHODOLOGY

Yearly data of number of storms in South Indian Ocean is obtained from the NOAA's, National Climate Data Center (NCDC). International Best Track Archive for Climate Stewardship (IBTrACS) of NCDC has the centralised data of tropical cyclones worldwide to aid in understanding of the distribution, frequency and intensity of the storms (Knapp et al., 2010). Data are available for all the basins in the Network Common Data Form (NetCDF). Figure 1 shows the plot of all the tracks of storms formed in the South India Ocean for the period of 1901 to 2014. Storm statistics are shown for the separate east and west regions of the SIO in the following section.

After the storm statistics, analysis of storm activity with the Indian Summer Monsoon Rainfall (ISMR) is carried out. Data on the amount of rainfall in the respective monsoon seasons is acquired from the IMD data archive. And subsequently, it is shown how the El Nino and La Nina episodes have affected the storm activity. Data on the El Nino and La Nina is acquired from the NOAA's Climate Prediction Center (CPC) for the period of 1950-2015.

RESULT AND DISCUSSION

Storm Statistics

Annual frequency of the storms for the period from 1901 to 2014 is derived from the IBTrACS data set. Later, data are seperated for the east as well as west basins of the South Indian Ocean in order to understand the difference of occurences of storms between the two regions. In Figure 1, data are plotted for the east (bottom), west (faint line in the middle) and whole SIO (bold line on top of the figure) regions.

It is observed that the storms formed in the eastern SIO are less in number compared to western SIO. Total 2142 storms have been formed for the whole SIO region during 1901-2014. Among them 1250 and 892 storms have occurred in the western and eastern SIO respectively. On an average 19 storms have formed in a year in the SIO, 8 storms in the eastern and 11 storms in the western basin.

Storms in the east were well below average for the first half of the 20th century and increased only after the mid twentieth century and then remained almost constant there after. The storms in the west were at their peak during the first half of the 20th century. Later, in the late 20th century and at the beginning of the 21st century, frequency of storms has reduced drastically. (Overall the storm activity is showing decreasing trend from eighties, mainly attributed to the reduced number of storms in the west). Highest number of storms recorded in SIO is 32 in both 1903 and 1935, while those in the eastern basin are 19 in 1971 and 31 in western basin in 1903.

ENSO Correlation with the Storm Statistics

El Nino and La Nina are part of a larger cycle called ENSO. ENSO episodes from 1991 to 2010 and are captured and analysed with the corresponding storm activity of the South Indian Ocean. During the ENSO episodes, El-Nino or La-Nina, Storms gets shifted to the West SIO and

Table 1. El-Nino and La-Nina Years with ISMR (1901-2010).

EL-Nino, Storms and Rainfall

El-Nino Years	No. of Storms in		Total no. of Storms	El-Nino Years R/F (mm)
	(WSIO)	(ESIO)		
1902	18	1	19	792.1
1905	20	0	20	718.5
1914	2	2	4	964.3
1918	18	4	22	736.5
1930	13	5	18	876.4
1940	10	3	13	905.0
1941	12	1	13	813.5
1951	12	5	17	749.2
1953	11	4	15	983.4
1957	8	12	20	898.1
1958	13	9	22	1012.9
1963	8	11	19	912.2
1965	17	12	29	738.3
1969	7	13	20	888.3
1972	9	9	18	697.4
1977	7	10	17	911.3
1982	9	15	24	767.4
1986	11	15	26	769.8
1987	8	6	14	774.6
1991	7	10	17	828.3
1994	8	15	23	1001.2
1997	7	13	20	927.3
2002	5	11	16	737.3
2004	8	7	15	774.1
2006	3	12	15	889.3
2009	9	9	18	698.2

La-Nina, Storms and Rainfall

La-Nina Years	No. of Storms in		Total no. of Storms	La-Nina Years R/F (mm)
	(WSIO)	(ESIO)		
1903	9	1	10	891.9
1909	17	5	22	927.9
1910	11	1	12	940.2
1916	4	6	10	1056.1
1917	12	7	19	1124.2
1922	24	2	26	957.5
1924	5	0	5	972.8
1933	8	2	10	1061.0
1938	14	2	16	1005.0
1942	6	5	11	1040.5
1950	7	4	11	923.2
1954	7	1	8	914.4
1955	7	9	16	962.0
1964	13	8	21	1031.5
1970	10	8	18	998.7
1971	10	19	29	925.5
1973	17	13	30	956.0
1975	13	14	27	1011.5
1988	9	6	15	1094
1998	10	5	15	943.1
1999	4	18	22	863.2
2007	9	5	14	942.9
2010	7	8	15	911.1

cause less rainfall over India during the Indian Summer Monsoon Season. Table 1 shows the El-Nino and La-Nina years with corresponding SIO storms and Indian Summer Monsoon Rainfall (ISMR). It is found that the correlation coefficient is -0.37 for the West SIO storms and all India rainfall during El-Nino years. Correlation coefficients are -0.13 and -0.17 for the East and West SIO storms with ISMR during the La-Nina years.

Decadal Analysis of Storms:

Figure 2 depicts the decadal frequency graph of storms of East SIO (ESIO), West SIO (WSIO) and overall SIO. The graph shows alternate ups and downs in the frequency till 1970. There is an increase in frequency in the decade 1971-80 compared to previous decade, and the frequency has been decreasing since 1981. The ratio of storms of East SIO to West SIO remains between 0.3 and 0.4 for the decade, i.e., 1851-60, 1871-80 and 1911-20. The same remains between 0.4 to 0.6 for decades 1861-70, 1881-90, 1921-30 and 1941-50. The ratio drops to 0.1 for decades 1891-00 and 1901-10. The storms in the east have been on the rise since 1941. In fact, since 1961, there have been more storms in the East than in the West. The ratio has been more than 1 and increasing since 1961. The activity over the West was relatively higher till 1950, which was nearly double than that of East. Thereafter, the activity over East is gradually on the rise while it is decreasing over the West.

Storms in SIO and the ISMR

Maximum number of storms occurs in this SIO region during the four months of December, January, February and March and the Indian summer monsoon is from June to September. There seems to be little correlation between the storms and the immediate Indian summer monsoon rainfall season, especially in the southern peninsular India. Respective correlation coefficients are -0.106 and -0.187 for the monsoon seasonal and southern peninsular India (SPIN) rainfall. Rainfall of All India June (AI June), All

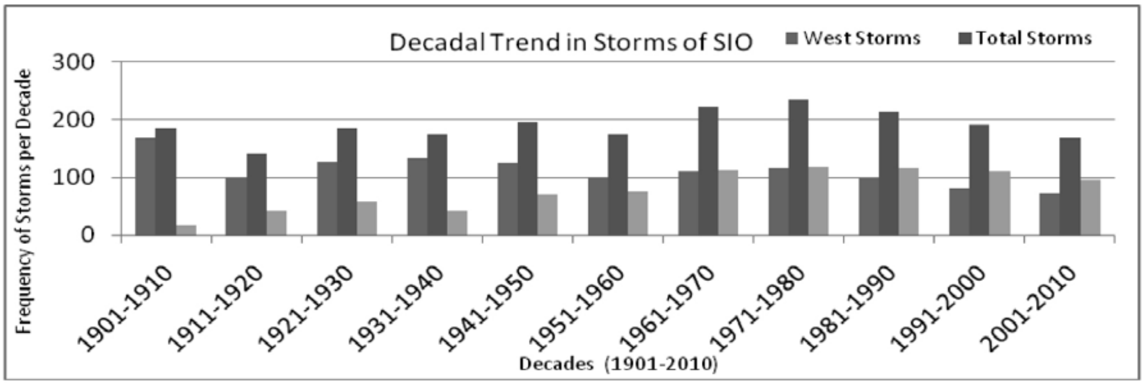

Figure 2. Decadal frequency of Storms of the South Indian Ocean.

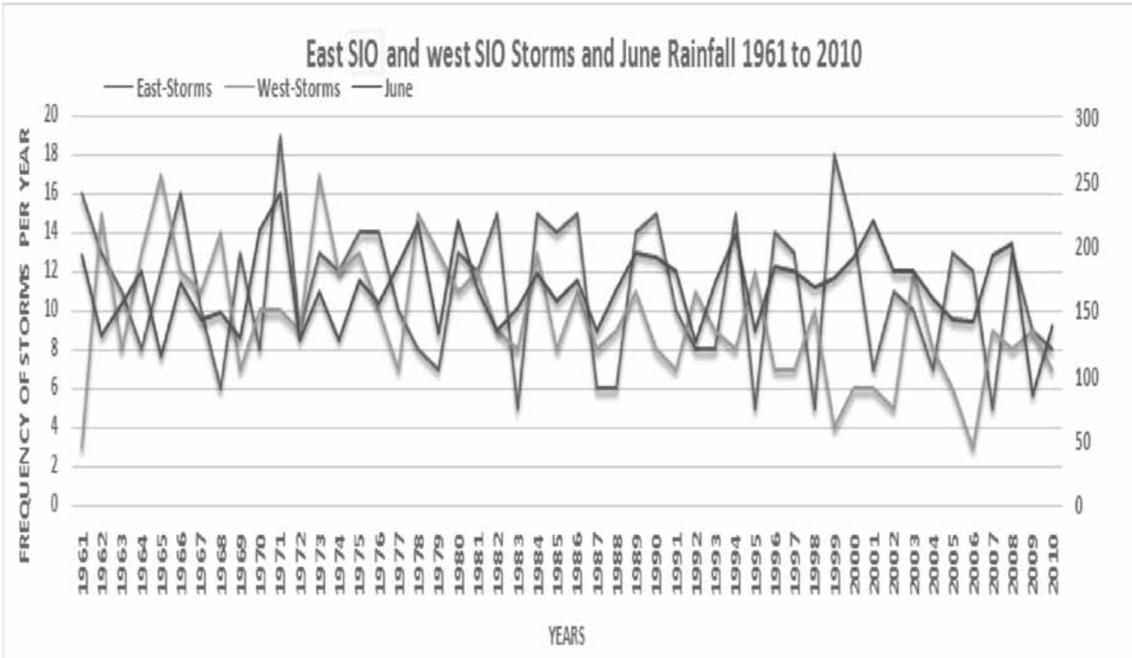

Figure 3. Rainfall in June, storms in East, West SIO (1961 -2010).

India (AI), Southern peninsular India (SPIN) and number of storms in East SIO (ESIO), West SIO (WSIO) for the period 1961-2010 are plotted in Figures (3, 4 & 5). The figures depict that storms in both West SIO and East SIO have been on the decline since last decade. The fluctuations in frequency of storms as well the number of storms is reducing.

At the same time, SPIN rainfall almost remains within the range of 922mm and 542mm. AI rainfall remains within the range of 1094 and 698mm. For the month of June, the rainfall range is from 85mm to 240mm; the SPIN and AI rainfall being a little on the higher side in the last 2 decades.

Figure 3 depicts storms in ESIO, WSIO and rainfall in June over India. For storms in WSIO and June rainfall, there is a negative correlation co-efficient (- 0.14619). For El Nino years 1965 and 2009, it is seen that Storms in WSIO increase in number and AI June rainfall decreases. For years 1963, 1977 and 1994, number of Storms in WSIO decreases and AI June rainfall increases. We can also see that for years 1969, 1972, 1982, 1986, 1987, 1991, 2002, 2004 and 2006, storms in WSIO and AI June rainfall both increase or both decrease together. For the year 1997, Storms in WSIO remain the same while AI June rainfall decreases.

For storms in ESIO and AI June rainfall, there is a positive correlation co-efficient of 0.26454. For El Nino years 1965, 1969, 1982 and 2002, it is seen that the number of storms in ESIO increases and AI June rainfall decreases. For years 1963 and 1977, storms in ESIO decrease and AI June rainfall increases. We can also see years 1972, 1986, 1987, 1991, 1994, 1997, 2004, 2006

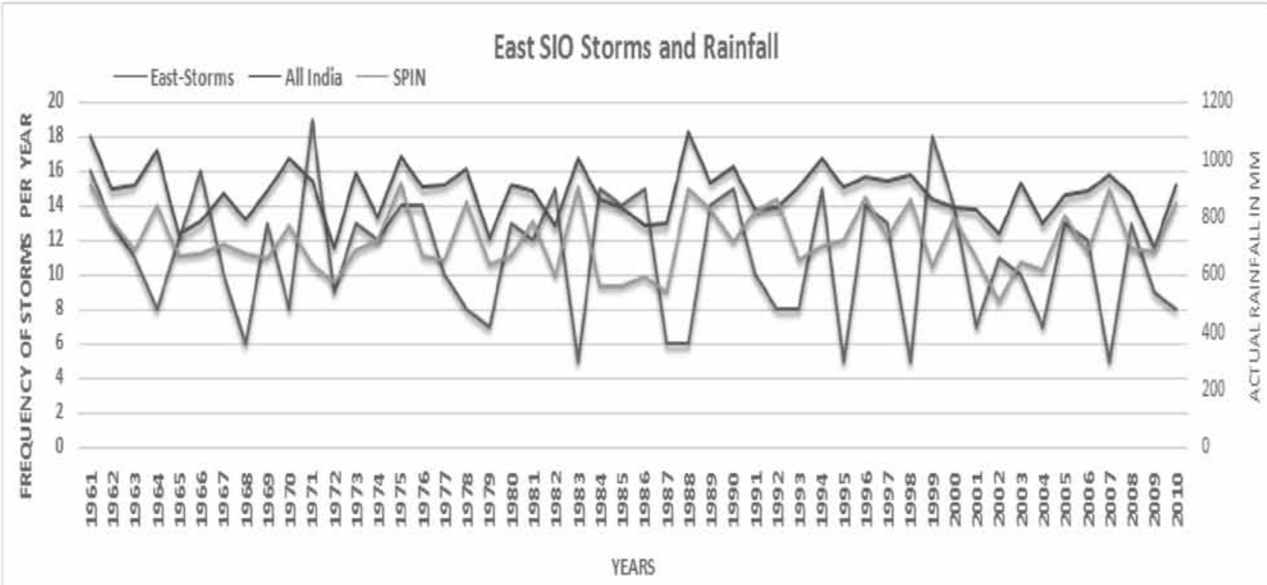

Figure 4. Rainfall AI, SPIN, storms in East SIO (1961 -2010).

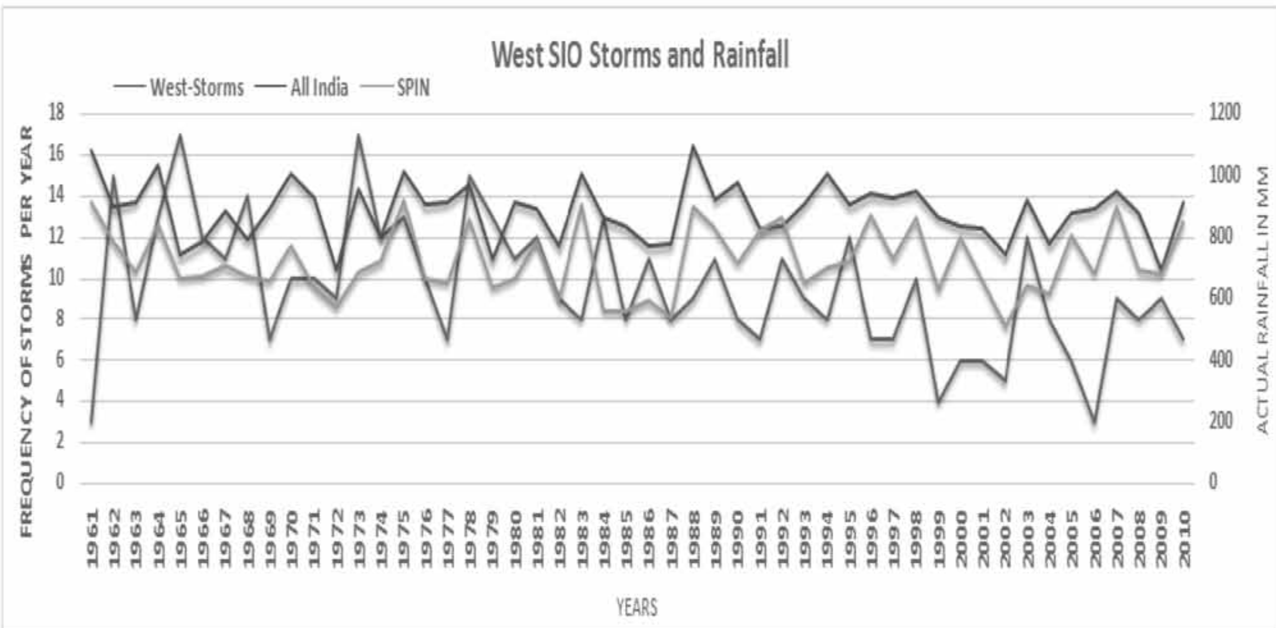

Figure 5. Rainfall AI, SPIN, Storms in West SIO (1961 -2010)

and 2009; where storms in ESIO and June rainfall both increase or both decrease together.

Figure 4 depicts rainfall of AI, SPIN rainfall and storms in ESIO. For the storms in ESIO and SPIN rainfall, there is a negative correlation co-efficient (- 0.21671). For El Nino years 1965, 1969, 1982 and 2002, it is seen that storms in ESIO increase and SPIN rainfall decreases. For year 1991, storms in ESIO decrease and SPIN rainfall increases. We can also see the years 1963, 1972, 1977, 1986, 1987, 1994, 1997, 2004, 2006 and 2009, when storms in ESIO and SPIN rainfall both increase or both decrease together.

For storms in ESIO and AI rainfall, no correlation is seen. For El Nino years 1965, 1982, 1986 and 2002, it is seen that storms in ESIO increase and AI rainfall decreases. For years 1963, 1977, 1987 and 2006, storms in ESIO decrease and AI rainfall increases. We can also see that for the years 1969, 1972, 1991, 1994, 1997, 2004 and 2009, storms in ESIO and AI rainfall both increase or both decrease together.

Figure 5 depicts graph of AI rainfall, SPIN rainfall and storms in WSIO. For the storms in WSIO and SPIN rainfall, no correlation is seen. For years 1965 and 2009, storms in WSIO increase and SPIN rainfall decreases. For years 1991 and 1994, storms in WSIO decrease and SPIN rainfall increases. We can also see that for the years 1963, 1969, 1972, 1977, 1982, 1986, 1987, 2002, 2004 and 2006, storms in WSIO and SPIN rainfall both increase or both decrease together. For year 1997, storms in WSIO remain the same while SPIN decreases.

For storms in WSIO and AI rainfall, no correlation is seen. For El Nino years 1965, 1986, 2009, it is seen that storms in WSIO increase and AI rainfall decreases. For years 1963, 1969, 1977, 1987, 1994 and 2006, storms in WSIO decrease and AI rainfall increases. We can also see years 1972, 1982, 1991, 2002 and 2004, where storms in WSIO and AI rainfall both increase or both decrease together. For year 1997, storms in WSIO remain the same while AI rainfall decreases.

CONCLUSIONS

1. Storms show decreasing trend towards end of the 19th century for whole SIO, although frequency of storms in the east SIO has increased. Decreasing trend is mainly attributed to the drastic reduction in number of storms in the west SIO.
2. The activity over the West SIO was relatively higher till 1950, which was nearly double than that of East SIO. Thereafter, the activity over East SIO is gradually on the rise and it is otherwise over the West.
3. AISMR is negatively correlated (-0.37) with storms in WSIO during the preceding months of the EL-Nino year.
4. All India June rainfall is negatively correlated (-0.14619) with the storms in WSIO and positively correlated (0.26454) with the storms in ESIO.

ACKNOWLEDGEMENTS

The authors express their sincere thanks to Shri B. Mukhopadhyay, Additional Director General of Meteorology, IMD, Pune for his guidance and encouragement in carrying out this research work. Thanks are due to Dr. Vinod Kumar for constructive review and suggestions. They also thank Prof. B. V. S. Murty for editing the manuscript. We thank the Chief Editor for his support and encouragement.

Compliance with ethical Standards

The authors declare that they have no conflict of interest and adhere to copyright norms.

REFERENCES

Alberto, F.M., Rydberg, L., Rouault, M., and Lutjeharms, R.E., 2009. Climatology and Landfall of Tropical Cyclones in the South-West Indian Ocean, Western Indian Ocean Journal of Marine Science, v.8, pp: 15-36.

Chang-Seng, D., and Jury, M., 2010a. Tropical Cyclones in the SW Indian Ocean. Interannual Variability and Statistical Prediction, Meteorol Atmos Phys, v.106, pp: 149-162.

Chang-Seng, D., and Jury, M., 2010b. Tropical Cyclones in the SW Indian Ocean. Structure and Impacts at the Event Scale, Meteorol Atmos Phys, v.106, pp: 163-178

Knapp, K., Kruk, M., Levinson, D., Diamond, H., and Neumann, C., 2010. The International Best Track Archive for Climate Stewardship (IBTrACS): Unifying tropical cyclone best track data. Bulletin of the American Meteorological Society, v.91, pp: 363-376.

Kumar, A., and Kumar, S., 2013. Tracking of Tropical cyclones and their intensity changes in the south pacific region using World-wide lightning location network, Proceedings of Pacific inter-science congress, USP.

Rao P.C.S., Kadam V.B., Lokhande K.R., and Gaonkar, S.B., 2012. A Climatological Study of Storms of South Indian Ocean in the Bygone Century, WMO, World Weather Research Programme. Extended Abstracts, Second International Conference on Indian Ocean Tropical Cyclones and Climate Change (IOTCCC-II), 14-17 Feb, 2012, pp: 38.

WMO/ESCAP Panel on Tropical Cyclones, 2015. Tropical Cyclone Operational Plan for the Bay of Bengal and the Arabian Sea, (Report No. TCP-21), World Meteorological Organization pp: 11–12.

Received on: 15.7.16; Revised on: 24.11.16; Re-revised on: 18.1.17; Accepted on: 29.1.17

NEWS AT A GLANCE

Forthcoming Events:

1) **FUTORES II — Future understanding of tectonics, ores, resources, environment and sustainability**
04 Jun 2017 - 07 Jun 2017,
Townsville, Australia
Contact Email: futores2@jcu.edu.au
Topics: New Insights in Mineral Deposit Understanding, New Technologies and Approaches in Mineral Exploration, Tectonics and Metallogenesis, Basins and Energy, Future Trends in the Minerals Industry
Event website: http://www.jcu.edu.au/futores.

2) **European Geosciences Union (EGU) General Assembly**
23 Apr 2017 - 28 Apr 2017
Vienna, Austria
Abstract: The EGU General Assembly will bring together geoscientists from all over the world to one meeting covering all disciplines of the Earth, planetary and space sciences. The EGU aims to provide a forum where scientists, especially early career researchers, can present their work and discuss their ideas with experts in all fields of geoscience.
Event website: http://www.egu2017.eu/

3) **GeoConvention 2017**
15 May 2017 - 19 May 2017
Calgary, Alberta, Canada
Contact: Dustin Menger; Email: dustin@geoconvention.com
Topics: geoscience, CSPG, CSEG, CWLS, geology, geophysics, exhibition, exhibit, earth, science
Event website: http://www.geoconvention.com

4) **79th EAGE Conference & Exhibition 2017 Energy, Technology, Sustainability - Time to open a new Chapter**
12 Jun 2017 - 15 Jun 2017
Paris, France
Abstract: The energy mix is changing but the world will need every form of energy - both fossil and renewable- to meet its growing demands. Our ability to respond effectively to all the changes in our industry especially during this low oil and gas price cycle, determines whether we stay in a time of crises or move to that of opportunity. In order to survive and ultimately thrive again, we need to change and adapt our approaches and historical norms.
Event website: http://www.eage.org/event/index.php?eventid=1488&Opendivs=s3

5) **79th EAGE Conference & Exhibition 2017 Student Programme**
12 Jun 2017 - 15 Jun 2017
Paris, France
Abstract: EAGE provides students with the opportunity to gain knowledge, skills and contacts to pursue a career in geosciences and the engineering industry. The next opportunity for students will be the student programme at the 79th EAGE Conference & Exhibition from 12 June to 15 June 2017.
Event website: http://www.eage.org/event/index.php?eventid=1490&Opendivs=s3

6) **Engineering Geophysics 2017 Conference and Exhibition**
24 Apr 2017 - 28 Apr 2017
Kislovodsk, Russia
Event website: http://www.eage.org/event/index.php?eventid=1508&Opendivs=s3

Awards and Recognition

1) Dr. N. Purnachandra Rao, Chief Scientist and an AcSIR Professor at CSIR-NGRI has been selected for the "Prestigious National Geoscience Award" by the Ministry of Mines, Govt. of India.

2) Dr. A. Keshav Krishna, Scientist at CSIR-NGRI has been selected for the "Prestigious National Geoscience Award" by the Ministry of Mines, Govt. of India.

Space Science & Technology News

Space science & technology has witnessed phenomenal success in the last two decades, encouraging our space scientists to face new challenges in exploring planets of our solar system. In this process series of technological innovations are being tested regularly, following strict security norms in the laboratory. Many of these exercises carried out by highly motivated scientists and technical experts do only receive accolades when a mission is successful. Such a committed involvement is not seen in other fields of science and technology (except in communication) due to absence of an organised planning and execution mechanism. It is learnt that for any space expedition well articulated schedules are planned at least 5 years in advance, as many inter linking sequential procedures are to be fine tuned and precisely executed. When we closely observe the strides made by NASA and our own ISRO it is evident considerable efforts have been made to ensure success of a space expedition, amidst known and unknown impediments. Starting from selection of data acquisition gadgets of small and big dimensions and ensuring the success of minute execution procedures need optimum use of precision technology. For Chandrayan and Mangalyaan voyages to Moon and Mars respectively, planning of various procedures was started long time back following in house and at times international interactions, without compromising our own interests. If and when we want to send a rover to collect various types of data from Mars or even Moon it is essential for us to select precise landing sites, as done by NASA for its upcoming Mars 2020 mission. Since we have entered in the race to explore different planets and have a shot at exoplanets we need to sharpen our capabilities, as a continuation of the success story in world record breaking, at a time launching of 104 satellites on 15th February, 2017. To familiarize with the existing scenario in space technology and space voyages I cover below some recent studies. If they excite your inquisitiveness a significant volume of literature is there to satiate your thirst for enhancing your knowledge base.

***NASA Shortlists Three Landing Sites for Mars 2020**

Mars 2020 is targeted for launch in July 2020 aboard an Atlas V 541 rocket from Space Launch Complex 41 at Cape Canaveral Air Force Station in Florida. The rover will conduct geological assessments of its landing site on Mars, determine the habitability of the environment, search for signs of ancient Martian life, and assess natural resources and hazards for future human explorers. It will also prepare a collection of samples for possible return to Earth by a future mission.

Participants in a landing site workshop for NASA's upcoming Mars 2020 mission have recommended three locations on the Red Planet for further evaluation. The three potential landing sites for NASA's next Mars rover include Northeast Syrtis (a very ancient portion of Mars' surface), Jezero crater, (once home to an ancient Martian lake), and Columbia Hills (potentially home to an ancient hot spring, explored by NASA's Spirit rover). There were 240 participants in the Feb. 8-10, 2017 workshop in Monrovia, California, and up to 60 who engaged online. More information on the landing sites can be found at:http://mars.nasa.gov/mars2020/mission/timeline/prelaunch/landing-site-selection/
NASA's Jet Propulsion Laboratory will build and manage operations of the Mars 2020 rover for the NASA Science Mission Directorate at the agency's headquarters in Washington. For more information about NASA's Mars programs, visit:http://www.nasa.gov/mars

***New timeline for our solar system estimated**

Astronomers have established a new timeline for the solar system that is helping to pinpoint when gas giants Jupiter and Saturn likely formed. Approximately 4.6 billion years ago, a swirling cloud of hydrogen gas and dust known as the solar nebula collapsed in on itself, giving way to the birth of the sun. The leftover material from this massive explosion then clumped together to form the planets, in a process called core accretion.

A new study suggests Jupiter and Saturn likely took shape within the first 4 million years of the solar system's formation, which further supports the core accretion model. Weiss and lead author Huapei Wang, a postdoctoral student at MIT, studied the magnetic orientations of four ancient meteorites called angrites. They fell to Earth at different times and were found in Brazil, Argentina, Antarctica and the Saharan desert. This type of space rock acts as a good marker for what the cosmic environment was like during the early days of the solar system. When the solar nebula was present, it generated a substantial magnetic field, which would in turn be recorded in meteorites formed during this time. However, the researchers observed little to no remnant magnetization in the oldest of the four angrites, which formed 3.8 million years after the formation of the solar system. That lack of magnetization suggests the gas and debris of the solar nebula had already dissipated by that time. Thus, the solar system's large-scale structure, including Jupiter and Saturn, must have already been established. Solar systems form out of the condensation of a gaseous nebula. The two scientists found an accurate and precise age for the lifetime of our solar system's ancient [solar] nebula and the magnetic field. They found that the [solar] nebula and [magnetic] field had dispersed 3.8 million years after the formation of the solar system.

The study, published on Feb. 9, 2017 in the journal Science, offers a more precise estimate of the solar nebula's lifetime and will therefore help to determine when and how other planets formed in the solar system. Since the solar nebula lifetime critically affects the final positions of Jupiter and Saturn, it also affects the later formation of the Earth, our home, as well as the formation of other terrestrial planets. The researchers said they plan to study other primitive asteroid samples to be collected by the Hayabusa 2 spacecraft and NASA's OSIRIS-REx mission, which are expected to return to Earth in the early 2020s. (**Source:** http://www.space.com/35662-solar-system-evolution-giant-planet-formation.html)

***Hubble Has Found the Ancient Galaxies That Gave the Universe Its First Light**

A new technique that removes the light of foreground galaxy clusters is giving astronomers a direct look at a generation of galaxies dating back to the universe's baby years. The discovery is considered a key piece of evidence for a critical, but poorly understood period of time when the universe switched from being dark to radiating light. Scientists theorize that energy from first-generation galaxies transformed the dark, electrically neutral universe into ionized and radiating plasma. But these faint galaxies are not easy to find.

University of Texas astronomer Rachael Livermore and colleagues describe a successful hunt thanks to a new technique that combines deep-field Hubble Space Telescope images with what is known as "wavelet decomposition" — a light-masking equivalent of noise-cancelling headphones — to computationally remove light from foreground galaxy clusters. The wavelet transform allows us to decompose an image into its components on different physical scales. Thus, one can isolate structures on large scales… and remove them, allowing objects on smaller scales to be identified more easily. Ironically, astronomers first have to rely on galaxy clusters, which warp spacetime with their massive gravity, to serve as naturally occurring lenses that boost Hubble's resolving power more than 100 times.

By then masking the light, Livermore, University of Texas astronomer Steven Finkelstein and Space Telescope Science Institute astronomer Jennifer Lotz found 167 galaxies that are 10 times fainter than any previously known, a number that shows "strong support" for how many early galaxies would have been needed to re-ionize the universe.

A more direct detection method will come after Hubble's successor, the James Webb Space Telescope, is launched next year.

(**Source:** http://www.space.com/35668-hubble-frontier-fields-lensing-astronomy-universe-ancient-galaxies.html)

***More Alien Worlds? New Data Haul Identifies 100+ Possible Exoplanets**

Astronomers have spotted more than 100 new potential alien planets, including one in the fourth-closest star system to the sun, a new study reports. This haul of newfound possible exoplanets, which have yet to be confirmed as bona fide alien worlds, comes from a new analysis of 20 years' worth of data gathered by the HIRES (High Resolution Echelle Spectrometer) instrument at the Keck Observatory in Hawaii.

HIRES detects exoplanets using the "radial velocity" method: The instrument picks up the tiny gravitational wobbles that orbiting worlds induce in their parent stars. This strategy is different from that employed by the most prolific planet hunter of all time, NASA's Kepler space telescope; Kepler watches for the tiny brightness dips caused when a planet crosses its star's face — called the "transit method." In the new study, the researchers identified 60 so-called planet candidates, as well as 54 other suggestive signals that require further investigation before they can be elevated to candidate status.

One of the official candidates circles the star GJ 411 (also known as Lalande 21185), which lies just 8.3 light-years from the sun. Only three star systems are closer. (The three-star Alpha Centauri is the nearest system to the sun. Last August, astronomers announced the discovery of a potentially Earth-like world orbiting Proxima Centauri, one of the Alpha Centauri trio. Proxima Centauri lies 4.22 light-years from Earth.) The possible GJ 411 planet is at least 3.8 times more massive than Earth, and it's probably too hot to be habitable, study team members said. The candidate world lies quite close to the star, completing one orbit every 10 Earth days.

The huge HIRES data set consists of nearly 61,000 measurements of more than 1,600 stars. To wring the most science possible out of this catalog — which study team members called the biggest compilation of radial-velocity planet-hunting observations ever the HIRES researchers have shared it with other exoplanet — researchers around the world. The best way to advance the field and further our understanding of what these planets are made out of is to harness the abilities of a variety of precision radial velocity instruments, and deploy them in concert. The new study, which was led by Paul Butler of the Carnegie Institution for Science in Washington, D.C., was published in The Astronomical Journal. To date, astronomers have discovered 3,450 confirmed exoplanets, about two-thirds of which were found by Kepler. Several thousand more await confirmation. And the finds should keep rolling in well into the future. For example, the European Space Agency's Gaia mission, which launched in December 2013, is expected to discover thousands of alien worlds before its work is done, as is NASA's Transiting Exoplanet Survey Satellite (TESS), which is scheduled to lift off in early 2018.

(**Source:** http://www.space.com/35687-100-potential-exoplanets-found-hires.html)

PSLV-C37 Successfully Launches 104 Satellites in a Single Flight

In its thirty ninth flight (PSLV-C37), ISRO's Polar Satellite Launch Vehicle successfully launched the 714 kg Cartosat-2 Series Satellite along with 103 co-passenger satellites on February 15, 2017 from Satish Dhawan Space Centre SHAR, Sriharikota. This is the thirty eighth consecutively successful mission of PSLV. The total weight of all the 104 satellites carried on-board PSLV-C37 was 1378 kg.

PSLV-C37 lifted off at 0928 hrs (9:28 am) IST, as planned, from the First Launch Pad. After a flight of 16 minutes 48 seconds, the satellites achieved a polar Sun Synchronous Orbit of 506 km inclined at an angle of 97.46 degree to the equator (very close to the intended orbit) and in the succeeding 12 minutes, all the 104 satellites successfully separated from the PSLV fourth stage in a predetermined sequence beginning with Cartosat-2 series satellite, followed by INS-1 and INS-2. The total number of Indian satellites launched by PSLV now stands at 46.

After separation, the two solar arrays of Cartosat-2 series satellite were deployed automatically and ISRO's Telemetry, Tracking and Command Network (ISTRAC) at Bangalore took over the control of the satellite. In the coming days, the satellite will be brought to its final operational configuration following which it will begin to provide remote sensing services using its panchromatic (black and white) and multispectral (colour) cameras.

Of the 103 co-passenger satellites carried by PSLV-C37, two – ISRO Nano Satellite-1 (INS-1) weighing 8.4 kg and INS-2 weighing 9.7 kg – are technology demonstration satellites from India.

The remaining 101 co-passenger satellites carried were international customer satellites from USA (96), The Netherlands (1), Switzerland (1), Israel (1), Kazakhstan (1) and UAE (1).

With successful launch, the total number of customer satellites from abroad launched by India's workhorse launch vehicle PSLV has reached 180.

(**Source:** http://isro.gov.in/update/15-feb-2017/pslv-c37-successfully-launches-104-satellites-single-flight)

Outstanding Contribution

Significant scientific studies have been carried out by many illustrious sons of India, Prof.C.V.Raman, Prof.Jagadish Chandra Bose, Prof.Ramanujam to name a few. Following their footsteps many carried out outstanding scientific research covering basic and applied branches of physical, chemical and life sciences. In earth Sciences we produced both theoretical as well as field scientists of international repute. Similarly in almost all the branches of Physical, chemical and life sciences significant contributions have been made by number of scientists of international repute.

I have covered in the News & Views section very senior earth system scientists who have made significant contributions to propagate the importance of this branch of science by bringing into focus the importance of solid earth, oceans, atmosphere & space. I selected some of those living legends to motivate our young researchers in carrying out such research studies that are basically useful to our society. There are many more who have contributed significantly in propagating the importance of our country`s area specific natural wealth. Due to some limitations I could not continue "Living Legends" subsection. I found it difficult to gather sufficient information about some of the stalwarts. I regret the subsection`s discontinuity. As and when I am confident that sufficient data has been gathered I will reintroduce it. Till then please bear with me.

Since scientific research in our country has to attain and maintain international standards it is essential for our young researchers to get motivated by going through the outstanding contributions made even in other branches of science. To achieve this I started from November 2016 issue the noteworthy and outstanding contributions made by those scientists who helped in propagating the importance of Indian Science in general and steps essential to address problems faced by the vulnerable segments of our society in particular through their path breaking scientific contributions in their fields of expertise. I have covered outstanding contribution to Indian Space Programme by Dr.Krishnaswamy Kasturirangan, outstanding contribution to Atomic Energy and India's Nuclear Weapons Programme by Dr.Rajagopala Chindambaram and outstanding contribution to Indian Food Security by Mankombu Sambasivan Swaminathan (Architect of Green Revolution). In this issue I have included the outstanding contributions made by Prof.C.N.R.Rao, well known expert in solid state and materials chemistry.

Prof.C.N.R. Rao

C.N.R. Rao was born in Bangalore in 1934. He attended Acharya Patashala high school in Basavanagudi, which made a lasting influence on his interest in chemistry. His father enrolled him to a Kannada-medium course to encourage his mother tongue, but at home used English for all conversation. He completed secondary school leaving certificate in first class in 1947. He studied BSc at Central College, Bangalore. His first research paper was published in the *Agra University Journal of Research* in 1954.

Research Expertise

Chintamani Nagesa Ramachandra Rao (C.N.R. Rao) is an Indian chemist, distinguished as one of the leading solid state and materials chemists around the world. His scientific career spanning over five decades saw him making significant contribution in development of the field that included his analysis on transition metal oxides. The study aided in comprehending the novel phenomenon and association of materials properties with that of structural chemistry of such materials. He was a front-runner in synthesizing two dimensional oxide materials like La_2CuO_4. For last twenty years, apart from working on hybrid materials, he has been making significant contribution to nanomaterials.

Professional Achievements

Professor C.N.R. Rao is the Linus Pauling Research Professor and Honorary President of the Jawaharlal Nehru Centre for Advanced Scientific Research, Bangalore. His main research interests are in solid state and materials chemistry, surface phenomena, spectroscopy and molecular structure. He is an author of over 1000 research papers and 36 books. He received the M.Sc. degree from Banaras, Ph.D. from Purdue, D.Sc. from Mysore universities and has received honoris causa doctorate degrees from 32 universities including Purdue, Bordeaux, Banaras, Mysore, IIT Bombay, IIT Kharagpur, Notre Dame, Novosibirsk, Uppsala, Wales, Wroclaw, Caen, Khartoum and Sri Venkateswara University. Besides being Fellow of the Indian National Science Academy and the Indian Academy of Sciences, Professor Rao is a Fellow of the Royal Society, London, Foreign Associate of the National Academy of Sciences, U.S.A., Foreign Member of the Russian Academy of Sciences, French Academy of Sciences, Japan Academy as well as the Polish, Czechoslovakian, Serbian, Slovenian, Brazil, Spanish, Korean and African Academies and the American Philosophical Society. He is a Member of the Pontifical Academy of Sciences, Foreign Member of Academia Europaea and Foreign Fellow of the Royal Society of Canada. He is on the editorial boards of 15 leading professional journals.

Awards and Recognition

Among the various medals, honours and awards received by him, mention must be made of the Marlow Medal of the Faraday Society (1967), Bhatnagar Prize (1968), Jawaharlal Nehru Fellowship (1973), Padma Shri (1974), Sir C.V. Raman Award (1975), Centennial Foreign Fellowship of the American Chemical Society (1976), S.N. Bose Medal of the Indian National Science Academy (1980), Royal Society of Chemistry (London) Medal (1981), Padma Vibhushan (1985), Honorary Fellowship of the Royal Society of Chemistry, London (1989), Hevrovsky Gold Medal of the Czechoslovak Academy (1989), Meghnad Saha Medal of the Indian National Science Academy (1990), Blackett Lectureship of the Royal Society (1991), CSIR Golden Jubilee Prize in physical sciences (1991), TWAS Medal in Chemistry (1995), Einstein Gold Medal of UNESCO (1996), Linnett Professorship of the University of Cambridge (1998), Centenary Lectureship and Medal of the Royal Society of Chemistry, London (2000), the Hughes Medal of the Royal Society, London for original discovery in physical sciences (2000), Karnataka Ratna (2001) by the Karnataka Government, the Order of Scientific Merit (Grand-Cross) from the President of Brazil (2002), Commander of the Order of Rio Branco from Brazil (2002) and the Gauss Professorship of Germany (2003), Order of Friendship(2009), National order of Scientific Merit(2012), Bharat Ratna (2013), Order of the Rising Sun (2015). Professor Rao is the President of the Third World Academy of Sciences, Member of the Atomic Energy Commission of India and of the Executive Board of the Science Institutes Group, Princeton, and Chairman, Indo-Japan Science Council. Prof. Rao was President of the Indian National Science Academy (1985-86), the Indian Academy of Sciences (1989-91), the International Union of Pure and Applied Chemistry (1985-87), the Indian Science Congress Association (1987-88), the Materials Research Society of India (1989-91) and Chairman, Advisory Board of the Council of Scientific and Industrial Research (India). He was the Director of the Indian Institute of Science (1984-94), Chairman of the Science Advisory Council to Prime Minister Rajiv Gandhi (1985-89) and Chairman, Scientific Advisory Committee to the Union Cabinet (1997-98), and Albert Einstein Research Professor (1995-99).

P.R.Reddy

J. Ind. Geophys. Union (May 2017)
v.21, no.3, pp: 240-241

TECHNICAL NEWS

Autonomously Deployed Deep-Ocean Seismic System (ADDOSS) – the emerging technology for Ocean Seismic Network

Raja Acharya
India Meteorological Department, Regional Meteorological Centre, Kolkata (Ministry of Earth Sciences)

The Autonomously Deployed Deep-Ocean Seismic System (ADDOSS) is primarily used with the goal to navigate the oceans with seismic instrumentation which will help in monitoring of earthquakes, advances in tsunami warning systems, and research on deep Earth structure.

Features of this system: This novel technology is introduced by the Scripps Institution of Oceanography at UC San Diego. It is autonomously deployable, communications gateway designed to provide long-term and near real-time data from ocean observatories. The new system has the ability to telemeter sensor data from seismometers deployed on the seafloor top shore via satellite and to be deployed without a ship, thereby greatly reducing life-cycle costs.

Ocean Surface Gateway: The system consists of a free-floating surface communications gateway which utilizes a Liquid Robotics wave glider.

Wave Glider: The surfboard-sized float is towed by a tethered, submerged glider, which converts wave motion into thrust. The surface float is equipped with solar panels, an Iridium satellite telemetry modem/GPS, and a small processor to provide commands to steer the system via a rudder on the glider. The Wave Glider has demonstrated the ability to "swim" thousands of kms across the open ocean and to hold station in a very small watch circle. The subsea instruments (ocean bottom package) and the surface gateway are connected through Acoustic Communications link, while communications between the gateway and land are provided by the Iridium satellite constellation.

Performance: Tests of the surface gateway in 4350 m depth of water demonstrated that it has the ability to send 4 channels of compressed, 1 sample per second data from the ocean bottom to the gateway with an average power draw of approximately 0.15 W and a latency of less than 3 minutes.

The Objective and Benefits of introducing ADDOSS: The establishment of approximately high quality broadband permanent ocean seismic stations has long been envisioned to provide seismic data coverage in areas lacking nearby island or continental sites. In the **IRIS** (Incorporated Research Institutions for Seismology) grand challenges report (Seismological Grand Challenges in Understanding the Earth's Dynamic Systems) the need to extend seismological observations to the seafloor was clearly articulated which will address the issue of OSN (Ocean Seismic Network). Of the 10 "Grand Challenges" identified, seven explicitly called for such seafloor stations to address the scientific problems such as improved tomographic imaging of the structure of the lower mantle (especially in the Southern Hemisphere), the core-mantle boundary, and the role of subducting slabs and plumes in deep mantle circulation. Studies of regional structure and tectonics of many areas also require observations from oceanic areas. The lack of good coverage in oceanic areas seriously degrades the accuracy of determination of earthquake parameters such as location and moment and this is particularly critical for tsunami warning systems.

Moreover, since the seafloor deforms under the loading of surface gravity waves, a broadband seafloor seismic sensor combined with a traditional bottom pressure sensor will respond to a tsunami travelling overhead and contribute useful real-time data to a tsunami warning system. While this system addresses a global seismic network (GSN), it has the potentiality for addressing other scientific problems including the monitoring of ice sheet and shelf breakup and telemetering data from many other types of seafloor and water column sensors. The life cycle costs for this system will be much less than the cost of maintaining buoys, with accompanying tethers, for scientific observations including climate. This sets the ground for introduction of an autonomously deployed, deep-ocean seismic system (ADDOSS) to provide long-term and near-real-time seismographic observations from the deep oceans. The system circumvents traditional ocean-floor seismometer deployments and data retrieval that involve ship time, expensive deployments via ships and long time lags in recovery.

Future Plans: ADDOSS is planned as a 20- station array with each unit spread 2,000 kms (1,242 miles) apart across the oceans where no islands exist. ADDOSS data will be integrated into Project IDA (the International Deployment of Accelerometers), the global seismographic network operated by Scripps Oceanography's Cecil H. and Ida M. Green Institute of Geophysics and Planetary Physics.

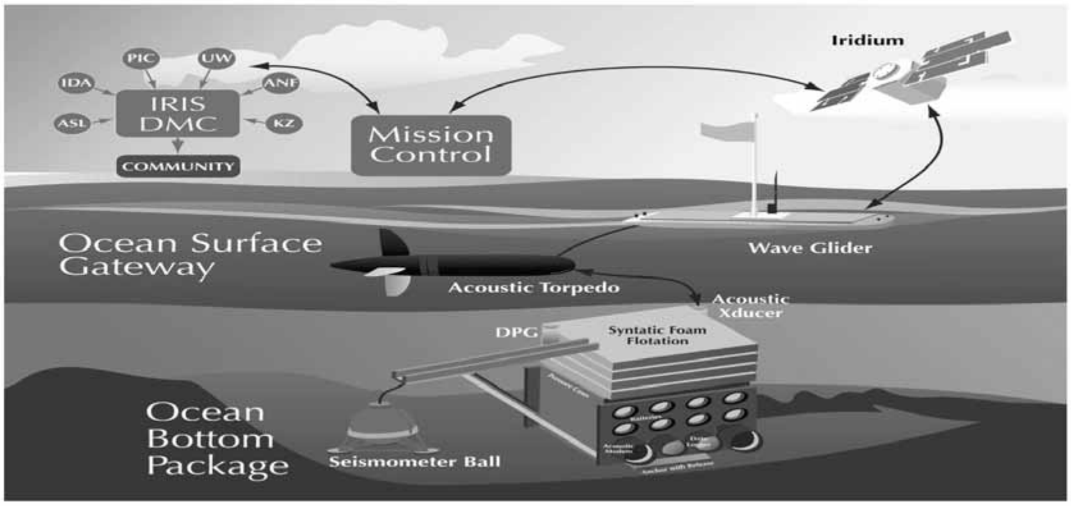

ADDOSS Schematic diagram

CONCLUSION

This new technological capability would make it realistic to consider the deployment of seafloor observatories in any remote areas of the oceans. In addition to addressing fundamental questions of Earth structure and tectonics, providing real-time data from stations in oceanic areas will significantly increase the accuracy of earthquake parameters such as location and moment.The next-generation wave gliders will be large enough to tow smaller, disposable OBS packages to a remote deployment site without the need of a ship. This provides independence from ship schedules, ship costs, and the possibility of deployments in very remote ocean locations. Ultimately the ADDOSS will also replace the need for ship deployment of ocean buoys for monitoring oceanic and meteorological parameters as it will have the potential to deploy such ocean buoys in future

ACKNOWLEDGEMENTS

This technical news has been compiled using internet information, basically to propagate the importance of ADDOSS.I unequivocally state that the technical details given above have not been developed by me either directly or indirectly. I thank the Chief Editor of JIGU for editing and publishing this technical news item.

BIBLIOGRAPHY

1. ADDOSS: Autonomously Deployed Deep-ocean Seismic System Communications Gateway for Ocean Observatories by Gabi Laske, Jon Berger, John Orcutt and Jeff Babcock
2. An autonomously deployed, deep-ocean, broadband seismic network Jon Berger (1), John Orcutt (1), Neil Trenaman (2), Tim Richardson (2), and Gabi Laske (1) (1) University of California, San Diego, Scripps Institution of Oceanography, La Jolla, United States (jorcutt@ucsd.edu), (2) Liquid Robotics, 1329 Moffett Park Drive, Sunnyvale, CA 94089
3. Development of an Autonomously Deployed Deep-Ocean Seismic System by Berger, Jonathan Orcutt, John Laske, M. Gabrielle Babcock, Jeffrey
4. Journal Nature Volume 507, issue 7491: Article: Global seismic network takes to the seas by Nicola Jones.
5. https://www.iris.edu/hq/workshops/2015/05/future_seismic_and_geodetic_facility_needs_in_the_geosciences
6. Connecting The Seafloor To Space With Persistent, Unmanned, Surface Vehicles By Justin Manley, Milsat Magazine, Oct 2016 Edition.

Diamonds from the deep

The oxidation state of Earth's silicate-rich mantle has had a profound effect on our planet's evolution, including core–mantle differentiation, mineral formation, and the distribution and availability of carbon, hydrogen, and oxygen. Most measurements derive from the highly oxidized upper mantle, yet theory and experiments suggest that the deep mantle should include chemically reduced regions and metallic iron alloys. Now Evan Smith of the Gemological Institute of America and colleagues report that a certain class of large gem-quality diamonds—including the 3106-carat Cullinan, the largest ever found—provides direct verification of those predictions: metallic inclusions of a solidified mixture of iron, nickel, carbon, and sulfur. (**Source:** Physics Today 70, 2, 80 (2017); doi: http://dx.doi.org/10.1063/PT.3.3475).

ANNOUNCEMENT

54th Annual Convention of
Indian Geophysical Union (IGU)

will be held at CSIR-NGRI, Hyderabad

During December 4-7, 2017

on

"RECENT ADVANCES IN GEOPHYSICS: SPECIAL REFERENCE TO EARTHQUAKES"

Hon. Secretary
Indian Geophysical Union
CSIR-NGRI Campus, Uppal Road
Hyderabad- 500 007, India
Email: igu123@gmail.com

GUIDE LINES TO AUTHORS

The Journal of Indian Geophysical Union (J-IGU), published quarterly by the Indian Geophysical Union (IGU), is an interdisciplinary journal from India that publishes high-quality research in earth sciences with special emphasis on the topics pertaining to the Indian subcontinent and the surrounding Indian Ocean region. The journal covers several disciplines of earth sciences such as the Geosphere, its watery and gaseous envelopes (the Hydrosphere, the Cryosphere and the Atmosphere), and life (the Biosphere). It also publishes articles on Space and Planetary sciences. J-IGU welcomes contributions under the following categories:

- Research papers reporting new findings, results, etc.
- Review articles providing comprehensive overview of a significant research field related to earth sciences

In addition, J-IGU also welcomes short communications on opinion and report on scientific activity, personal information, book reviews, news and views, etc.

The manuscript should be submitted electronically as a single pdf file including the main text, figures, tables, and any other supplementary information along with the signed "Declaration Letter". The manuscript should be submitted by email ((jigu1963@gmail.com) to the Editor.

After acceptance of the manuscript the corresponding author would be required to submit all source files (text and Tables in word format) and figures in high resolution standard (*.jpg, *.tiff, *.bmp) format. These files may be submitted to the Editor as a single *.zip file along with the "Copyright Transfer Statement".

IMPORTANT INFORMATION

Ethics in publishing

J-IGU is committed to ensuring ethics in publication and takes a serious view of plagiarism including self-plagiarism in manuscripts submitted to the journal. Authors are advised to ensure ethical values by submitting only their original work and due acknowledgement to the work of others in case used the manuscript. Authors must also refrain from submitting the same manuscript to more than one journal concurrently or publish the same piece of research work in more than one journal which is unethical and unacceptable. Editor of J-IGU is committed to make every reasonable effort to investigate any allegations of plagiarism brought to his attention, as well as instances that come up during the peer review process and has full authority to retract any plagiarized publication from the journal and take appropriate action against such authors if it is proven that such a misconduct was intentional.

Similarly, Editor and Reviewers are also expected to follow ethical norms of publishing by ensuring that they don't use any unpublished information, communicated to them for editorial or review purpose, in their own research without the explicit written consent of the author. They are also expected to keep manuscript/ data/ observations/ any other information related to the peer review confidential to protect the interest of the authors. Reviewers should refrain from reviewing the manuscripts in which they have conflicts of interest resulting from competitive, collaborative, or other relationships or connections with any of the authors, companies, or institutions connected to the manuscript.

Conflict of interest

All authors are requested to disclose any actual or potential conflict of interest including any financial, personal or other relationships with other people or organizations within three years of beginning the submitted work that could inappropriately influence, or be perceived to influence, their work.

Submission declaration

Submission of a manuscript implies that the work has not been published previously and it is not under consideration for publication elsewhere, and that if accepted it will not be published elsewhere in the same or any other form, in English or in any other language, without the written consent of the publisher. It also implies that the authors have taken necessary approval from the competent authority of the institute/organization where the work was carried out.

Copyright

After acceptance of the manuscript the corresponding author would be required to sign and submit the "Copyright Transfer Statement".

MANUSCRIPT PREPARATION

The corresponding author should be identified (include E-mail address, Phone/Mobile number). Full affiliation and postal address must be given for all co-authors.

Abstract:

An abstract of not more than 300 words must be included.

Text:

The manuscript should be structured to include a front page containing the title, Author(s) name, affiliation and address of the institute where the work was carried out, a short title, and 5-to-6 index terms/Key words. Author(s) present address, if different from the above mentioned address, may be given in the footnote. The corresponding author should be identified with an asterisk and his/her email ID should be provided. This page should be followed by the main text consisting of Abstract, Introduction, Methods/ Techniques/ Area description, Results, Discussion, Conclusions, Acknowledgements, and References. Tables and Figures with captions should be inserted in the main text of the manuscript at appropriate places.

Figures/ Illustrations:

All figures should be provided in camera-ready form, suitable for reproduction (which may include reduction) without retouching. Figures in high-resolution (at least 300 dpi) standard formats (*.jpg, *.tiff, *.bmp) are acceptable. Figures should be numbered according to their sequence in the text. References should be made in the text to each figure. Each figure should have a suitable caption.

Tables:

Authors should take note of the limitations set by the size and layout of the journal. Table should not exceed the printed area of the page. They should be typed on separate sheets and details about the tables should be given in the text. Heading should be brief. Large tables should be avoided and may be provided as supplementary information, if required.

Equations:

Equations should be numbered sequentially with Arabic numerals and cited in the text. Subscripts and Superscripts should be set off clearly. Equation writing software that presents each equation as an object in MS Word will be accepted. Style and convention adopted for the equations should be uniform throughout the paper.

References:

All references to publications cited in the main text should be presented as a list of references following the text and all references in the list must be cited in the text. References should be arranged chronologically, in the text. The list of references should be arranged alphabetically at the end of the paper.

References should be given in the following form:

Kaila, K.L., Reddy P.R., Mall D.M., Venkateswarlu, N., Krishna V.G. and Prasad, A.S.S.S.R.S., 1992. Crustal structure of the west Bengal Basin from deep seismic sounding investigations, Geophys. J. Int., v.111,no., pp:45-66.

REVIEW PROCESS:

All manuscripts submitted to the journal are peer-reviewed. It is advisable to send the contact details of **4 potential reviewers** along with the manuscript to expedite the review process. Editor has the option to select reviewers from the list or choose different reviewers. The review process usually takes about 3 months. All enquiries regarding the manuscript may be addressed to the Editor.

GALLEY PROOF:

Technical editing of manuscripts is performed by the editorial board. The author is asked to check the galley proof for typographical errors and to answer queries from the editor. Authors are requested to return the corrected proof **within two days** of its receipt to ensure uninterrupted processing. The editor will not accept new material in proof unless permission from the editorial board has been obtained for the addition of a "note added in proof". Authors are liable for the cost of excessive alterations to galley proof.

PUBLICATION CHARGES:

There are no page charges for publication and printing charges for b/w figures. However, in view of substantial cost involved in printing of color figures, author will be charged for printing of pages containing color figures @ Rs. 2,500/- per page. The charges may be revised at any time based on cost of printing and production. Author will receive an estimate/ invoice of the color figures reproduction cost along with the galley proof. It is the responsibility of the author to remit the color figures reproduction cost **within one month** of the receipt of the estimate/invoice.

The corresponding author will receive a soft copy (pdf format) of his/her published article. Should the author desire to purchase reprints of his/ her publication, he/she must send the duly signed Reprint Order Form (accompanies the galley proof and contains price details) along with the corrected galley proof to the Editor. The reprint charges must be paid **within one month** of sending the Reprint Order Form.

Any payment related to printing of color figures and/or purchase of reprints should be made in the form of a Demand Draft in the name of **Treasurer, Indian Geophysical Union**, payable at **Hyderabad**.

You may download the pdf file here: Guide for Authors